EXC-5 Controls Intracellular Trafficking in Order to Maintain the Apical Structure of the *C. elegans* Excretory Canal

BY

Brendan Christopher Mattingly

Submitted to the graduate degree program in Molecular Biosciences and the Graduate Faculty of the University of Kansas in partial fulfillment of the requirements for the degree of Doctor of Philosophy.

_____
Chairperson Dr. Matthew Buechner

_____
Dr. Robert Cohen

_____
Dr. Erik Lundquist

_____
Dr. Kristi Neufeld

_____
Dr. Kathy Suprenant

_____
Dr. Craig Martin

Date Defended: April 21st, 2011

The Dissertation Committee for Brendan Mattingly
certifies that this is the approved version of the following dissertation:

EXC-5 Controls Intracellular Trafficking in Order to Maintain the Apical Structure of the *C. elegans* Excretory Canal

_____
Chairperson Dr. Matthew Buechner

Date approved: April 26th, 2011

Abstract:

The goal of this work is to understand how cells form and maintain tubular shapes. The protein EXC-5 is necessary for a small tubular structure in *Caenorhabditis elegans* to maintain its shape. *C. elegans* is a small, easily manipulable, genetically tractable, and transparent nematode with a unicellular excretory canal system. The *C. elegans* excretory canal cell is a long "H"-shaped tubular structure that serves as the osmoregulatory organ for the animal. EXC-5 is a guanine nucleotide exchange factor (GEF). GEF proteins work by binding to GDP-bound small GTPases and facilitating the exchange of GDP with GTP, thus activating the GTPase. The activated GTPases are effectors themselves and interact with numerous other proteins to direct various cellular processes.

In this dissertation I discuss the various methods by which I examined how EXC-5 functions in order to maintain the tubular structure of the excretory canal. I describe an EMS non-complementation screen to identify new alleles of EXC-5, an EMS screen to identify genetic enhancers of EXC-5, methods to create an excretory canal-specific RNAi strain of *C. elegans*, the genetic interactions between *exc-5*, *cdc-42*, *mig-2*, *ced-10* and other genes, the organization of subcellular organelles within the canal cell and in *exc-5* mutants, the generation of intein containing proteins to create conditional alleles, and the generation of antibodies that bind to EXC-5.

The data from these studies lead to a model of tubular maintenance where the sorting of material to the apical surface is only required at certain points along the canal where it is undergoing significant restructuring because of growth or physical damage. When *exc-5* is mutant, materials are not efficiently sorted to the apical surface where they are needed to maintain the apical surface. Failure of the actin network under osmotic pressure from fluid within the lumen causes cysts to form in the canal cell. When EXC-5 is overexpressed, sorting to the apical surface is enhanced at the expense of sorting to the basal surface. This leads to an inability of the basal surface to adhere to the basement membrane and grow out, causing a convoluted tubule phenotype.

Acknowledgements

Thank you to Dr. Matthew Buechner who has been a great mentor and a valuable friend. Special thanks to my family, Mom, Dad, and my brother Brian for all their unending love and support over the years and their encouragement of me to follow my interest in science. Thank you to my love Mandie for putting up with me and making life so wonderful.

My thanks to all the members of the Buechner lab, past and present, for their help, especially Elinor Brown and Derek Setter. Thank you to the Lundquist, Timmons, Ackley, and Neufeld labs for strains, reagents, conversations, criticisms, and use of their lab equipment. Thank you to Dr. Edina Harsay for helpful conversations about my work. Thank you to all my committee members, Drs. Bob Cohen, Erik Lundquist, Kristi Neufeld, Kathy Suprenant, and Craig Martin for their generous help and support. Thanks to the *Caenorhabditis* Genetics Center for strains. Many thanks to the Grant lab for providing the subcellular markers, K. Matsumoto for the *exc-5::gfp* construct, the White lab for the *GBD::wsp-1* cDNA, and T. Oka and M. Futai for the pCV01 plasmid.

Thank you to the University of Kansas for providing a wonderful environment to do research and for financial support. Thank you to other funding sources including the NIH and NSF. Thank you to all the students I have taught at KU, I enjoyed helping you learn and learning from you.

Last, but not least, thank you to the millions of worms that unwittingly, reluctantly, forcibly, or unavoidably gave their lives for science.

Table of Contents

To my family and friends who have selflessly provided their love, support, and kindness to me over the years. Thank you.

Chapter 1: Introduction

Forward/Scope of Research

The nature of life is complex and messy. It is truly remarkable that life exists and a challenge to be able to understand it. While day-to-day experimentation may temporarily subvert the naïve wonder that I felt as an adolescent and the general curiosity about how life exists and how things work, those feelings have never truly gone away. I would like to take just a moment to address you and ask that you take a moment to reflect upon the beauty, wonder, and complexity of the natural world.

The natural world is a big place, planet-sized for some, universal to others. The diversity and scope of trying to study all of it is staggering, yet our species has undertaken the role. Although there seems to be an infinite number of aspects to studying life on this planet, the most appealing to me has always been those processes that occur at a genetic and cellular level. It is from a seemingly simple combination of a few nucleic acids that life arose and formed cells. Those cells, under directions from the nucleic acids contained within, have become the fundamental unit of life on this planet.

The scope of my research has focused on examining how cells are able to form and maintain tubes. This process is essential in order for large multicellular organisms to exist. (As a large multicellular organism with many complex tubular organ systems, I can attest to this life-dependent importance.) Without transportation systems to allow all cells to obtain the nutrients they need and get rid of waste products, life would remain a strictly microscopic pursuit. In this dissertation I examine one model of tube formation and maintenance, the *Caenorhabditis elegans* excretory canal cell and the gene *exc-5*.

Tubular Structures

Cellular tubes are formed by polarized epithelial tissue. While skin may be the first thing that springs to mind at the mention of epithelial tissue, epithelia do more than just separate, contain, or protect other tissues from their surroundings. A working definition of epithelia might be any cells or tissues that are designed to interface with the outside environment. The function of epithelium is diverse and includes *sensation*, *diffusion*, *secretion*, *adsorption*, and *excretion*. In order for many epithelia to perform these latter tasks, the epithelial cells that make up the tissue must work together to form tubular structures.

The ways in which cells form tubes varies and much is already known about the underlying morphological processes. There are five mechanisms by which tubes can form: wrapping, budding, cavitation, cord hollowing, and cell hollowing [1]. Different tubes use different mechanisms to form and those mechanisms are correlated to their size. The largest tubes are generally made by wrapping, cavitation, or cord hollowing. Smaller tubes, some consisting of only a single cell, use budding and cell hollowing. While the way in which these cells form tubes may differ, there is an underlying biology that they all share.

As polarized cells, epithelia have an apical and a basal or basolateral surface (Fig. 1.1). In a single-celled layer, these cells are firmly attached to each other through tight junctions and adherens junctions that mark the boundary between the apical and basal/basolateral surfaces. Beside their mechanical role to bind the two interfacing cells together through claudin and occludins for tight junctions or cadherins and catenins for linking actin together in adherens junctions, these junctions have also been shown to be an important site of polarization. Tight junctions in particular are associated with the PAR proteins, PTEN, and CDC42 in order to maintain the boundary between the apical and basolateral surfaces [2,3]. The basolateral surface of a cell contacts its neighboring epithelial cell and each one is anchored at the basal surface to a basement membrane through integrins. All of this remains true when these cells form a tubular shape. In a tubular structure, the apical surfaces of the cells form a continuous surface that creates an enclosed space called a lumen where fluids are free to flow past the cells. The basal surface of the cells similarly forms a continuous outer surface that is anchored to and surrounded by a basement membrane (Fig. 1.1B).

Not all of the underlying cellular mechanisms by which these cells form a tube are entirely clear, but much is known about the processes involved. Perhaps most important to lumen formation is cell polarization. It is clear that CDC42, PAR proteins, aPKC, and PTEN function together to alter the phospholipid composition of the apical and basolateral surfaces, enriching the apical membrane with PIP_2 [3,4], while PIP_3 is enriched in basal and basolateral membranes [5]. The segregation of these phosphoinositides is fundamental to apical and basal membrane identities and is closely linked to intracellular transport and proper protein and vesicle targeting through the interactions between these phosphoinositides, the Rho-family of GTPases (especially CDC42), and the PAR complexes [2,4].

Morphogenic processes are perhaps the second most important part of tube formation. The cellular movements and cell shape changes that cells must undergo in order to organize themselves into a functional tube require rearrangements of cells' cytoskeletons, the extracellular matrix, and a luminal matrix [6-9].

Figure 1.1 -- Polarized Epithelia Form Tubes

(A) A diagram illustrating a single-celled layer of polarized mammalian epithelial cells. Apical surfaces are lined in red while basal and basolateral surfaces are lined in blue.

(B) A diagram illustrating a cross-section of a mammalian multicellular epithelial tube.
(C) A diagram illustrating a cross section of the unicellular *C. elegans* excretory canal cell.
(D) A 3D representation of the excretory canal cell. The arrow indicates movement of fluid through the lumen of the canal.

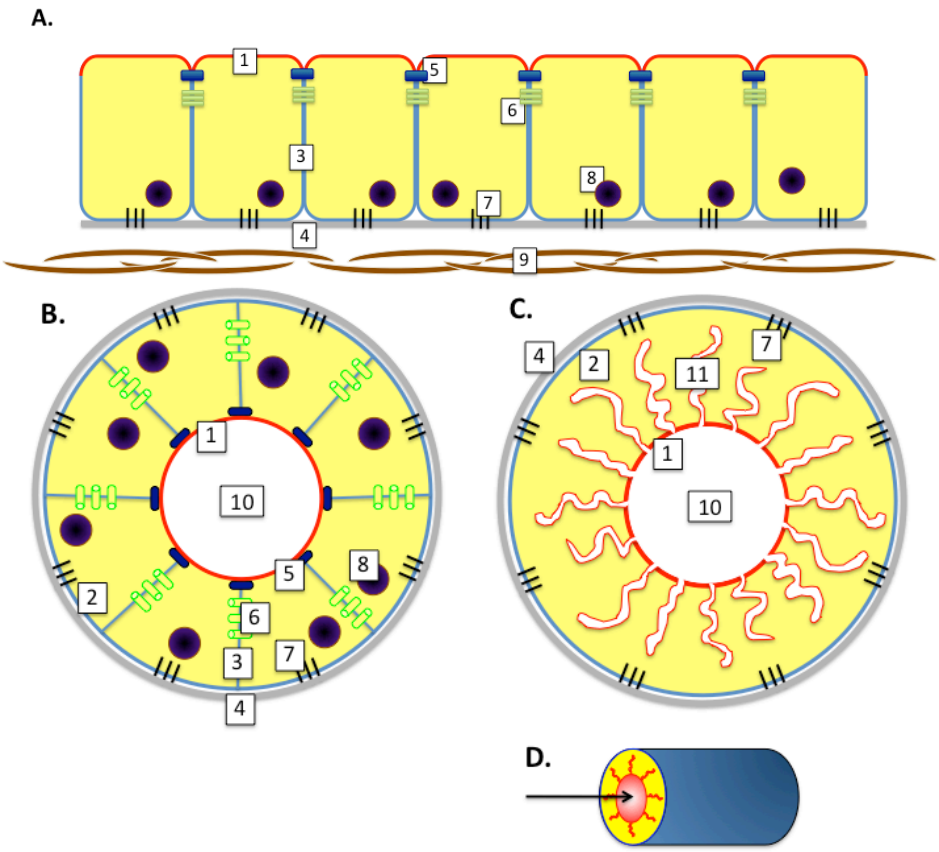

1. The apical surface of a polarized epithelial cell contacts the external environment and is enriched in phosphatidylinositol 4,5-bisphosphate (PIP_2).
2. The basal surface of a polarized epithelial cell contacts the basement membrane and is enriched in phosphatidylinositol 3,4,5 triphosphate (PIP_3).
3. Basolateral surface of an epithelial cell contacts neighboring epithelial cells and the basement membrane. It is enriched in phosphatidylinositol 3,4,5 triphosphate (PIP_3).
4. The basement membrane is a thin layer of fibrous proteins that help anchor the epithelium to the underlying tissue.
5. Tight junctions physically anchor two cells together using claudin and occludins in vertebrates. Tight junctions also serve as centers for polarization through their association with PAR proteins, PTEN, and CDC-42 [2,3] and enrichment of the apical membrane with PIP_2. These junctions form the boundary between the apical and basolateral surface of the cell.
6. Adherens junctions physically anchor cells together using cadherins and catenins and link to the actin cytoskeleton. These junctions are typically basal to tight junctions in vertebrates and may recruit PI3K to enrich PIP_3 on the basolateral surface [3].
7. Integrins anchor the basal surface of epithelial cells to the basement membrane.
8. Cell Nucleus.
9. Extracellular Matrix (ECM).
10. Lumen of the tubule where fluid flows through the organ.
11. Canaliculi are small tubular invaginations that connect to the lumen and extend into the cytoplasm of the canal cell.

While the initial formation of tubes from the cellular milieu is fascinating, it represents only a small portion of the biology of these structures. The majority of the lifetime of these tubular systems is spent carrying out their biological function - transporting fluids. How do these tubes maintain their shape while under constant pressure? How do they stay in working condition in such a dynamic and often harsh environment? The cells that form these tubes are dynamic and maintain sensitivity to the fluids that flow through them [10-13]. These cells must also be able to regenerate themselves, remain flexible and robust while being bent and moved, and be able to repair damage when it occurs. Cells are able to do all of these things (and more!) through regulation and formation of cytoskeleton components, cell signaling, and intracellular transport.

Polarized Membrane Trafficking

Cells are able to move membrane proteins, add or subtract membrane surface, and interact with their environment through the exchange of materials by means of membrane trafficking. The recycling and targeting of materials occurs through vesicular movement to and from many different membrane compartments or the plasma membrane via actin formation and microtubule transport. These compartments are primarily sub-regions and components of a large and dynamic tubulo-vesicular network whose parts are identified more by the proteins they contain than their gross morphology [14,15].

This complex system of membranous compartments allows material to be taken into the cell at the plasma membrane through endocytosis and sent to specific destinations in the cell through sorting. During sorting, material may be sent back to the plasma membrane and recycled while other cargo may be broken down and metabolized in lysosomes. Sorting also directs material that has been synthesized within the cell to be incorporated into the proper membrane or to be secreted by transport to the plasma membrane and exocytosis.

These processes become more complicated in polarized epithelial cells. As mentioned previously, polarized cells have an apical and a basal surface that differ in composition, have different functions, and require different components to be delivered to each surface. The organization of the organelles and the control of the progression from one compartment to the next are largely directed by RABs, small G-proteins of the Ras superfamily [16]. The cytoskeleton (actin, microtubules, and associated motors) as well as the Rho and Rac GTPases also play distinct roles in the movement and progression of material through the trafficking pathways [17-19]. A general model of polarized membrane trafficking is provided in Figure 1.2, and summarized below.

Material is endocytosed from the plasma membrane at either the apical or basolateral surface. This process can be clathrin-dependent or clathrin-independent. In clathrin-dependent endocytosis (CDE), the clathrin coat forms around the plasma

Figure 1.2 -- A General Model of Polarized Intracellular Transport

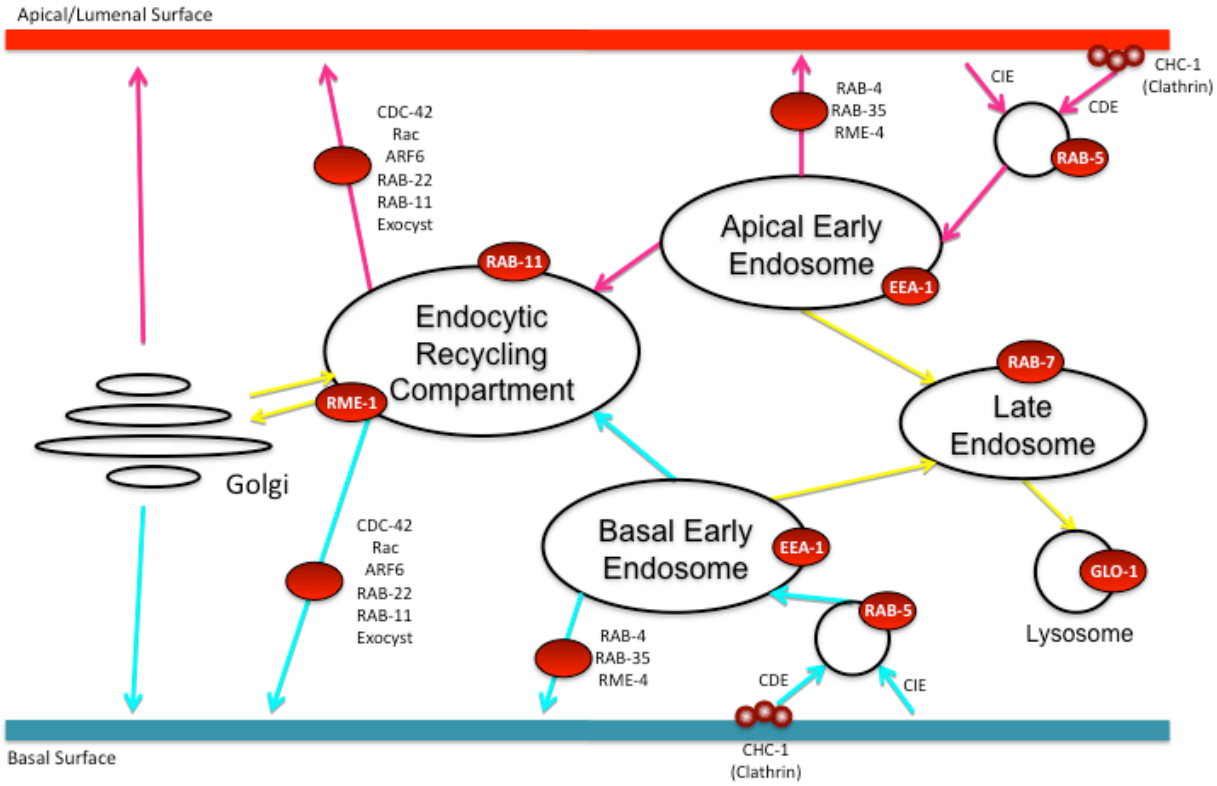

Endocytosis occurs through either clathrin-dependent endocytosis (CDE) or clathrin-independent endocytosis (CIE). Early endocytic vesicles are enriched in RAB-5 and fuse together to form early endosomes through the aid of EEA-1. Material from either the basal or apical early endosomes can mature into late endosomes and eventually be degraded in the lysosome. Alternatively, material can either be 'rapidly recycled' to the plasma membrane through RAB-4, RAB-35 (RME-5), and RME-4; or 'slow-recycled' to the endocytic recycling compartment (ERC) through RAB-11. Material in the ERC can then be sorted back to the plasma membrane or to the Golgi via several routes, each using different proteins. CDC-42, RAB-11, RME-1, and the exocyst are involved in the transport of material from the ERC to the plasma membrane.

membrane and helps create a membrane invagination. This invagination is then severed from the membrane in order to produce an endocytic vesicle, also known as a primary vesicle. The endocytic vesicle loses this clathrin coat as it is transported to a membranous organellar compartment termed the early endosome.

Clathrin-independent endocytosis (CIE) can be achieved through several different pathways. One method involves a caveolin coat and dynamin to make a vesicle from the plasma membrane. Another involves CDC42, ARF1, and actin in a dynamin-independent process. Yet another clathrin- and dynamin-independent process uses the ARF6 GTPase. Interestingly, cargo of ARF6-associated endocytosis has been shown to include β_H-spectrin and cell-extracellular matrix-interacting proteins. Regardless of the method of internalization, clathrin-independent endocytosis results in endocytic vesicles that are then transported to the early endosome [15].

The early endosome is defined as the membrane compartment that receives material from primary vesicles derived from both clathrin-dependent and clathrin-independent endocytosis and is first characterized by the presence of RAB-5. RAB-5 is a small GTPase that binds to the PI3P present on early endocytic membranes and is necessary for the fusion of endocytic vesicles together to form the early endosome [16]. In order for this fusion to occur, RAB-5 binds to EEA-1 (early endosomal antigen 1, which itself contains a PI3P binding FYVE domain and is recruited to endocytic membranes) along with other adaptor proteins to form a fusion complex [20,21]. It is thought that EEA-1 provides a tether to connect RAB-5 proteins on other vesicles in order to facilitate their fusion into the early endosome.

The early endosome serves as the first cargo-sorting organelle and is a tubular-vesicular network. In polarized cells, there exists both a basolateral early endosome and an apical early endosome [22]. Material in the early endosomes has three general ways of being sorted [23].

The default pathway for material that has not been selected to exit the early endosome for recycling is degradation. As the early endosome (also termed the sorting endosome) matures, it turns into a more acidic and spherical compartment termed the late endosome [23] and is characterized by the presence of RAB-7 [24]. RAB-7 has several functions and is essential in several trafficking events including the movement of late endosomal material into multi-vesicular bodies and lysosomes [25,26] where the cargo will be degraded and metabolized. Interestingly, RAB-7 has been shown to directly interact with Rac [27] and when over-active, RAB-7 has been shown to cause Charcot-Marie-Tooth disease type 2B (CMT2B) [28].

The second method of early endosome exit is sometimes termed 'rapid recycling'. Rapid recycling occurs when material is directly taken from the early endosome and replaced on the plasma membrane from whence it came. Although the precise function of rapid recycling is unclear, RAB-4, RAB-35 (RME-5), and RME-4, all seem to be necessary for the process [15].

The third method of early endosome sorting is sometimes termed 'slow recycling'. For apical early endosomes, this involves moving material into a compartment called the apical

recycling endosome (ARE) [22] or the endocytic recycling compartment (ERC) [15], or the recycling endosome. Material in the ERC can then be sorted back to the plasma membrane [15,22]. It should be noted that there is debate as to whether the ARE is a distinct compartment separate from the CRE, or whether they are both subdomains of a larger recycling complex [29,30].

Both the ERC and recycling endosomes are enriched for RAB-11. Slow-recycling material from the basal early endosomes also moves into the recycling endosome, joining with slow recycling material from the apical surface [22]. It is in this compartment that the apical and basal endocytic transport routes converge and allow material from either of the polarized surfaces to be recycled back to the plasma membrane or to another membrane compartment. In *C. elegans*, movement from the recycling endosome to the plasma surface or back to the Golgi requires RME-1/EHD1 [31,32]. Although the specific proteins required for any particular cargo to be sorted out of the recycling endosome and into sub-domains of the plasma membrane will vary, CDC-42, Rac, ARF6, RAB-22, RAB-11, and members of the exocyst complex are involved in the process [15,33,34].

The Rho Family of GTPases

The Rho family of GTPases (Rho-GTPases) is a sub-family of the Ras superfamily of small GTPases. Like all small GTPases, these Rho family members are activated when bound to GTP (Fig. 1.3). As their name implies, they have a GTPase activity that will eventually cleave the terminal phosphate of their GTP-bound substrate, turning it into GDP and thereby inactivating the small GTPase. There are three proteins associated with the activation and inactivation of GTPases: Guanine nucleotide exchange factors (GEFs) help activate these proteins by facilitating the release of the inactive GDP-bound molecule, and the binding of an activating GTP molecule; GTPase -activating proteins (GAPs) stimulate the GTPase activity inherent in the GTPase, causing inactivation of the protein as it cleaves GTP into GDP; Guanine nucleotide dissociation inhibitors (GDIs) slow the release of the inactive GDP molecule from the GTPases, causing the GTPase to remain in its inactive form for longer periods.

The most-studied members of the Rho-GTPases include Rho, Rac, and CDC-42. All three proteins are well known for their involvement with modulating the actin cytoskeleton. They are involved in a vast array or cellular processes, most of which require movement or changes in cell shape. These include cell migration, cell death, cell polarization, and tubulogenesis.

Figure 1.3 – Activation of RhoGTPases

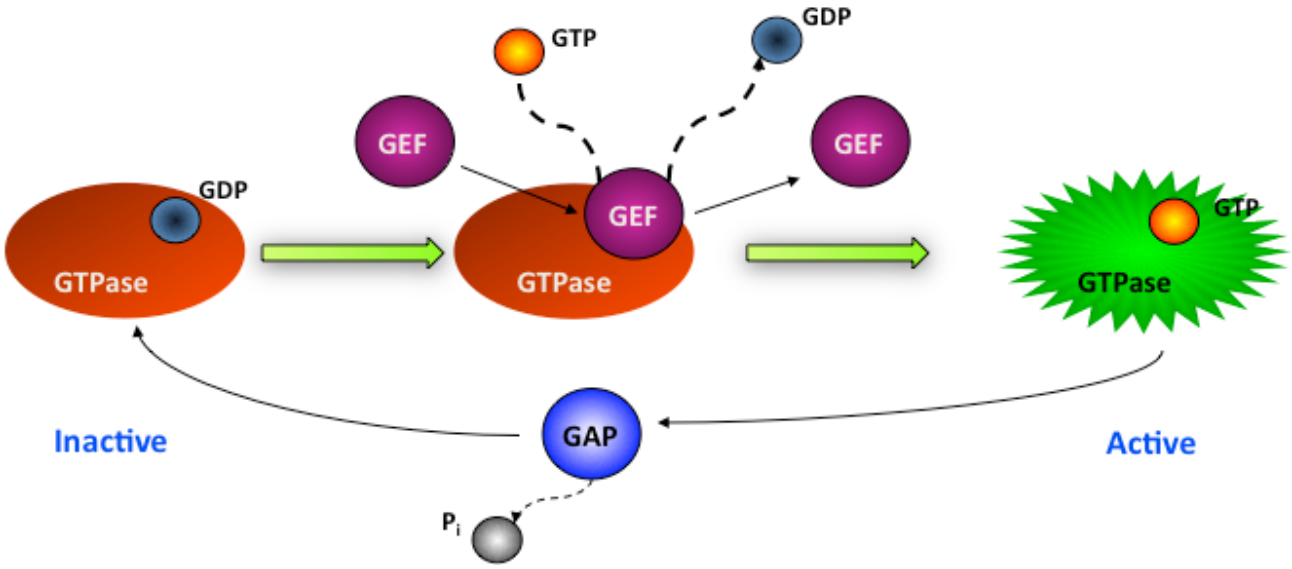

RhoGTPases are activated when bound to GTP. Guanine nucleotide exchange factors (GEFs) bind to the inactivated GTPase and facilitate the release of GDP and the binding of GTP in order to activate the protein. Activated GTPases will eventually inactivate themselves through their own GTPase activity by removing the terminal phosphate on GTP and turning it into GDP. GTPase activating proteins (GAPs) can catalyze this activity and enhance the inactivation of the GTPase.

Rho-GTPases have also been shown to be involved in intracellular trafficking. CDC-42 in particular is well known for its role in the polarization of cells [35] and its involvement in membrane trafficking [36]. CDC-42 has recently emerged as a link between cell polarization, which is essential in lumen formation, and intracellular transport [34,37]. CDC-42 activity is required for vesicle trafficking in polarized cells. When CDC-42 activity is altered or reduced, sorting and recycling to the apical and basolateral surfaces is disrupted [38] and sometimes causes mis-targeting of basolateral cargo to the apical surface [39,40]. In addition, endocytosis is also disrupted in *cdc-42* mutants. Endocytosis from either the apical or the basal surface (or both) is impaired and can cause apical membrane proteins to accumulate in sorting endosomes [41]. CDC-42 has also been shown to interact with the exocyst in regulating vesicle trafficking [42].

The specifics of how CDC-42 and the other Rho GTPases influence trafficking are not well known. Considering the functions of these proteins, it is likely that the effects are mediated through modification or rearrangement of the actin cytoskeleton.

Your friend: *Caenorhabditis elegans*

The small, free-living, temperate soil nematode *Caenorhabditis elegans* can be found ubiquitously on earth. As an adult, it can grow to approximately 1mm long. While relatively simple, *C. elegans* contains most of the major tissue types found in much larger organisms. These tiny animals have a host of inherent properties that make them excellent organisms to use to study genetics as well as developmental and cellular biology [43].

The nematodes are hermaphroditic, which allows the maintenance of genetic backgrounds without the need for mating. Male animals do exist, and arise spontaneously at a very low frequency. Using males, it is also possible to set up genetic crosses to introduce and combine different genes or mutations as well as any transgenic integrated constructs.

C. elegans matures rapidly and is prolific. From the time it is laid as an egg, until the time it lays its own eggs is a little over 2 days (approximately 50 hours at 25°). Each hermaphrodite is capable of laying 300-400 eggs [44]. In a relatively short amount of time, you can alter the genotypes of the animals and have a large population of animals for phenotypic analysis.

The lifecycle of *C. elegans* consists of 6 stages [44]. The animals begin life as eggs inside of their mother and are generally laid within 2-4 hours of fertilization (growth times are given at 25°). After 8 hours of embryonic development, the animal hatches from the egg in its first larval stage, termed L1. Twelve hours later, the animal goes through another molting process and emerges in its second larval stage, L2. After seven hours, the L2 animals molt, and emerge in their third larval stage, L3. After another seven hours, the L3 animals molt and emerge in their fourth larval stage, L4.

Figure 1.4 – *Caenorhabditis elegans*

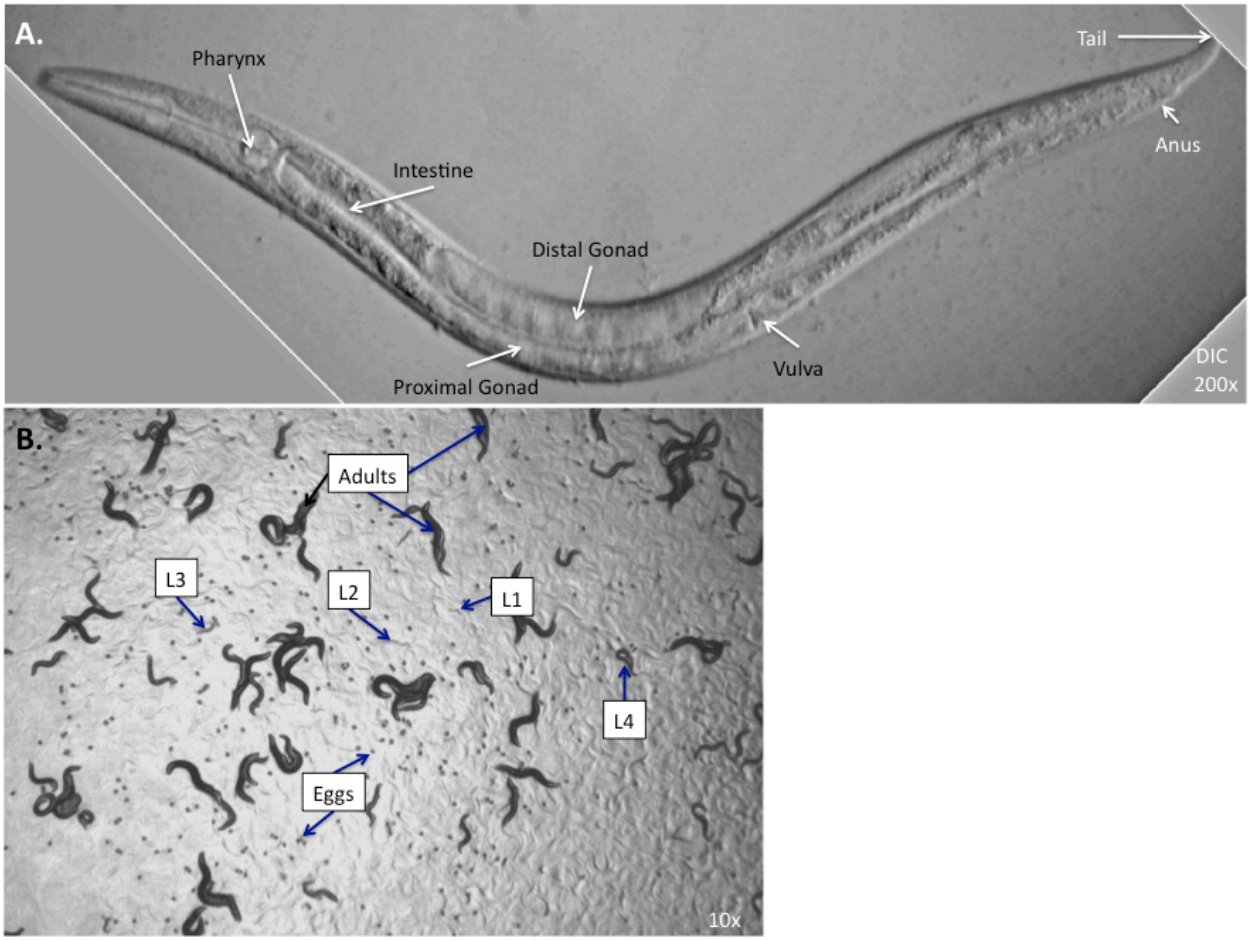

(A) A DIC micrograph of a live L4 animal at 200x magnification. As adults these animals reach about 1mm in length. Their transparency makes it easy to identify cells and organs within the animal. Most of the body cavity is filled with the intestine and gonad. The anterior of the animal is to the left; the posterior of the animal is to the right; dorsal is up and ventral is down.
(B) A micrograph taken of animals growing on an NGM plate with a lawn of *E. coli* BK16. *C. elegans* has six primary life stages: egg, L1, L2, L3, L4, and adult.

During the L4 stage, the animal reaches the end of gonadogenesis and spermatogenesis. Nine hours after becoming an L4, the animal undergoes its final molt into an adult and begins to lay eggs. In our work, we have largely focused on L4 and young adult animals. Older adults begin to accumulate eggs that fill the body cavity and disrupt the morphology of many of the organs in the animal, often causing breakdown of the affected tissues. Animals younger than the L4 stage are quite small and underdeveloped, which makes the canal cell difficult to see. Due to the large number of animals, as well as their ability to survive adverse conditions, it is possible to freeze the animals and store them in liquid nitrogen or low-temperature freezers (-80°C) for years. This greatly reduces the amount of work required to maintain genetic strains and facilitates storage of a huge library of different mutations and transgenic animals.

In addition to the already mentioned aspects of *C. elegans* biology, the nematodes are transparent. This property allows for easy observation of whole, living animals under the microscope (Fig. 1.4A). Every cell of the animal is observable at any time point in development. Because of this, and one more unique property – the invariant cell lineage of the somatic tissues of the animal, the cell lineage for every one of the 959 cells (1031 in the male) has been mapped out [45]. This eutelic nature provides a powerful tool to look at the development of the animal as well as the cellular biology underlying it.

C. elegans Excretory Canal Cell

Of all the cells in *C. elegans*, one stands out as particularly useful for examining tubule formation and maintenance, the excretory canal cell. The excretory canal cell is a large and highly organized unicellular tubule. It has a single basal surface, and a circular apical surface that forms the lumen of the tube (Fig. 1.1C). Invaginations that form from the luminal surface and extend into the cytoplasm of the canal cell are called canaliculi. These form even smaller tubulo-vesicular structures. The excretory canal cell provides both a sensitive and relatively simple single-celled model of the mechanisms required for tubule formation and maintenance.

The excretory canal cell is only part of the excretory system of *C. elegans*, though it is the largest. The entire excretory system is composed of the canal cell, two fused gland cells, and a duct cell that connects the canal cell to the pore cell. The pore cell connects the excretory duct to the outside environment (Fig. 1.5). The excretory system serves as an osmoregulatory organ and is vital to the survival of the animals. Laser ablation of the canal cell leads to death within a few hours [46].

Figure 1.5 – The Excretory System of *C. elegans*

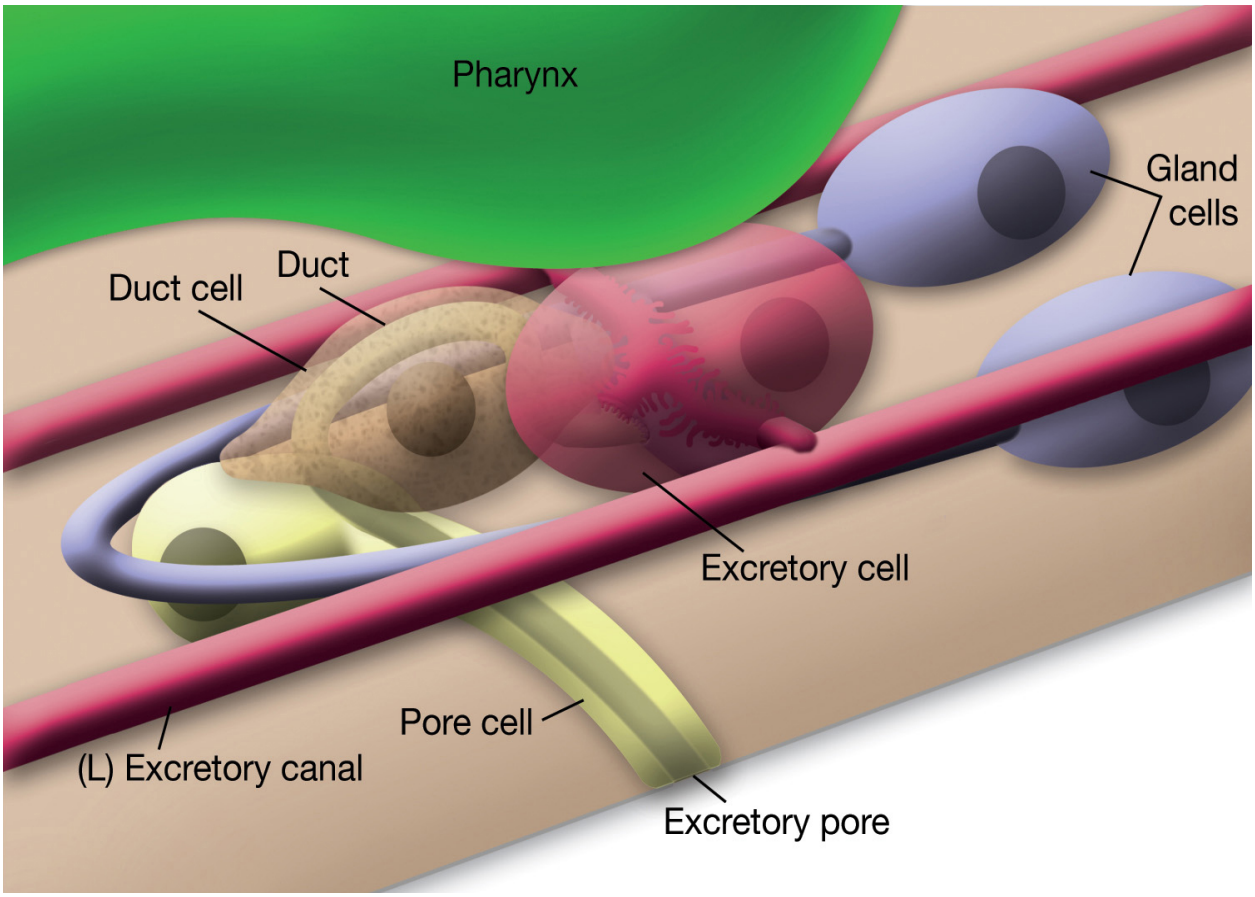

The excretory system functions as the osmoregulatory organ of *C. elegans* and is essential for its survival. The cells that make up the excretory system are primarily located ventrally to the terminal bulb of the pharynx (*green*). The excretory canal cell (*red*) collects fluid from the body of the animal and connects to the duct cell (*speckled brown*). The duct cell creates a passage between the excretory canal cell and the pore cell (*yellow*). The pore cell then empties into the outside environment. The excretory gland cells (*blue*) are connected to the duct and pore and secrete materials into the lumen. Image reprinted with permission from WormAtlas [47].

The canal cell originates at the end of gastrulation as a spherical non-polarized cell ventral to the posterior bulb of the developing pharynx. As the cell grows, it starts to extend two processes dorsolaterally, one to the left of the animal and one to the right (Fig. 1.6). At the same time as the cell is growing out, vacuoles accumulate and fuse to form a large hollow structure within the cell. This structure then becomes apically polarized and begins to form a luminal structure within the cell that extends with the growing processes. Once the left and right processes reach the midline of the animal, they bifurcate to the anterior and posterior of the animal. When the animal hatches, the canal cell has only extended halfway along the posterior length of the animal. The cell continues to grow rapidly through the L1 stage until it reaches the posterior end of the animal. Since the canal cell maintains its length relative to the animal, the canal cell must continue to grow in proportion with the animal through the larval stages and into adulthood.

Excretory cell growth results in a large "H"-shaped structure that is composed of one cell and a continuous lumen. The nucleus remains at the cell body, largely unmoved from its place of origin. Morphologically, there are two long canals on either side of the animal that extend from the head of the animal to the anus (Fig. 1.7). These are connected through the cell body of the canal cell and then fused to the duct cell, where the collected contents of the canals can be emptied through the pore cell and into the environment.

Figure 1.6 – Development of the Excretory Canal Cell

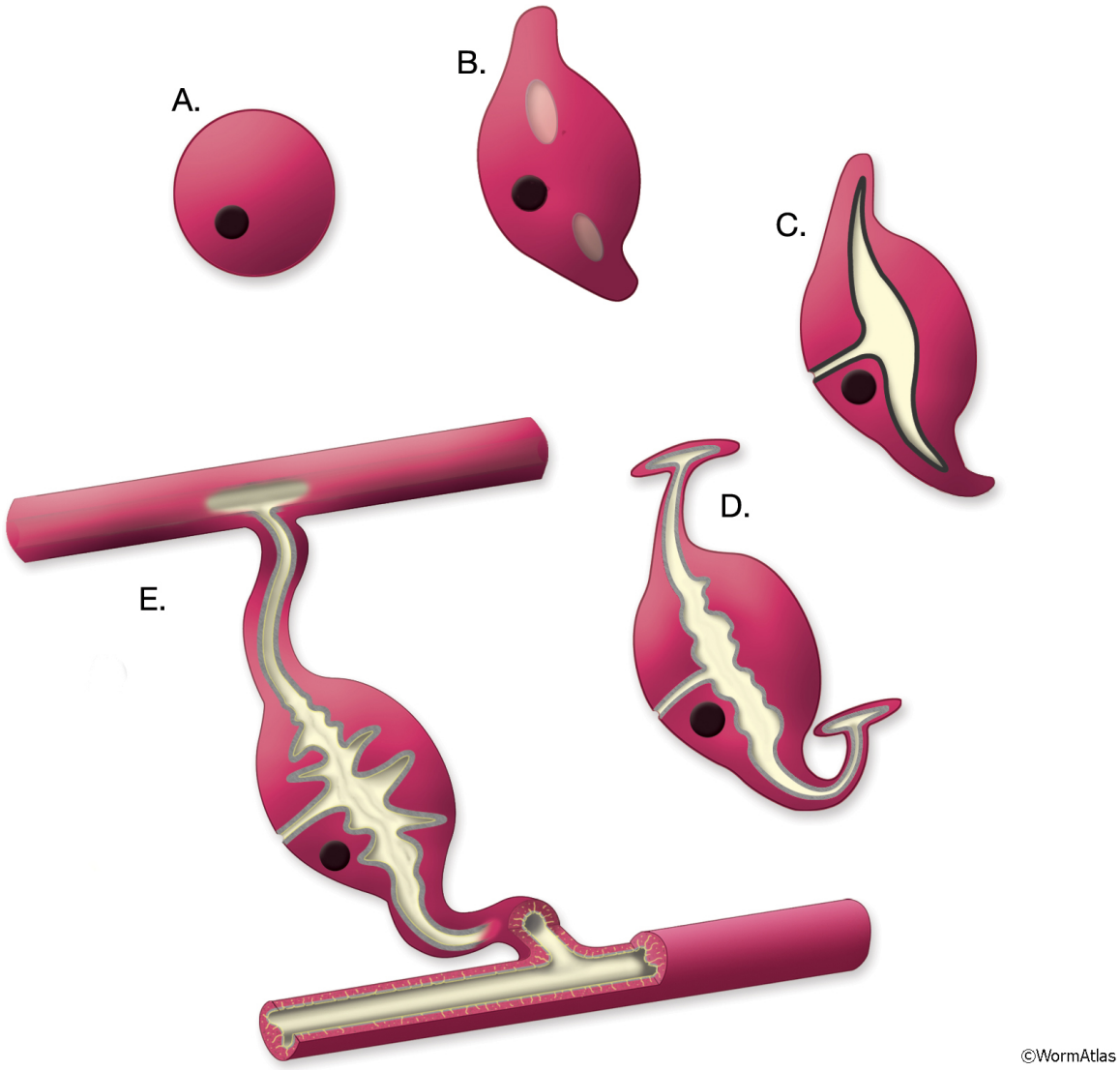

(A) The excretory canal cell originates as a spherical non-polarized cell at the end of gastrulation. **(B)** As the cell grows, it extends two processes dorsolaterally. During this time the cell also accumulates vacuoles that fuse together to form large hollow structures within the cell. **(C)** The hollow structures fuse and become apically polarized. The compartment begins to take on a luminal structure and extends with the growing processes on either side of the canal. **(D)** When the growing processes reach the midline of the animal, they bifurcate and extend both anteriorly and posteriorly. **(E)** These processes continue to grow and extend to the head and tail of the animal and form two long canals on both the left and right side that are connected through the excretory canal cell body. Image reprinted from WormAtlas.org with permission [47].

Figure 1.7 – The *C. elegans* Excretory Canal Cell

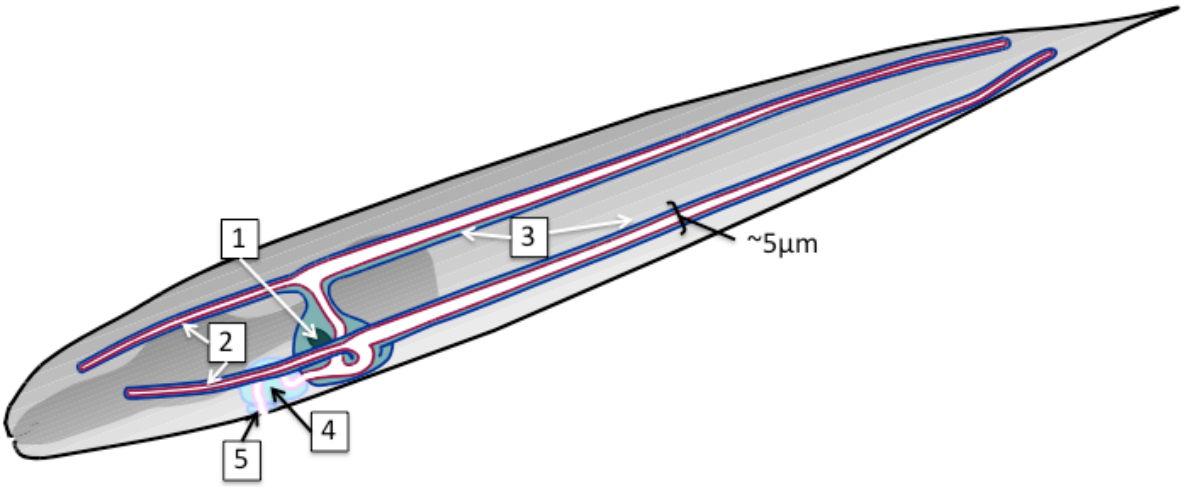

The excretory canal cell forms a large "H"-shaped structure that is composed of one cell and a continuous lumen (*white*). The luminal/apical surface of the canal is in red. The basal surface of the canal is in blue. The cytoplasm of the canal cell is in light blue. The relative position of the pharynx is shaded in dark grey. Morphologically, there are two long canals on either side of the animal that extend from the head of the animal to the anus. These are connected through the cell body of the canal cell and then fused to the duct cell, where the collected contents of the canals can be emptied through the pore cell and into the environment. Adapted from Buechner 2002.

1. The nucleus of the excretory canal cell remains at the cell body, largely unmoved from its place of origin.
2. The anterior canals extend towards the mouth of the animal and are shorter and have a smaller diameter than the posterior canals.
3. The posterior canals extend towards the tail of the animal. Their diameter is largest near the cell body but gradually decreases towards the tail. On average, the approximate diameter of the canal is 5µm.
4. The canal duct cell connects the excretory canal cell to the pore cell.
5. The excretory pore cell opens to the environment and allows the contents of the excretory system to be released from the animal.

exc Mutations

In a wild-type animal, the diameter of the canals remains relatively constant. The anterior canals (anterior to the excretory canal cell body) are both shorter and have a narrower diameter than do the posterior canals (posterior to the excretory canal cell body). The posterior canals reach their largest diameter right at the excretory canal cell body then gradually taper in diameter as they reach the tail of the animal (Fig. 1.7).

In a collection of mutations, first identified in the Edward Hedgecock laboratory [48] and termed *exc* mutants (for excretory canal cell abnormal), this consistent canal cell morphology is disrupted. While the severity and specific phenotype of these mutations vary, they all share the common characteristic of disrupting the continuous lumen diameter of the canal and forming enlarged, fluid-filled cysts.

Many of the *exc* genes have been cloned and their encoded proteins characterized. EXC-4 is a chloride channel [49], EXC-7 is an RNA transport protein [50] and EXC-9 is a LIM-domain-containing CRIP homologue [51]. Recent work by Kelly Grussendorf has indicated that EXC-1 is homologous to a mammalian class of interferon-inducible GTPases of the Ras family. Other genes producing an Exc phenotype include *sma-1*, a β_H-spectrin [52], *let-653*, a secreted mucin [53], *let-4* [48], *lpr-1*, a lipocalin that causes defects in the duct cell [54], and *erm*-1, an ezrin, radixin, moesin homologue [55].

By identifying and characterizing the mutations that disrupt the morphology and maintenance of the canal, we can gain a better understanding of the mechanisms involved in the processes of normal tubule formation and maintenance.

EXC-5: Past and Present

Exc-5 encodes a guanine nucleotide exchange factor (GEF) for CDC-42 [56,57]. Although EXC-5 has previously been identified as the homologue of FGD1, more members of the FGD family have been discovered. Through studies based on homology, we have identified EXC-5 as sharing similarities with the entire mammalian FGD family (Fig. 1.8). This family is named for the human disease associated with mutations in FGD1, FacioGenital Dysplasia [58]. In this disease, also known as Aarskog-Scott syndrome, there are mild morphological defects of the face (widely spaced eyes, anteverted nostrils, broad upper lip) and scrotum. Mutations in another member of this family, FGD4, cause the human muscular dystrophy Charcot-Marie-Tooth disease type 4H (CMT4H) [59]. CMT4H is a progressive demyelinating neuropathy that leads to pain as well as loss of movement and sensation in the distal limbs [60].

Figure 1.8 – EXC-5 Belongs to the FGD Family of Proteins

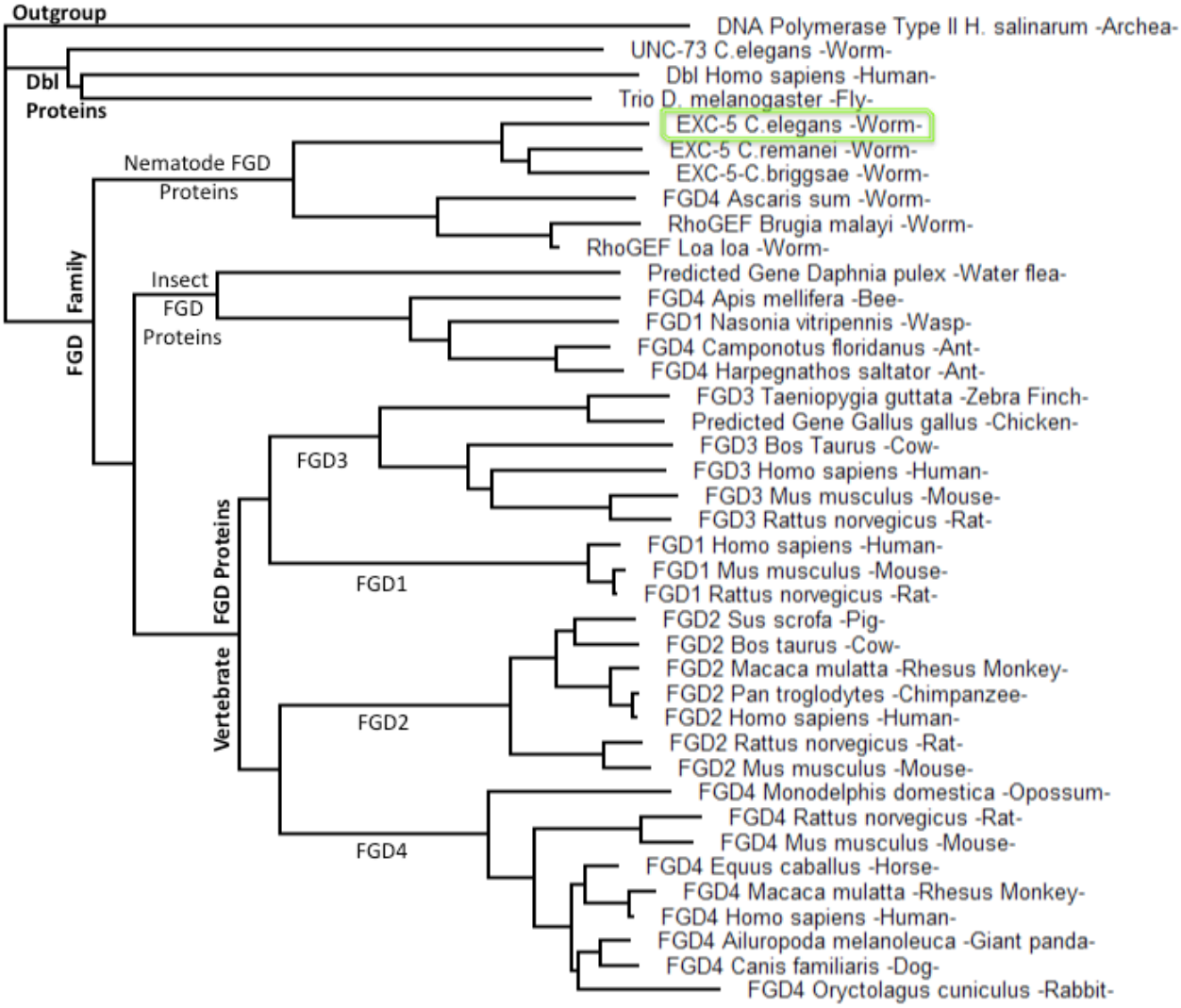

Although previously characterized as being the equivalent of FGD1 in humans, EXC-5 shares similarity to the entire family of FGD proteins. While nematodes and insects seem to have only one member of the family, vertebrates have several members including FGD1, FGD2, FGD3, and FGD4. These proteins have been implicated in several human diseases including Faciogenital Dysplasia and Charcot-Marie-Tooth disease type 4H. The FGD proteins are part of a larger family of Dbl guanine nucleotide exchange factors (GEFs). These GEFs contain a Dbl homology (DH) domain in tandem with a Pleckstrin homology (PH) domain. DNA polymerase Type II from *Halobacterium salinarium* was used as an outgroup. Sequences were aligned using ClustalW's PHYLIP algorithm. Distances between groups are proportional to their similarity.

EXC-5, like other FGD family members, is a member of the Dbl (diffuse B-cell lymphoma) family of GEFs. It contains a Dbl Homology domain (DH) in tandem with a Pleckstrin Homology domain (PH), common to the Dbl family of GEFs. The DH domain contains the GEF activity of these proteins as well as the Rho-GTPase binding site. Interestingly, some of these proteins may bind more than one GTPase but have GEF activity for only one specific GTPase [61]. Like the other members of the FGD family of proteins (which has had its official name changed to mean FYVE, RhoGEF, and PH domain-containing protein), EXC-5 also contains a FYVE domain, as well as a second PH domain (Fig. 1.9B). While the DH domain interacts with Rho-GTPases, the PH domains have been shown to interact with phosphatidylinositol 4,5-bisphosphate (PIP_2) [62], which is enriched on plasma membranes. The FYVE domain is a Zinc-finger domain that has been shown to associate with phosphatidylinositol 3-phosphate (PI3P) [63,64], a phospholipid that is enriched on endosomal membranes.

exc-5 is located on chromosome IV in *C. elegans*. There are two reported splice forms of the gene, a longer form consisting of 16 exons [57] and a shorter form that contains 15 exons [56] (Fig. 1.9). The shorter form excludes exon 14 and removes a small, slightly less conserved N-terminal portion of the second PH domain. *exc-5* cDNA we have isolated does not contain exon 14, and therefore we suggest that this shorter transcript is the more predominant form. This is in agreement with previous studies that reported the shorter isoform exists at about a 20-fold excess over the longer isoform [56]. It remains unclear what the functional difference is, if any, between these two transcripts. Regardless, I will refer to EXC-5 as containing 16 exons and being 844 amino acids long (and not 826 as the shorter isoform encodes) as this represents the most inclusive form of the gene. *exc-5* is expressed in the excretory canal and in several other tissues including the pharynx, rectal epithelial cells, and several head and tail neurons [57]. Although *exc-5* is expressed in other tissues, there does not appear to be any obvious defects in *exc-5* mutants in cells other than the excretory canal.

In *C. elegans*, loss-of-function mutations in *exc-5* cause large fluid-filled cysts to form approximately halfway through the animal (Fig. 1.10, Table 6.2) [48,57]. These cysts form early in development, shortly before or after hatching, and grow larger as the animal ages (Fig. 6.10). Generally, these cysts appear at the canal termini, but that does not preclude other cysts from forming at discrete points along the length of the canal. The lumen of the canal before and after these cysts retains its structure, which indicates that cyst formation occurs at discrete points along the canal. Previous electron microscopy work has shown that the apical structure surrounding the lumen has broken down at the places where these cysts have formed [57]. Our current model for the formation of these cysts is that there is a weak point in the apical cytoskeleton. Due to the osmotic stress that the canal cell is under, this weak point fails under osmotic pressure and causes the canal cell to lose its structural integrity. As the animal grows older, the osmotic pressure continues to enlarge and deform the canal to form the large fluid-filled cysts characteristic of the Exc-5 phenotype.

Figure 1.9 – Genetic and Protein Architecture of EXC-5

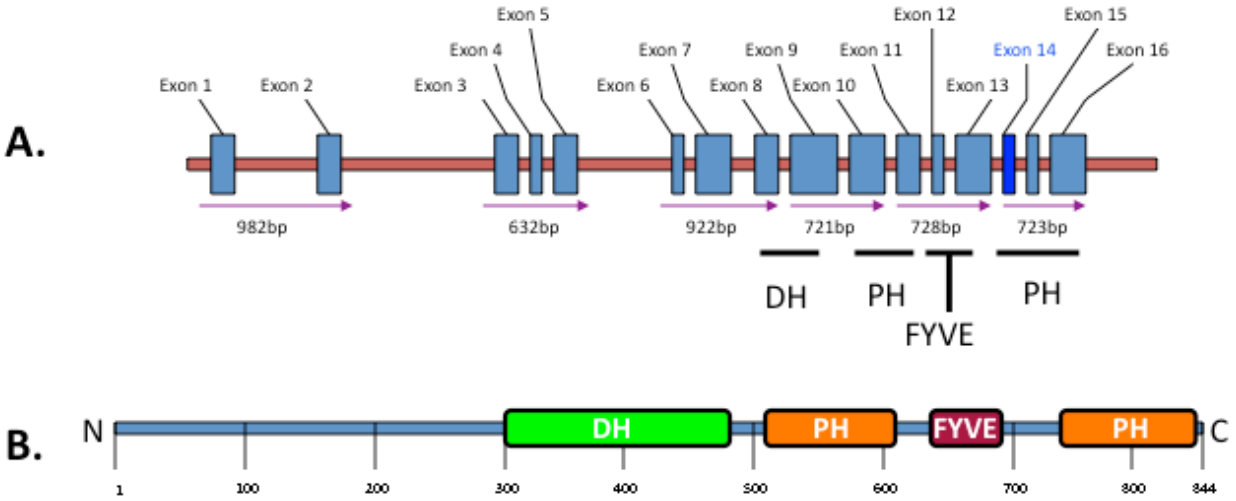

exc-5 is located on chromosome IV in *C. elegans* and is 5766bp long (2535bp of coding sequence). **(A)** *exc-5* has 16 exons (blue). Exons 8 and 9 contain the DH domain sequence; exons 10 and 11 contain the first PH domain sequence; exons 12 and 13 contain the FYVE domain sequence; exons 14,15, and 16 contain the second PH domain sequence. *exc-5* has a shorter isoform that does not include exon 14 (dark blue). This shorter isoform is 2481bp and does not include some sequence of the second PH domain. Purple arrows indicate the segments and their lengths that were used to amplify the coding region of *exc-5* for Chapter 2. **(B)** EXC-5 is 844 aa long (826 aa for the shorter isoform). The DH domain extends from amino acids 301-479, the first PH domain extends from 510-613, the FYVE domain 631-693, and the second PH domain 736-829.

Figure 1.10 – *exc-5* Mutants Develop Cysts or Convoluted Tubules

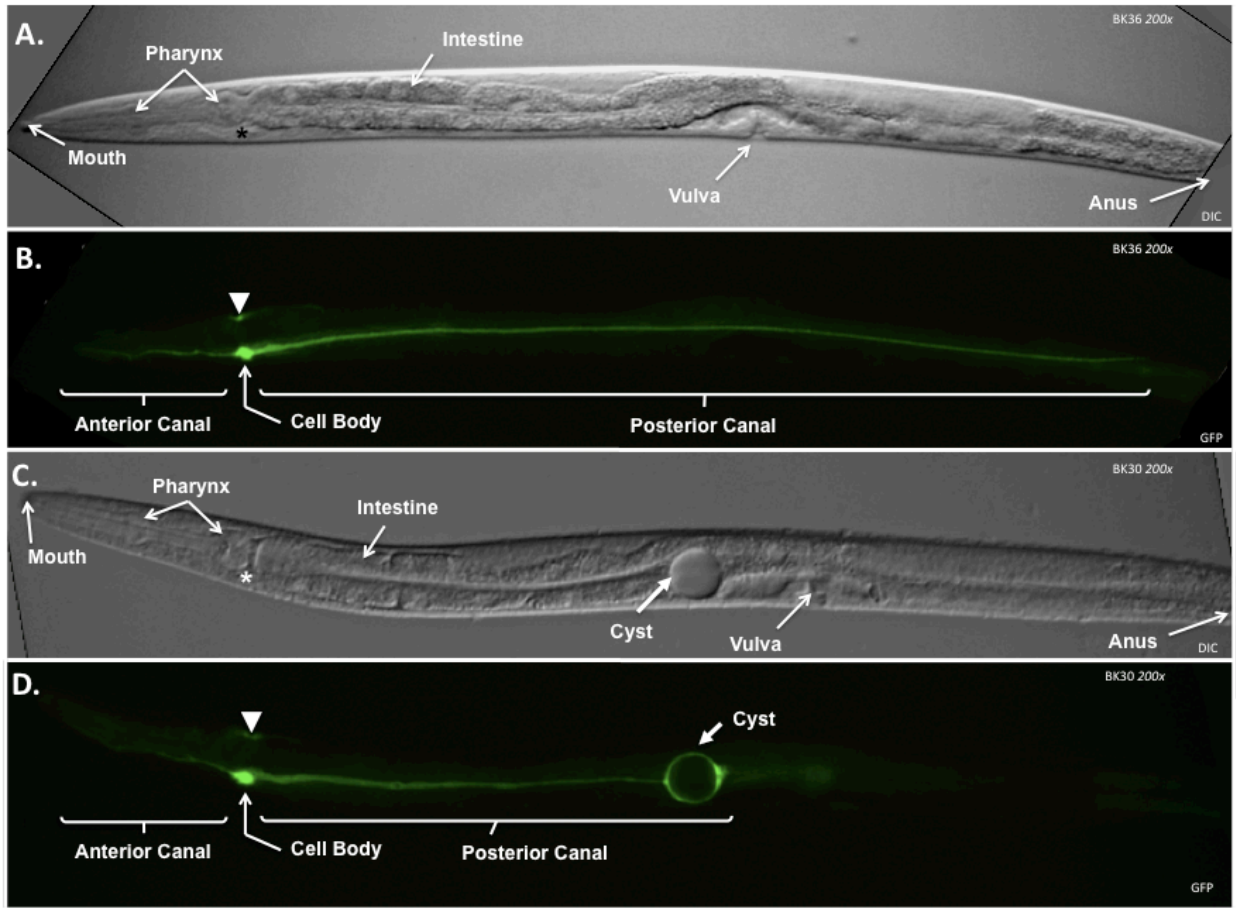

(A) A DIC micrograph of an L4 BK36 animal at 200x magnification. The pharynx is a muscular structure that contains two bulbous structures. The excretory canal cell body (asterisk) lies ventrally to the posterior bulb. No cysts are obvious along the length of the animal. **(B)** BK36 animals are phenotypically wild-type but contain an integrated transgene (*qpIs11*) that expresses a canal-specific GFP maker. This construct uses the promoter for *vha-1*, part of a vacuolar ATPase expressed only in the canal and the head mesodermal cell (arrowhead). The left canal is visible in the plane of focus. The anterior canals are thinner and shorter than the posterior canals and almost reach the buccal opening of the animal. The cell body is the brightest part of the excretory cell and contains the nucleus. The posterior canal's largest diameter is next to the cell body and gradually thins as it progress to the end of the canal near the anus of the worm. There are no cysts present and the diameter of the canal remains uniformly thin and continuous. **(C)** A DIC micrograph of an L4 BK30 animal at 200x magnification that is homozygous for the *exc-5* (*rh232*) null allele. A large cyst is visible in the center of the animal. **(D)** BK30 animals contain the *qpIs11* insertion in addition to the *rh232* allele. Typical for the *exc-5* null phenotype, the canal extends only halfway through the animal and ends with a large cyst.

Figure 1.10 E-F – EXC-5 Mutants Develop Cysts or Convoluted Tubules

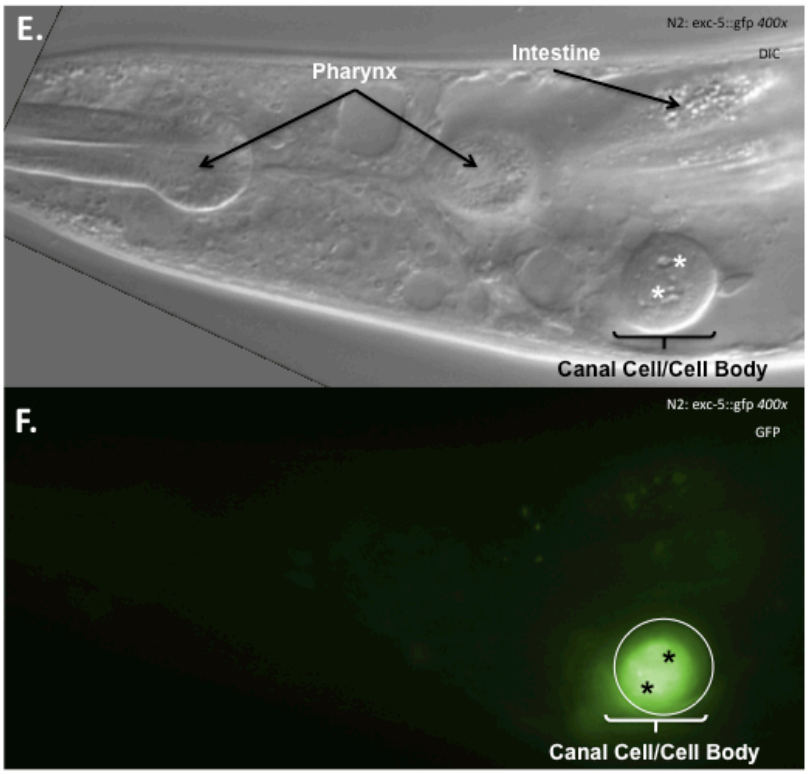

(E) A DIC micrograph of an adult animal overexpressing a genomic copy of *exc-5* linked to *gfp* at 400x magnification. The canal cell has not extended along the length of the animal. The lumen structure remains intact but is confined to a smaller space and coils within the cell body. The lumen passes in and out of the plane of focus, but cross sections of it appear as small holes (asterisks).
(F) EXC-5 is expressed in the entire canal cell but is most strongly associated with the luminal surface (asterisks). The white circle outlines the cell body.

Interestingly, this phenotype is similar to the defect seen in patients with CMT4H. In these individuals, the Schwann cells develop properly to wrap around the neurons and insulate them with a tubular myelin sheath. As the patients age, discrete points of failure occur along the insulating tubule in the Schwann cells and cause progressive degeneration of the nervous system [65].

In addition to the cystic phenotype seen in animals having no EXC-5 activity, there is also a phenotype associated with overexpression of EXC-5. In animals overexpressing EXC-5, the canal fails to extend along the length of the animal (Fig. 8). The canal cell becomes spherically shaped due to the apparent inability of the basal surface to adhere to the hypodermis and extend. The apical surface, however, appears unaffected except for the fact that is trapped within the confines of the un-extended basal surface and therefore becomes convoluted as it forms [51,57]. We have termed this phenotype a convoluted tubule phenotype. This phenotype is similar to those seen in mosaic animals that are mutant in basolateral proteins such as β-integrin and laminin [66,67].

Although *exc-5* has been cloned and its phenotype has been characterized previously, the underlying mechanisms that determine where and why cysts form in an *exc-5* mutant and why overexpression of EXC-5 causes a convoluted tubule phenotype remain unclear. In this dissertation, I present a series of experiments the aim of which is to examine how EXC-5 works within the *C. elegans* excretory canal cell in order to maintain its tubular shape. In Chapter Two, I describe my attempts to identify novel temperature-sensitive alleles of EXC-5 as a means of determining when during the excretory canal's growth EXC-5 activity is required. In Chapter Three, I describe the isolation of two genetic enhancers of EXC-5 activity as a means to determine what cellular pathways EXC-5 might be working in. In Chapter Four, I describe my attempts to create an excretory canal-specific RNAi strain as a tool to look at knockdown of gene function only in the excretory canal without disrupting other tissues. In Chapter Five, I describe the genetic interactions that EXC-5 has with some of the RhoGTPases as well as other EXC proteins. Next, in Chapter Six, I describe the disruption of trafficking within the excretory canal cell when EXC-5 activity is lost or gained. In Chapter Seven, I describe the construction of a conditional allele of EXC-9 and EXC-5 using inteins. In Chapter Eight, I describe the work that has been done to isolate antibodies specific to EXC-5. In the last chapter, Chapter Nine, I summarize the observations made from this work and present a new model for EXC-5 function within the excretory canal cell.

Chapter 2: Identification of Novel Temperature-Sensitive Alleles of EXC-5

Abstract

Previously isolated alleles of *exc-5* (*rh232*, *n2672*, *tm412*, *ok271*, and *rh275*) are all null mutations. In order to ascertain the developmental requirements of EXC-5 during the growth of the excretory canal cell, we devised an EMS non-complementation screen to identify new temperature-sensitive alleles of EXC-5. Through this screen we produced forty-three isolates. Two new alleles, *qp39* and *qp21*, have premature stop codons in the last PH domain of *exc-5* and have null phenotypes. Three isolates, *qp35*, *qp37*, and *qp56*, all had hypomorphic canal phenotypes but did not contain any mutations within the coding regions of *exc-5*. One isolate, *qp49*, did show temperature-sensitive effects but when sequenced still contained the original *rh232* deletion. This indicates that we have isolated an extragenic temperature-sensitive mutation in a suppressor of EXC-5. Although a temperature-sensitive allele of *exc-5* was not isolated, I discuss the insight these new strains have provided on our view of EXC-5 activity.

Rationale

"When during development is EXC-5 required?"

Only animals homozygous for the mutant *exc-5* allele *rh232*, and therefore lacking any EXC-5 activity since their conception, show a cystic phenotype. Is EXC-5 activity only required during the early larval stages (the point at which cysts initially form)? Is it required for the entire life of the animal, constantly providing an essential activity to maintain the canal shape? Is it possible to reduce or even reverse or repair the cysts in the canal by supplying EXC-5 activity after cysts have formed? To answer these questions we needed a conditional allele of *exc-5*, one that we could turn on and off during different times as the canal cell develops and grows. The most efficient type of allele for this purpose is a temperature-sensitive (TS) allele.

The *rh232* allele is a null allele consisting of a large EMS-induced deletion that removes the first twelve exons of *exc-5* as well as fourteen kilobases of upstream sequence. The other mutant alleles of *exc-5* available from the *Caenorhabditis* Genetics Center (*n2672*, *tm412*, *ok271*, and *rh275*) are similarly null mutations. We had to make our own TS allele and we attempted to do so using an ethyl methanesulfonate (EMS) non-complementation screen (Fig. 2.1). By using this scheme, we isolated several new alleles of *exc-5* by their inability to complement the *rh232* null allele. Alleles that we recovered were screened to verify them as new alleles and tested for temperature sensitivity.

Materials and Methods

Strains Used

In order to have a genetic marker for the *rh232* deletion and avoid re-isolating the same mutant allele, I created a recombinant chromosome that included the *exc-5* (*rh232*) mutation and the *unc-44* (*e362*) mutation approximately 1.1cM away. This was done by mating male animals that were heterozygous for the *rh232* mutation with hermaphrodites that were homozygous for the *e362* mutation (CB362). Progeny from this mating were allowed to self-fertilize. At this step, there is a small possibility for a recombination to occur, and any progeny showing an Exc-5 phenotype were kept, and allowed to self-fertilize again. Progeny from these animals were isolated that appeared both Exc and Unc, as these animals had become homozygous for an *rh232 e362* recombinant chromosome (BK50). BK50 hermaphrodites were then mated with male animals containing a GFP transgene (BK44) on chromosome I (*qpIs11* [unc-119;Pvha-1::gfp]) that labels the canal. Animals that were homozygous for *rh232*, *e362*, and *qpIs11*were re-isolated (BK51) and used in the EMS non-complementation screen.

EMS Non-Complementation Screen

BK44 animals were collected into 2ml of M9 buffer. Animals were then added to an additional 2ml of M9 buffer with 20µl of ethyl methanesulfonate (EMS) dissolved. Animals were left to agitate in a rotary shaker for four hours, and then washed to remove the EMS solution. Mutagenized BK44 L4 males were isolated and mated to BK51 hermaphrodites in a ratio of 4:2 at a temperature of 25°C.

Progeny from these matings were screened for animals showing the Exc phenotype. These animals are presumed to contain a mutant allele from the mutagenized father, as their copy of *exc-5* fails to complement the *rh232* deletion provided by the mother. In order to isolate homozygous strains for these new alleles, Exc animals were allowed to self-fertilize. Any animals that produced Unc progeny were discarded as the presence of the *unc-44* gene indicated that the *rh232* mutation was still present in the genome. Animals breeding true for the Exc phenotype at 25° were considered new alleles of *exc-5*.

Temperature-Sensitive Screening of New Alleles

In order to test whether these new alleles were temperature-sensitive, animals were grown at 25° and 15°C by one of two methods. The first took forty animals homozygous for each of the new alleles and placed them on separate plates. Twenty plates were grown at 25° and twenty at 15°C. Alternatively, homozygous animals were chunked onto two plates to be grown at 25°, and two plates to be grown at 15°. The worms were compared approximately three days later. Alleles that were cystic at 25° but not at 15° were considered temperature-sensitive.

Figure 2.1 – EMS Non-Complementation Scheme

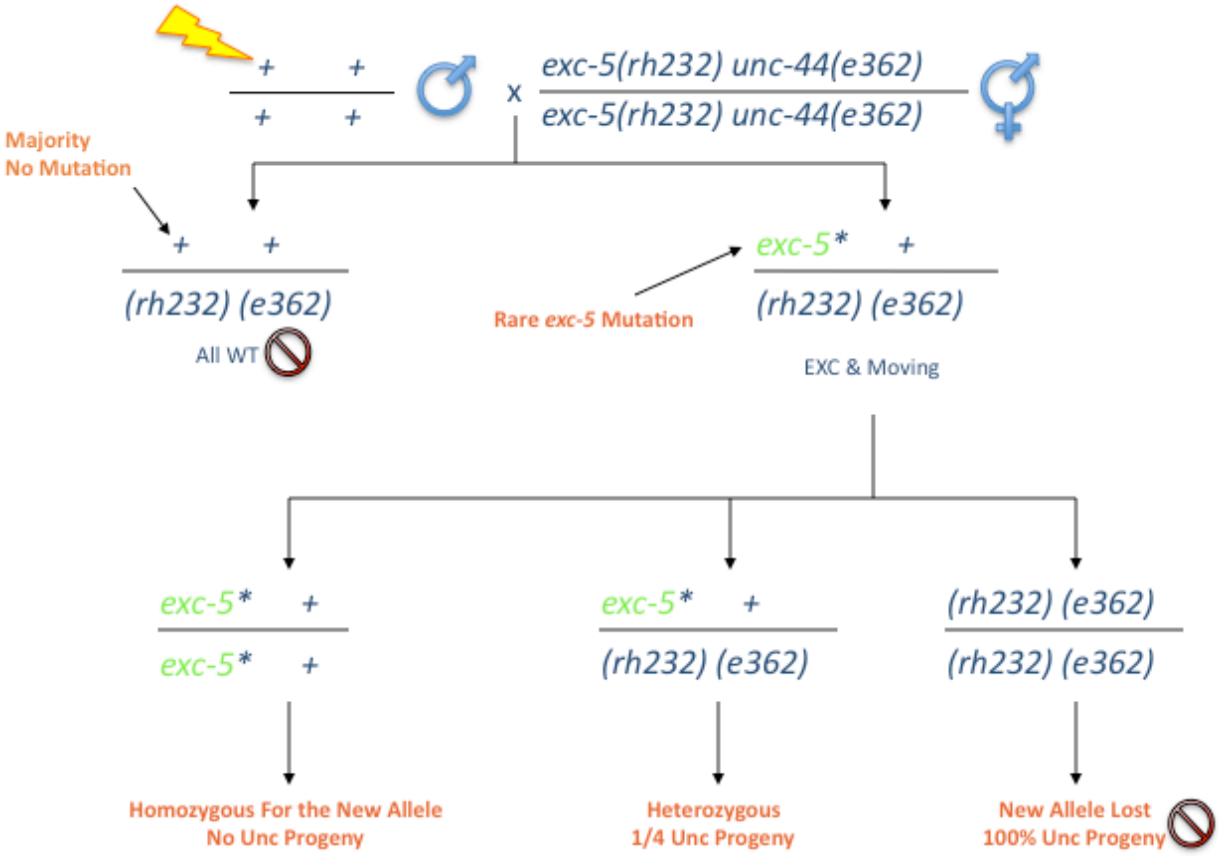

BK44 animals contain wild-type alleles of both *exc-5* and *unc-44.* These animals are mutagenized and then mated to BK50 animals that are homozygous for the *rh232* and *e362* mutant alleles. The majority of the mutagenized chromosomes will not contain a mutation in *exc-5* and will complement the mutant *rh232* allele with a wild-type version, producing a wild-type phenotype. On rare occasions a new mutation will have been induced in *exc-5*. These mutations will no longer be able to complement the *rh232* allele and will produce animals with an EXC phenotype. Since the *rh232* allele is linked to the *e362* allele, we can isolate the new allele from *rh232* by identifying animals that look Exc but no longer produce Unc progeny.

Characterizing the Cystic Phenotype between Animals

In conjunction with Dr. Xiangyan Tong, I developed a scoring method to characterize the cystic phenotype of *exc-5* and *exc-9* mutants (Fig. 2.2) [51]. Using this scale, the canal is given a length between zero and four. Canals that do not extend are scored as having a length of 0, whereas canals that are full-length are scored as a 4. Canals that end halfway through the animal are scored as a 2.

In addition to canal length, I also defined cysts into three sizes: small, medium, and large. Cysts that are larger than half the body diameter of the worm are considered large, cysts that were less than half the diameter of the animal, but larger than ¼ the diameter of the animal were considered medium, and cysts smaller than ¼ of the diameter were considered small.

Sequencing the *rh232* Deletion

In order to create a quick molecular screen to determine if the new alleles were in fact new alleles and not re-isolates of *rh232*, the ends of the *rh232* deletion first needed to be identified. By designing primers to small (~1kb) exon-rich regions of *exc-5* (Fig. 1.9), I was able to identify the exons that were present in the *rh232* deletion. I then used this point as an anchor to design a reverse primer. I then designed a series of primers in 5kb increments upstream of the deletion point in *exc-5*. Presence of a PCR (polymerase chain reaction) product indicated the existence of upstream sequence where the forward primer was designed. I then made a series of primers that were designed closer and closer to the break point. The final result was a PCR product ~500bp in length using a forward primer 14.5kb upstream of the *exc-5* start codon (5'-CCGAATACTTTTACTCGTTAGC-3') and a reverse primer located near the end of exon 13 (5'-GCGAAGGTGCTAGAATTAGGTC-3'). This product was then sequenced to determine the precise endpoints of the *rh2332* deletion.

The *rh232* allele was found to be missing 18,866 bp of sequence. This removes the first twelve exons of *exc-5* as well as the first three base pairs of exon 13. In addition to almost total deletion of the gene, *rh232* also removes 14kb of upstream sequence, removing any upstream genetic elements that would ordinarily regulate the transcription of *exc-5*. The sequence of the 21bp on either side of the deletion is as follows:
TTATTTTATTTAACGTTATA---18866bp Deletion --- CCTATCACGGGGTCGAAATG.

Sequencing New Alleles

The series of new alleles was first screened using a set of three primers in a Multiplex-PCR reaction (Fig. 2.3). Two of these were the primers that bridged the ~19kb deletion in *exc-5*; a forward primer 15kb upstream of the *exc-5* start codon (5'-TGCGCGAAACTGAGATGAATG-3') and a reverse primer at the end of exon 16 (5'-GAGGGATGAGATGAGATGAACGTAT-3'). The third was a forward primer near the beginning of exon 9 (5'-CTCGACTTCTTGCCAATGTGT-3'). Any strains that contained the deletion would produce an ~1.5kb size band in a PCR reaction, whereas those strains that had a novel non-deletion allele would not be able to amplify a ~19kb product, and instead amplify using the exon 9 primer site that is not present in the deletion, and produce a product ~2kb in size. Those strains that produced a ~2kb band and therefore did not contain *rh232* were amplified in six pieces using the primers designed to the six exon segments of *exc-5* and sent to a sequencing facility at Idaho State University.

Figure 2.2 – Measuring Canals and Cysts

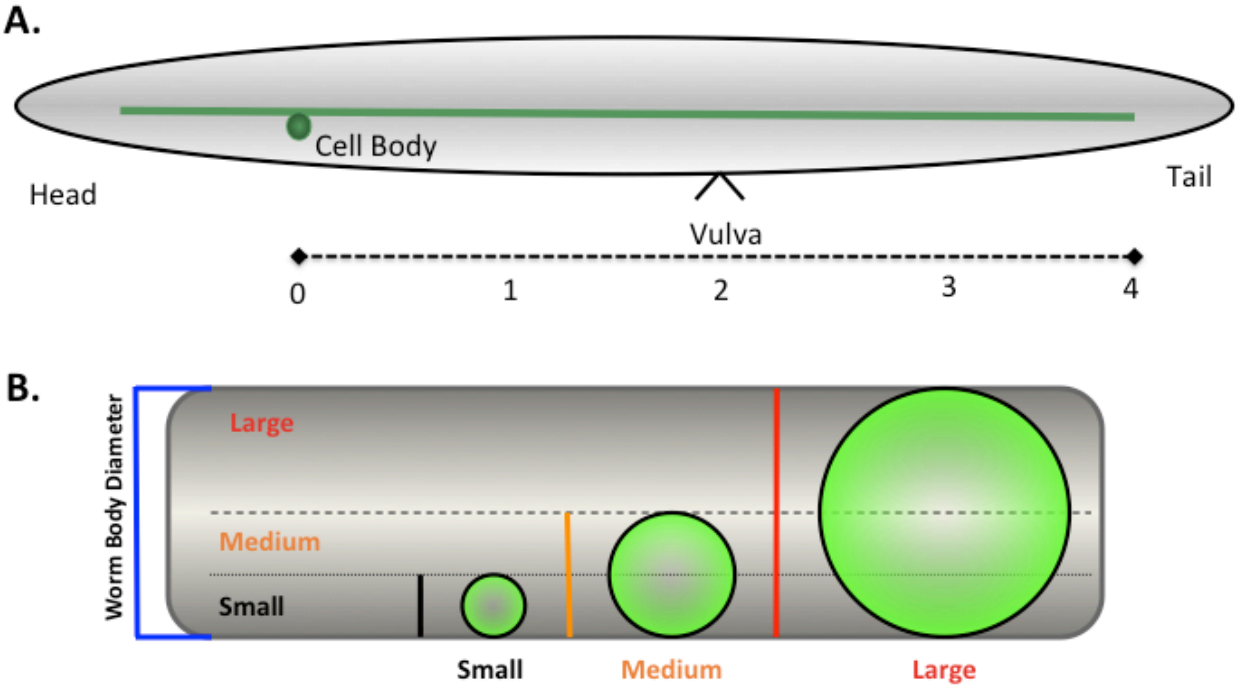

(A) A diagram representing a wild-type canal in an animal. Canal length is measured relative to the cell body, the vulva, and the anus of the animal. Canals that do not extend and remain at the cell body are scored as 0. Canals that extend halfway to the vulva are scored as 2. Canals that extend full-length to the anus of the animal are scored as 4.
(B) A diagram representing the body cavity of the worm. Cysts are defined as large if their diameter is larger than half the diameter of the animal. Medium cysts are defined as ¼ to ½ the diameter of the animal. Small cysts are defined as ones that are ¼ or less of the diameter of the animal.

Figure 2.3 – Multiplex-PCR Screen to Confirm New Alleles

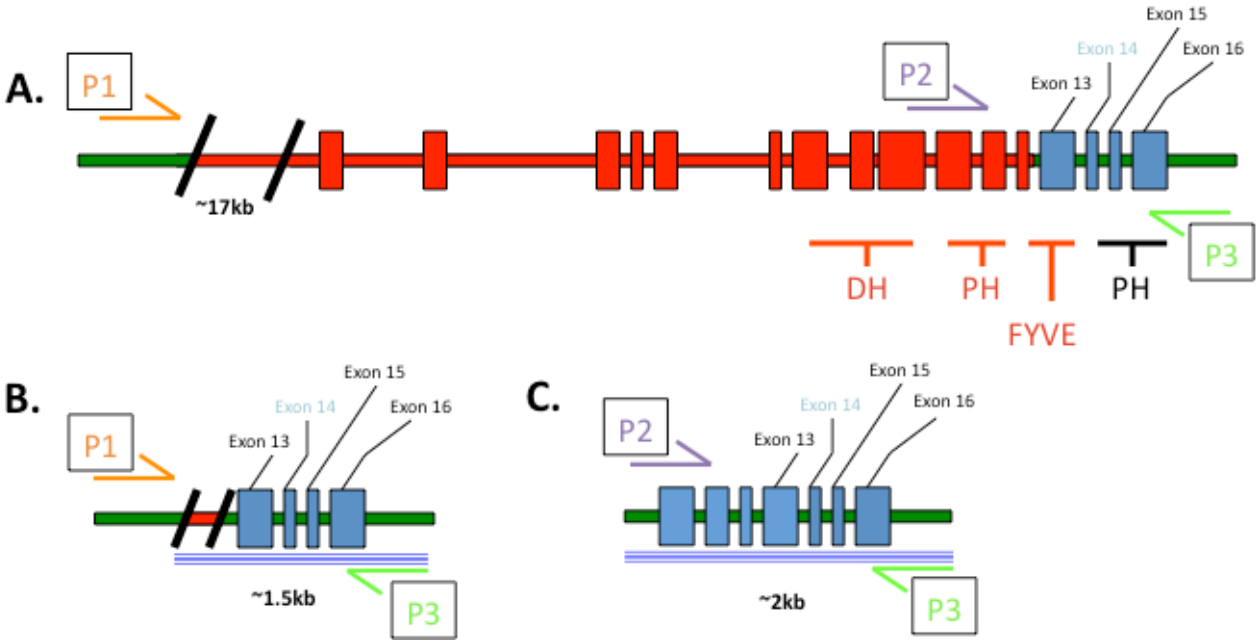

(A) A diagram of the genetic structure of *exc-5* and the *rh232* deletion. Areas in red are missing in the *rh232* allele. P1 represents the primer-binding site upstream of the deletion. P2 represents the primer-binding site that will be present in non-deletion alleles and missing in the *rh232* deletion. P3 represents the reverse primer-binding site for the reaction. **(B)** The PCR reaction will proceed using the P1 and P3 primers and amplify a 1.5kb product in animals containing the *rh232* deletion. **(C)** Animals that do not contain the deletion won't produce a 19kb product using the P1 and P3 primers. Instead, the smaller 2kb product using the P2 and P3 primers will be amplified.

Results

Twenty-seven rounds of mutagenesis resulted in an estimated 50,855 genomes screened and produced forty-three isolates. Of these, six had properties of interest but none of them were novel TS alleles of EXC-5.

Two of the isolates were novel mutations in *exc-5*, but did not show any temperature-sensitive effects. Both alleles, *qp39* and *qp21,* contained premature stop codons in the last PH domain, encoded by exons 14-16. *qp39* has a C → T transition in exon 15 that changes amino acid 756 from an arginine to a stop (CGA → TGA). *qp21* also contains a C→T transition in exon 16, changing amino acid 815 from a glutamine into a stop codon (CAA→ TAA). The last PH domain consists of amino acids 743-830. Therefore, *qp39* excludes almost the entire second PH domain whereas *qp21* only removes the last 15 amino acids (Fig. 2.4). Both of these strains had a null phenotype and looked similar to the *rh232* allele.

Three of the isolates had hypomorphic phenotypes: *qp35*, *qp37*, and *qp56*. These animals had much less severe phenotypes and frequently did not look mutant at all. When mutant, these animals had shortened, slightly malformed canals (Fig. 2.5). Sequencing of these animals, however, showed no mutations in the coding regions of *exc-5*. The frequency of slightly mutant canal phenotypes was not altered by temperature in these mutants.

The last isolate, *qp49*, showed temperature-sensitive effects, but did not show an absence of cysts at the lower temperature (Table 2.1). *rh232* showed little variation when moved between 15° and 20°. 19% of the animals had canals that formed large cysts at either temperature in the posterior canals, and roughly 20% had cysts in the anterior canals at both temperatures. In contrast, *qp49* was free of anterior canal cysts at 15°. Additionally, when *qp49* was moved to 25°, the number of canals that had large cysts rose to 38%, nearly double that of *rh232*. Sequencing of *qp49*, however, showed that it contained the original *rh232* deletion.

Table 2.1 – Temperature Sensitive effects of *rh232* and *qp49*

	rh232		*qp49*	
	15°	**25°**	**15°**	**25°**
% Canals with Large Cysts[a]	19%	19%	17%	**38%**
Total # of Cysts[b]	5	9	6	5
% Anterior Canals with Cysts[c]	21%	17%	**0%**	12%
n[d]	88	69	46	87

The *exc-5* null allele *rh232* shows little difference in phenotype between 15° and 25°. In contrast, at 15° *qp49* shows a slight decrease in the number of canals with large cysts. More significantly, it shows complete suppression of cyst formation in the anterior canals (green). At 25° this suppression is eliminated. In addition, at 25° the number of canals with large cysts in *qp49* doubles over that of *rh232* (red). [a]The percentage of canals that contained large cysts at a given temperature. [b]Average total number of cysts counted per canal. [c]Percentage of anterior canals that contained cysts. [d]Number of canals examined.

Figure 2.4 – New Null Alleles of *exc-5*

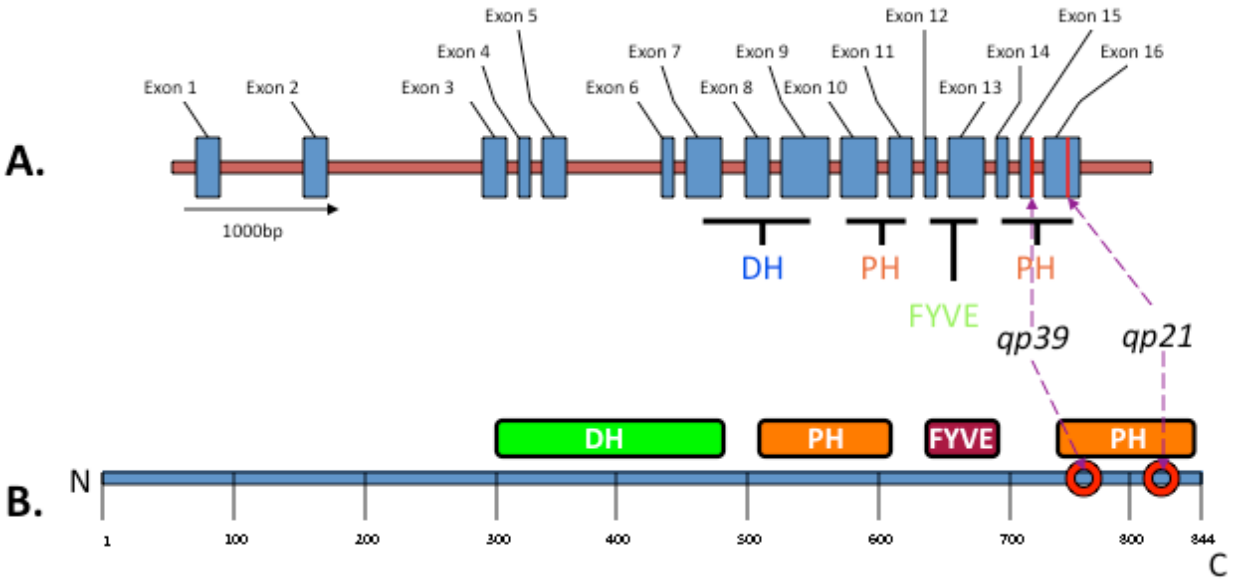

(A) Genetic structure of *exc-5* showing the locations of the *qp39* and *qp21* mutations. *qp39* has a C → T transition in exon 15 that changes amino acid 756 from an arginine to a stop (CGA → TGA). *qp21* also contains a C→T transition in exon 16, changing amino acid 815 from a glutamine into a stop codon (CAA→ TAA). **(B)** Both mutations disrupt the last PH domain of EXC-5. Both of these alleles have phenotypes similar to that of *rh232*.

Figure 2.5 – Hypomorphs Show Minor Canal Defects

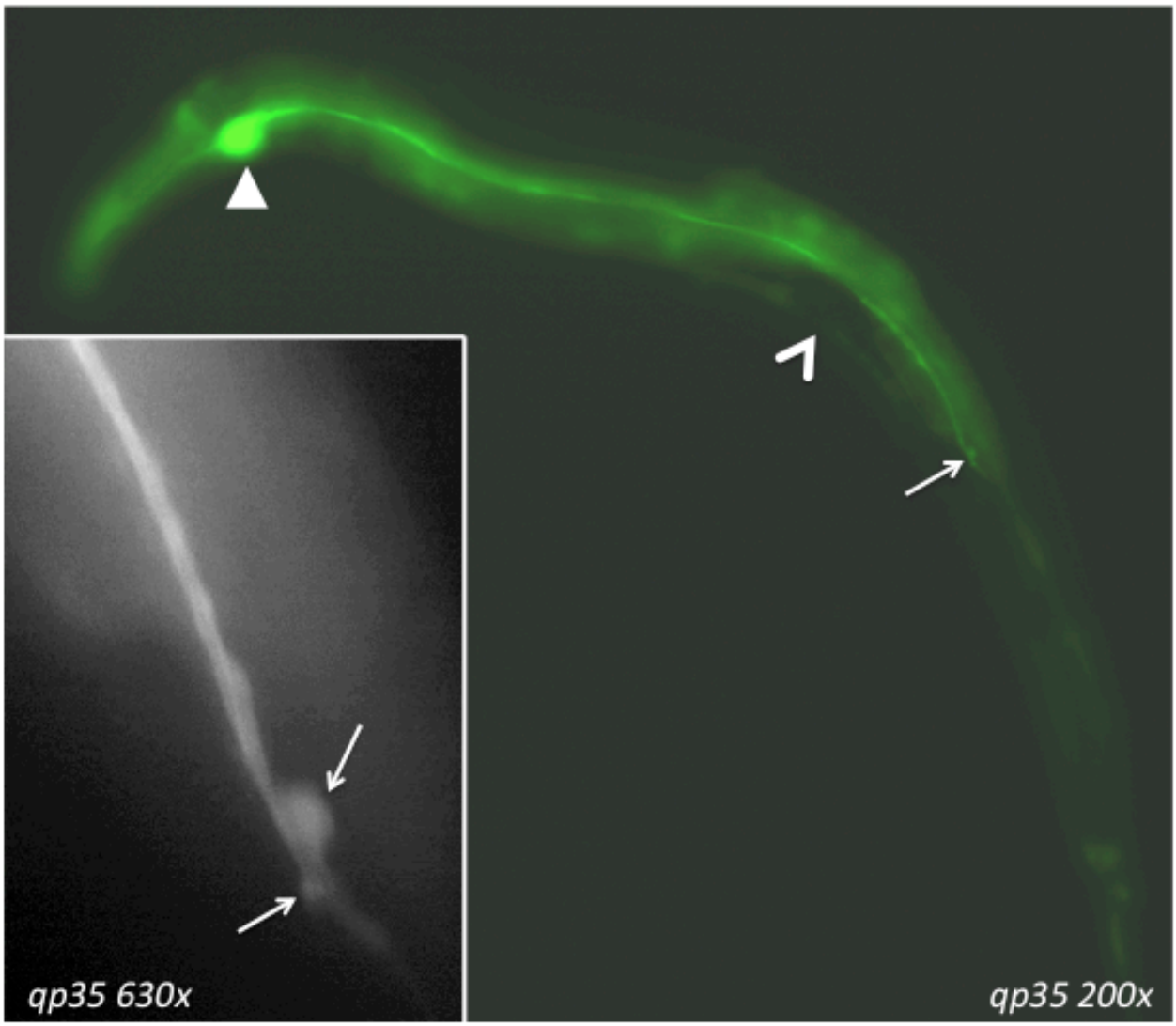

A micrograph taken under fluorescence of an L4 *qp35* animal at 200x magnification. Hypomorphic phenotypes are all similar to the animal depicted here. Canals extend two-thirds of the way to the tail and do not have visible cysts. Instead, the canals often end in slightly malformed protrusions (arrows). Inset is of the same animal at higher magnification. Sequencing of the exons of alleles *qp35*, *qp37*, and *qp56* did not show any mutations present.

Discussion

Although no new temperature-sensitive alleles of *exc-5* were found, six strains were isolated that provide some information, and the *rh232* deletion was successfully identified. Two of the isolates, *qp39* and *qp21*, were novel alleles of *exc-5*. Both contained C->T transitions within the last PH domain of the gene. This type of point mutation is common for EMS-induced mutations [68]. Interestingly, although these nonsense mutations only remove a small portion of the gene, the phenotypes of these animals were as severe as was the *rh232* deletion. This indicates that the last PH domain of EXC-5 is essential for function within the excretory canal. Mutations in the lipid-binding site of the first PH domain of FGD1 have been shown to cause disease effects [69]. If destroying the function of the last PH domain in EXC-5 causes a null phenotype, this would indicate that the DH/PH tandem domains are not the only essential domains in EXC-5, and that the activity of EXC-5 does not lie solely in its ability to function as a GEF. The related Vav family of proteins has been shown to have effects independent of its GEF activity [70,71]. It is also possible that the second PH domain in EXC-5 is important for determining the location of the protein within the excretory cell, and without it EXC-5 is unable to reach the correct membrane surfaces to activate/interact with its binding partners to maintain the canal shape. Future experiments would include creating a GFP-labeled version of EXC-5 that removed the terminal PH domain and then check its subcellular location as compared with that of WT EXC-5. A difference in location would indicate that EXC-5 is located improperly without the last PH domain. Additional experiments could be done to determine the roles of the other domains of EXC-5 by creating several different forms of the protein, selectively removing the different domains and observing whether these proteins retained their activity by preventing cysts to form within the canal. Previous studies of this kind have been done with FGD1; these experiments, however, have indicated that the N-terminal proline-rich domain in FGD1 is largely responsible for its location in the plasma membrane and Golgi complex [72] and that FGD1's Src homology (SH3) domain is responsibly for its interaction with cortactin and Arp2/3 [73]. Interestingly, EXC-5 does not contain these domains.

Alternatively, the transcript from *qp39* and *qp21* could be degraded through nonsense-mediated decay [74]. I suggest that this is unlikely due to the proximity of the new premature stop codons to the native ones. No experiments were done to ascertain the presence or absence of an *exc-5* mRNA or EXC-5 protein in these strains to verify this assumption, so the possibility remains that the mRNA is being degraded and no EXC-5 protein is being produced. The presence of a persistent *exc-5* mRNA in these strains could be checked using either RT-PCR (Reverse Transcriptase PCR) or a 5' RACE-PCR (Rapid Amplification of cDNA Ends). Determining whether or not the protein is present in these animals could be checked by using an antibody specific for EXC-5.

Screening through an estimated 51,000 genomes did not produce a TS allele that was suitable for our purposes. Ideally, we would have recovered an allele that had a 100% penetrant cystic phenotype at 25° and 0% (no cysts at all) at 15°, and then used this to look at the effects of removing or adding EXC-5 activity at different developmental time points during the growth of the animal and the excretory canal. The nature of the protein and phenotype may have made finding a TS allele improbable. The phenotype of an *exc-5* null mutant is stochastic. Although there is a 100% chance that it will form cysts, where and

how many cysts form is not predictable for any one animal. If there was a subtle TS effect, it may have gone unnoticed in the variation between animals at the two different temperatures. The value of such a subtle TS allele for our purposes would be low.

In addition, EXC-5 activity is not required to maintain the entire length of the canal. On a cellular level, this indicates that EXC-5 is only essential at certain points along the canal (where the cysts form) and not along other parts of the canal (which maintain their normal lumen diameter). The points along the canal that do fail, fail catastrophically and create large cysts. Our screen was sensitive enough to identify three hypomorphic alleles, which indicates that we were able to isolate alleles that had reduced activity. These strains also indicate that even a small amount of EXC-5 activity is enough to eliminate the cystic phenotype. As heterozygotes, they were unable to fully complement the *rh232* allele. When homozygous, they had enough activity to only allow minor defects in the canal to form. To generate a TS allele, a mutation that completely eliminated all EXC-5 activity at 25° would have to be induced. At the same time, this mutation would have to restore activity at 15°. It is feasible that such an EMS-induced mutation may not be possible for EXC-5. We have pursued other methods to generate TS alleles of EXC-5 in a more directed approach by engineering conditional alleles using inteins (see Chapter 7).

Our screen does indicate that it is possible to identify temperature-sensitive alleles of other genes that work with EXC-5. *qp49* was TS for its cystic phenotype even though it still contained the *rh232* deletion, which indicates that *qp49* is a TS mutation in a gene other than *exc-5*. At 15°, *qp49* acts as a mild suppressor of EXC-5, eliminating the formation of cysts in the anterior canals and slightly reducing the number of canals with large cysts. At 25°, *qp49* no longer suppressed the formation of cysts in the anterior canals. Interestingly, at 25° *qp49* also increased the number of canals with large cysts to nearly double that from *rh232*, which indicates that at higher temperatures *qp49* exacerbates the Exc-5 mutant phenotype. Currently there is no mapping data for this allele. Identifying what gene is being affected could be very interesting and future work will require *qp49* to be mapped.

Chapter 3: Identification of Genetic Enhancers of *exc-5*

Abstract

In order to identify more proteins that interact with EXC-5, we set up an EMS screen to identify mutations that suppressed the Exc-5 gain-of-function phenotype. We isolated two strains, BK188 and BK190, which contain mutations that act as enhancers of EXC-5 activity. Both mutations are recessive and do not show linkage to chromosomes I or X. Additional mapping information for BK188 shows that it is not linked to the middle of chromosomes II, III, IV, or V.

Rationale

"What other gene products interact with EXC-5?"

Several proteins have been shown to interact with FGD family members. CDC-42 and Rac have both been implicated in interactions with FGD proteins either directly or indirectly [75-78]. We wanted to broaden our search over the entire *C. elegans* genome to look for novel proteins that might interact with EXC-5. By identifying novel genes that interact with *exc-5*, we can gain insight into the pathways involved in regulating and maintaining the tubular shape of the excretory canal. The isolation of *qp49* suggested that suppressors of *exc-5* function exist. We were interested in also identifying enhancers of *exc-5*.

In order to do this, we took advantage of the gain-of-function phenotype of *exc-5* and set up an EMS suppressor screen to identify genes whose products normally contribute (enhancers) to EXC-5 function. Animals overexpressing EXC-5 show shortened and sometimes convoluted canals (Fig. 1.10). By mutagenizing animals that stably overexpressed EXC-5, we can screen for animals that appear suppressed; animals that have normal length canals. These animals will have had a mutation in a gene that normally contributes to EXC-5's function, and helps shorten the canal cell. Once mutated, the gene will alleviate the mutant gain-of-function phenotype of EXC-5 overexpression. By using this type of EMS suppressor screen, we isolated two genetic enhancers of *exc-5.*

Materials and Methods

Strains Used

In order to carry out this screen we first needed to build a strain that stably overexpressed EXC-5. This becomes particularly difficult as the overexpression of EXC-5 is deleterious, and at very high levels lethal; therefore transgenic arrays of EXC-5 are lost from the population at high rates.

A plasmid containing a genomic copy of *exc-5* under its own promoter and fused N-terminally to GFP (7.2kb of upstream sequence from *exc-5* and 5.3kb of *exc-5* coding region placed into pPD95.75 (gift from A. Fire) in front of the *gfp* gene and an *unc-54* 3' UTR) (gift from K. Matsumoto) was used to introduce excess copies of *exc-5* into wild-type (N2) animals. After many injections of the plasmid at various concentrations, I was ultimately successful in producing a worm strain containing an unstable array at a very low transmission rate (0.6-1% of animals would inherit the array, n=300) by injecting *exc-5::gfp* at 15ng/µl in combination with purified N2 genomic DNA at a concentration of 25ng/µl. The inclusion of the N2 DNA was designed to provide additional carrier DNA so that the transgenic array built by the animal would incorporate random wild-type DNA and prevent incorporation of a lethal, highly repetitive, high-copy-number array of only *exc-5::gfp* DNA.

The low-transmission array was then integrated into the chromosome by use of 4,5',8-trimethylpsoralen (TMP) [79]. Nematodes were washed off plates with M9 buffer, pelleted, and resuspended in a minimal volume. TMP was added to a final concentration of 30µg/ml. Animals were soaked in the TMP solution for 15 minutes in the dark and washed twice in M9 buffer. Nematodes were then plated and irradiated by use of a Spectrolinker™ (Spectronics Corporation, New York) set to 350µJ at 360nm. F_2 progeny from the irradiated animals were isolated and screened for integrants. Plates containing all fluorescent transgenic progeny were identified as having the transgene homozygously integrated. The resultant strain (BK157) has the *exc-5::gfp* array, *qpIs78*, integrated on the X chromosome. The strain was then outcrossed five times. . The GFP expression was so low in this strain that it was not suitable for screening through a fluorescent dissecting scope. To enhance canal visibility, I crossed the bright canal marker integrant *qpIs11* ([*unc-119*;*Pvha-1*::*gfp*] on I) into the outcrossed BK157 strain to create BK178. This strain was then used in the EMS suppressor screen.

EMS Suppressor Screen

Animals were mutagenized similarly to the manner described in Chapter 1. BK178 animals were collected into 2mL of M9 buffer. Animals were then added to an additional 2mL of M9 buffer containing 20µl of ethyl-methanesulfonate (EMS)(for a final 1% EMS solution). Animals were left to agitate in a rotary shaker for four hours, and then washed to remove the EMS solution. Mutagenized BK178 young adult hermaphrodites were moved to new plates and allowed to self-fertilize. The F_1 progeny were allowed to self-fertilize in order to isolate animals that may need to be homozygous for a suppression effect, and the F_2 generation was screened for animals that showed full-length canals. Animals with full-length canals were picked to separate plates and allowed to self-fertilize. Animals that bred

true for the suppressed phenotype were considered to have new mutations that suppressed *exc-5* gain-of-function.

Mapping the Genetic Locus of the Suppressors

In order to identify where the suppressors are located, test-crosses were done between BK188 or BK189 heterozygous males and a series of different hermaphrodites containing the following mutations linked to each of the six chromosomes of *C. elegans* respectively: *dpy-5*(*e61*) I; *dpy-10*(*e128*) *unc-4*(*e120*) II; *dpy-17*(*e164*) *unc-32*(*e189*) III; *dpy-20*(*e1282*) *unc-22*(*e66*) IV; *dpy-11*(*e224*) *unc-42*(*e270*), *dpy-11*(*e224*) *unc-76*(*e911*), and *unc-51*(*e369*) V; and *dpy-6* (*e14*) *unc-3*(*e151*) X.

Matings that did not result in the expected frequency of animals containing both the marker gene(s) and the suppression phenotype were considered to have the suppressor mutations linked to the chromosome associated with the marker gene(s).

Scoring of strains was carried out as in Chapter 2, with a length equal to 0 indicating no canal extension and a length of 4 indicating complete canal extension.

Results

Four rounds of mutagenesis resulted in an estimated 2,000 genomes screened and the isolation of two suppressor strains, BK188 and BK190.

The parent strain, BK178, has an average canal length of 1.8, although the range of canal lengths can vary between 0.5 and 3.5 (n=66). The two suppressor strains were identified through two selection criteria: First, individual animals that had full-length canals; and second, the progeny of these animals showed the same lengthening effect. Although not every animal in the second stage of selection had a full-length canal, the effect on the population of animals had to be observable. For both BK188 and BK190, approximately 75% of the animals have full-length canals.

Both suppressors are recessive and do not appear to be on chromosomes I or X. In addition, BK188 did not show linkage to the center of chromosomes II, III, IV, or V. Unfortunately, it also did not show linkage to the center or right side of chromosome V. BK190 was isolated with the assistance of Tekalign Burka and remains to be tested for chromosomes II, III, IV, and V.

Discussion

Although there have been several attempts to map these suppressors, we have currently not identified the genetic locus for the suppression effect. There are several reasons this has been difficult. The first is that these suppressors are only identifiable through their population effect. Individual animals may not always show a full-length canal. The second is that the suppressors are recessive, so only animals homozygous for the mutation will show the suppression phenotype. Thirdly, the suppression phenotype can only be seen with *qpIs78*. The inclusion of *qpIs11* in these strains was necessary to be able to screen the animals under the dissecting scope. The intensity of this canal marker, however, masks the GFP expression from *qpIs78*, and therefore animals must be known to contain *qpIs78* through the generation of animals with shortened canals and not through fluorescence. When creating the testcrosses in order to determine linkage, at least three different genetic elements (*qpIs78*, the suppressor locus, and the tester gene or genes) need to be homozygous in order to determine if the suppressor is linked to the chromosome. We are confident that the suppressors are not on chromosome I or X, as they show no linkage to either *qpIs78* or to *qpIs11.* Therefore, they cannot be mutations in *exc-1*, which has been shown to interact with *exc-5* (Chapter 5). While it is possible that the BK188 mutation is on the ends of chromosomes I, II, III, IV, or the left end of V, the initial crosses did not show it to be linked to any of the chromosomes.

These suppressors do not appear to affect *qpIs11* fluorescence, and therefore are unlikely to be nonspecific suppressors of transgene activity. It is possible that these suppressors are mutations that affect the expression of the *exc-5::gfp* transgene through either transcriptional or translational effects. Although these kinds of mutations would not be ideal in determining what proteins are interacting with the EXC-5 protein itself, they would still provide insight as to how *exc-5* is being regulated within the excretory canal cell.

Future work on this project requires these suppressors to be identified. We have shown that it is possible to isolate new strains that suppress the gain-of-function phenotype of EXC-5. Identifying what these mutations are could provide new insight into the molecular pathways in which EXC-5 works to maintain tubular shape.

Chapter 4: Creating a Canal-Specific RNAi System

Abstract

Loss-of-function mutations in several of the genes thought to be involved in the growth and maintenance of the excretory canal are lethal when mutated in the entire animal. In order to manipulate these genes and others in a cell-specific manner, we require a technique that allows us to manipulate gene function only in the excretory canal cell. In this chapter I describe two attempts, one using RNAi hair-pins and one using cell-specific expression of RDE-1, as well as current methods being implemented to create an excretory canal cell-specific RNAi technique.

Rationale

"What other gene products interact with EXC-5?"

Many of the genes that may or may not interact with EXC-5, in particular the RhoGTPases and CDC-42, are lethal when completely knocked out. Some mutations of these genes do exist, but are not null phenotypes. For instance, the *cdc-42* allele *gk388* must be maintained as a heterozygote. Animals that are homozygous for this allele are viable, but are sterile. The fact that animals homozygous for a presumably null allele of *cdc-42* are viable at all indicates that there is a maternal effect and, while genetically these animals may be null for *cdc-42*, cellularly they are not. The excretory canals in these animals do not appear to have major defects (see Chapter 5).

To date, most of the *exc* genes identified have been expressed primarily in the canal cell. This indicates that single-cell tubulogenesis and tubule maintenance are largely cell autonomous processes. Another possible explanation is that more generally expressed genes that would cause cysts to form in the canal also cause defects in other tissues and are lethal when mutated. In addition to testing particular genes of interest, a canal-specific method to knockout genes would allow the implementation of high-throughput genomic screens to identify genes that are involved in tubulogenesis, but would otherwise not be found through more traditional genetic screens.

In order to manipulate theses genes in a cell-specific manner and not affect the general development or morphology of the animal, we needed a way to disrupt these genes only in the excretory canal. We decided to use the robust RNAi (RNA interference) system within *C. elegans* [80] as a means to selectively knock down genes within the excretory canal cell while not perturbing other tissues within the animal. We have approached this technical hurdle in several ways.

The first attempt relies on the transcription of a construct only in the canal cell. The transcript is designed to bind back on itself to form a dsRNA hairpin. The second method is based on the *rde-1* (RNAi-defective) mutant.

Materials and Methods

1. Creating Excretory-Canal-Expressed RNAi Hairpins

By designing a DNA construct that has a canal-specific promoter, ~600bp of a cDNA of interest (forward fragment), followed by a ~300bp fragment containing the same ending sequence of the same cDNA in a reverse orientation (reverse fragment), we intended to create a transgene that would transcribe an mRNA that would fold back on itself and produce ~300bp of dsRNA sequence to trigger the RNAi mechanism within the excretory canal cell. To prevent the RNAi effect from spreading out of the canal cell, these constructs were to be injected into animals mutant for *sid-1,* which encodes a dsRNA transporter required for systemic RNAi in *C. elegans*.

The construct was assembled in a pCR-XL-TOPO® (Invitrogen™ Corporation, California) vector. The promoter used to drive the expression of the hairpins was a 1528bp fragment upstream of the *vha-1* gene and was inserted using the TA site of the vector. cDNA fragments were cloned from mRNA prepared from wild-type (N2) animals. Primers were designed to amplify both a ~600bp and ~300bp reverse fragment from *exc-5*, *cdc-42*, *mig-2*, *rho-1, rac-2*, *chw-1*, and *crp-1*. *exc-5* and *cdc-42* fragments were successfully amplified and used in subsequent cloning reactions as a control and test case, respectively. The ~600bp forward fragments were inserted at the XbaI site while the ~300bp reverse fragments was inserted into the vector at the ApaI site.

Although creating constructs of *cdc-42* and *exc-5* that contained the canal-specific P_{vha-1} promoter and the ~600bp forward fragment of each gene was made, cloning the smaller ~300bp inverted sequence into the construct was unsuccessful. Despite many attempts in several bacterial strains, we were unable to retrieve sequences that had the sequence in an inverted orientation. Clones were recovered that contained the second sequence in the forward orientation, but not the reverse. No functional constructs were created.

Failure to create the canal-expressed RNAi hairpin constructs was likely due to the length of the sequence to be inserted in an inverse orientation. An inverted repeat of this size was not accommodated by the bacteria and was heavily selected against, producing DNA constructs that only contained the reversed fragment in the forward orientation. Future work on this project would require reducing the sizes of the gene-specific elements and designing a more forced orientation cloning strategy.

2. Creating an RNAi-competent canal cell in an animal deficient in RNAi

rde-1 mutant animals are defective in RNAi even though they are able to produce siRNAs (short interfering RNAs) from a dsRNA (double-stranded RNA) injected trigger [81,82]. This indicates that the animals are not defective in their systemic response to injected dsRNA, but rather in a later process after siRNAs have been formed. We hypothesized that introducing *rde-1* back into the canal cell in an *rde-1* mutant background would restore the RNAi effect in the canal cell without disrupting other tissues of the animal.

A plasmid containing the promoter for *vha-1* and *gfp* (pCV01, gift from gift of T. Oka and M. Futai) was used as the backbone for canal expression of RDE-1. A genomic copy of *rde-1* was amplified and inserted in-frame upstream of *gfp* as a SacI-AgeI ~3.5kb fragment. This plasmid was then used for injection into *rde-1*(*ne219*) animals.

High levels of RDE-1 expression (caused by injections of 25ng/µl or higher of the construct) were deleterious to canal morphology. Injection of lower concentrations of the construct made GFP fluorescence almost undetectable. In order to identify transgenic progeny, a second plasmid containing the promoter for *CO3F11.1* fused to GFP was used as a co-injection marker. This marker labels some of the head neurons, and does not interfere with RDE-1's expression in the canal. Injection of the $P_{vha\text{-}1}$*::rde-1::gfp* construct at 5ng/µl and the $P_{C03F11.1}$*::GFP* construct at 100ng/µl resulted in a strain containing a stable high-transmission (~90%) array (*BK142*, *qpEx67*). Integration of this array through TMP (similarly as described in Chapter 3) resulted in four integrants: BK143, BK144, BK145, and BK146. BK143 was determined to have *qpEx67* integrated on chromosome II and used for further testing.

<u>Testing BK143 for RNAi Sensitivity</u>

The gene *sma-1* encodes β_H-spectrin and is necessary for proper elongation of *C. elegans* as well as the morphogenesis of the excretory canal cell and pharynx [52]. When mutated, *sma-1* creates defects in both the body of the animal (short and dumpy body type with a blunted nose) as well as the excretory canal (shortened length, enlarged lumen, and occasional cysts). Therefore, this gene makes an excellent test for a canal-specific RNAi strain. If the strain works, RNAi for *sma-1* will cause defects in the canal but not in the body morphology of the animal.

sma-1 dsRNA was produced by first PCR-amplifying a genomic copy of *sma-1* through use of primers that contain a T7 transcription site on both ends. This PCR product was then used as a template for an *in vitro* transcription reaction by use of the MEGAscript® T7 kit (Ambion® Incorporated, Texas). The resultant dsRNA was then injected into BK143 animals in addition to a co-injection marker, the dominant *rol-6* (*su1006*) allele that causes the animals to have a twisted body morphology [83]. Transgenic animals that showed a *rol-6* phenotype were examined for their canal morphology. Wild-type animals (N2) were also injected with the *sma-1* dsRNA and *rol-6* marker as a control.

Results

Surprisingly, RDE-1 had a strong deleterious affect on the canal cell. High concentrations (injection of 25ng/µl or greater) RDE-1 caused extremely shortened canals and a punctate expression pattern of GFP (Fig. 4.1). Even at lower concentrations (10ng/µl),some punctate expression and luminal defects near the end of the canal were observed. At lower concentrations (5ng/µl) most of the canals appeared normal and the punctate expression of RDE-1::GFP was eliminated, producing a continuous cytoplasmic expression pattern.

Injection of the *sma-1* dsRNA caused a robust *sma-1* phenotype in N2 animals (Fig. 4.2A). Injection of the same *sma-1* dsRNA into the BK143 strain showed no RNAi effects in either the body or the canal cells of the animals (Fig. 4.2B,C).

Figure 4.1 – Overexpression of RDE-1 Causes Canal Defects

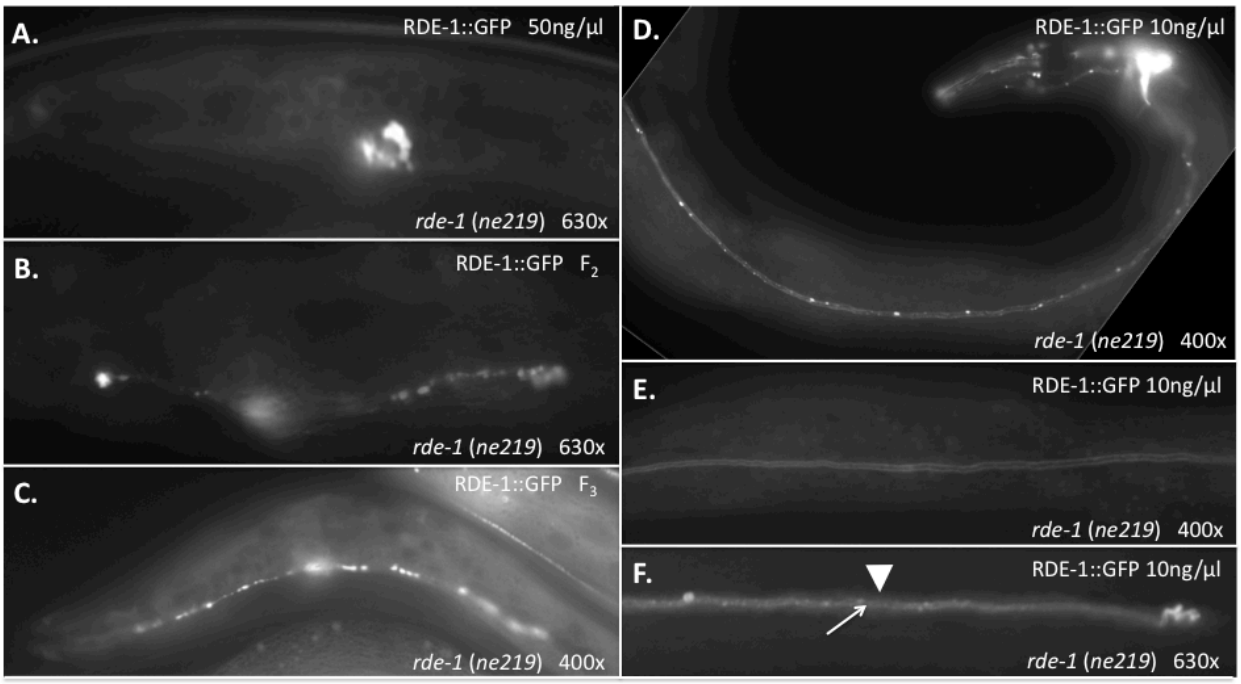

Expression of RDE-1 at high levels disrupts excretory canal morphology. **(A)** Progeny of animals injected with the *Pvha-1::rde-1::gfp* construct at 50ng/µl display excretory canals that have failed to extend. Unlike the convoluted tubule phenotype, these canals display defects at the luminal surface as well as the basal surface. RDE-1::GFP collects in large aggregates in the cell. **(B)** In the subsequent F_2 generation the *rde-1::gfp* array shows reduced deleterious effects. The canals extend further but still do not reach the vulva. Expression of RDE-1::GFP is still highly punctate and is not distributed evenly in the canal. Canal morphology is still highly disrupted. **(C)** In the F_3 generation, the array exhibits even less deleterious effects. Although short and still containing RDE-1::GFP puncta, the canal begins to take on normal morphology. The reduction of the RDE-1 overexpression phenotype over multiple generations indicated that a lower amount of RDE-1 would be non-detrimental to the canal. **(D)** Injection of the *Pvha-1::rde-1::gfp* construct at 10ng/µl (along with the $P_{C03F11.1}$*::gfp* construct at 100ng/µl as an injection marker) has little effect on canal morphology. Although some animals still have RDE-1::GFP puncta, diffuse expression can be seen in the canal. **(E)** In other animals, canal morphology is wild-type and expression of RDE-1::GFP is continuous throughout the canal. **(F)** RDE-1 expression is enriched at the luminal surface of the canal (arrow) and not the basal surface (arrowhead) when overexpressed. All images are fluorescent micrographs taken of L4 animals, except D. The animal pictured in D is a young adult. Magnification is as labeled.

Figure 4.2 – RNAi of *sma-1* is Ineffective on Animals Expressing RDE-1 in the Canal

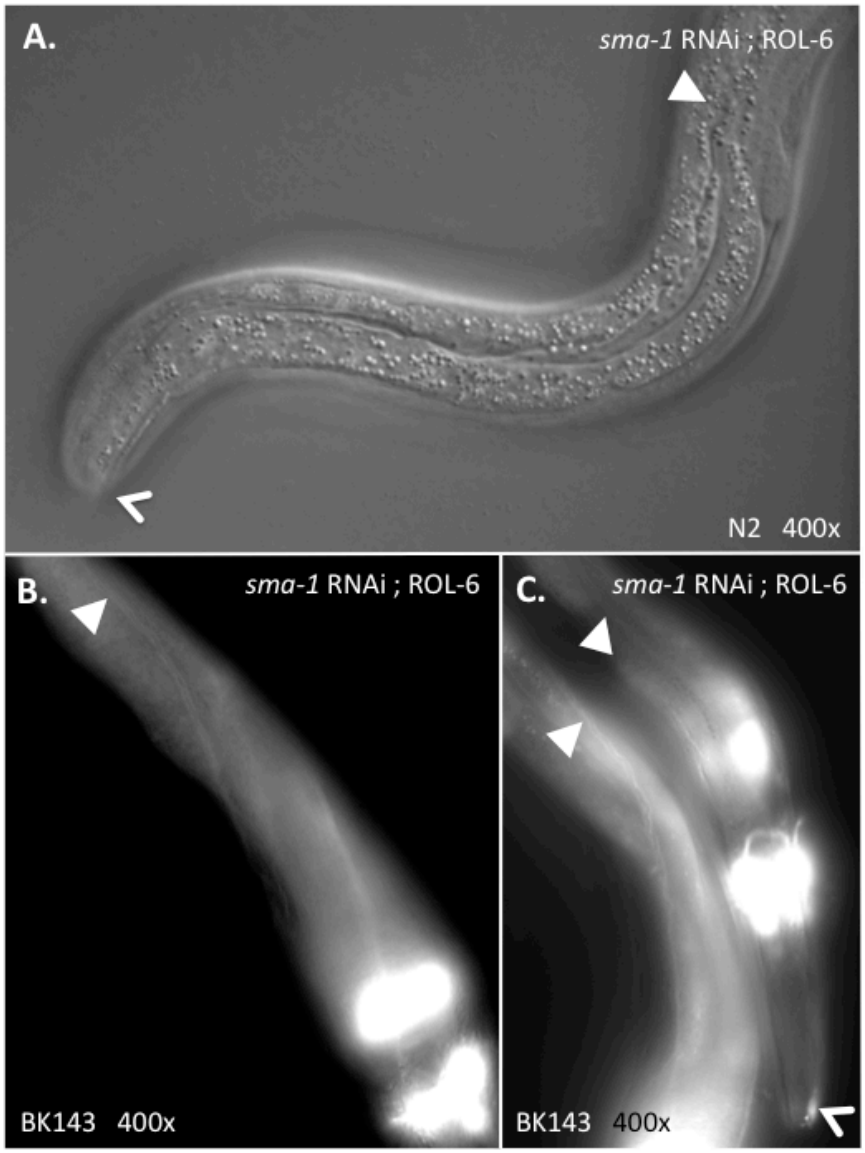

(A) Injection of dsRNA of *sma-1* into a wild-type (N2) background causes a characteristic body defect (open arrowhead) in the head of the animal to produce a short blunt nose. *sma-1* RNAi also causes short excretory canals with larger than normal lumen diameter (solid arrowhead).
(B) In BK143, animals express RDE-1 only in the canal. *sma-1* RNAi, however, has no effect on canal morphology (solid arrowhead).
(C) In addition to no canal defects, (solid arrowheads) BK143 animals also do not display the *sma-1* head defect (open arrowhead). All images are of L4 animals at 400x magnification. All animals were co-injected with *rol-6* as an injection marker. This causes the animals to twist along the body axis which is most evident in animals pictured in B and C. In addition, BK143 animals contain the $P_{C03F11.1}$*::gfp* construct that is expressed in head neurons (B,C).

Discussion

RDE-1 is an Argonaute protein that is required to process siRNAs. It has an RNase H activity that separates the siRNA duplex so that the resultant single-stranded siRNAs can be used for mRNA targeting [84]. It is interesting that the canal cell is sensitive to overexpression of this protein. Parts of the RNAi mechanism, specifically those that are involved in miRNA (micro RNA) processing and include the Argonaute proteins, are involved in the normal developmental regulation of eukaryotes [85,86]. Phenotypic defects have normally been associated with loss-of-function mutations in these proteins and their inability to process small RNAs. *rde-1* (*ne219*) mutants, however, show no canal defects even though they are deficient in RNAi activity. Only when RDE-1 was overexpressed in the canal was there a defect. Why this occurred is unclear. Perhaps there is an increase of the normal small RNA silencing mechanisms present in the canal when RDE-1 is overexpressed. The increased activity of RDE-1 may cause too much gene silencing to occur, the effect of which is to knock down genes that are essential to proper canal formation and create morphologically defective excretory canals.

Failure of BK143 to show any RNAi effects in the canal may be a result of the canal being refractory to RNAi. Other tissues, specifically neurons, have also been shown to be refractory to RNAi effects [87]. Since 2006, when this work was done, another group successfully used a similar strategy to perform tissue-specific RNAi in the muscle and hypodermis of *C. elegans* [88]. This suggests that the canal cell may indeed be less susceptible to RNAi than are other tissues.

There have been two methods successfully described for RNAi in neurons. The first is similar to the previously described hairpin method. Instead of creating one construct with both a forward and reverse element in it, the authors used two different constructs [89]. Both had the same cell-specific promoter, but one construct contained a coding sequence in the forward orientation, while the other construct contained the coding sequence in a reverse orientation; eliminating the problem of cloning an inverted repeat in a single DNA construct. They then injected both constructs into the animals where they were expressed only in the intended cell, and created a dsRNA by the transcription of separate but complementary mRNAs. Future work to create DNA constructs that express dsRNA only in the canal could use this method.

The second method is based on SID-1, a dsRNA transporter required for systemic RNAi in *C. elegans* [90,91]. Recently, a group showed that overexpression of SID-1 enhanced RNAi effects in neurons using an RNAi feeding trigger, and that cell-specific expression of SID-1 can produce cell-specific RNAi [92]. We have just started to implement this method by adapting SID-1 expression only in the canal cell. Our plans include using this technique for a genome-wide, canal-specific RNAi feeding screen.

Chapter 5: Genetic Interactions of *exc-5*

Abstract

EXC-5 is a putative GEF for CDC-42. In addition to examining the genetic interactions between these two proteins, we also looked at genetic interactions of *exc-5* with *mig-2* and *ced-10*, genes encoding Rac GTPases. Previous reports have indicated that EXC-5 interacts with MIG-2. In support of these previous observations, we found that EXC-5 shows interactions with both CDC-42 and MIG-2 and that these interactions indicate that all three proteins may work in the same pathway either directly or indirectly. In addition, we found that EXC-5 works downstream of two other EXC proteins, EXC-1 and EXC-9.

Rationale

"What other gene products interact with EXC-5?"

The *C. elegans* genome contains seven members of the Rho-family of GTPases: one Rho protein (RHO-1), three Racs (CED-10, MIG-2, RAC-2), CDC-42, and two CDC-42- related proteins (CRP-1, CHW-1) [93,94]. EXC-5 is a putative GEF for CDC-42. Previous work, however, has shown that a gain-of-function Rac mutation (*mig-2*(*gm38*)) can also rescue the Exc-5 mutant phenotype ([57] and personal observations). We examined the genetic interactions between *exc-5*, *cdc-42*, *mig-2*, and *ced-10*. CED-10 and MIG-2 act redundantly in several neuronal processes and both may interact with EXC-5 [95].

In addition to our interest in the interactions between the RhoGTPases and EXC-5, we were also eager to explore the possible genetic interactions between other *exc* genes. While all *exc* mutants cause cyst formation in the canal, the size and location of those cysts varies depending on the gene mutated. Two of the *exc* genes, *exc-1* and *exc-9*, show very similar mutant phenotypes to that of *exc-5*, which indicates that they may function in the same genetic pathway. I looked at the effects of introducing increased EXC-5 activity into several other *exc* mutant strains to see if EXC-5 was able to alter the other mutant phenotypes.

A classical way to demonstrate genetic interactions between different genes is to look at epistatic effects between them. In an effort to identify genetic interactions between *exc-5* and other RhoGTPases, I looked at animals containing mutations in a loss-of-function *cdc-42* (*gk388*) allele, a *cdc-42* dominant-negative (DN) mutation, a *cdc-42* constitutively active (CA) mutation (both generous gifts from E. Lundquist), a loss-of-function *mig-2* (*mu28*) allele, a gain-of-function *mig-2* (*gm38*) allele, or a hypomorphic loss-of-function *ced-10* (*n2993*) allele in conjunction with *exc-5* (*rh232*) (also a gift from E. Lundquist), and recorded the changes in canal length and cyst formation. If gain-of-function mutations can rescue or reduce the mutant phenotype of *exc-5* mutant animals, it is likely that EXC-5 is working upstream of these gain-of-function proteins. If combinations of other knockout or knockdown mutations can increase the severity of the EXC-5 mutant phenotype and produce a synergistic effect, then the two mutations may act in separate parallel pathways or have redundant roles. If there is no synergistic effect when combined with other loss-of-function alleles, then it is likely that the two mutations are in the same pathway.

Overexpression of EXC-5 or EXC-9 causes convoluted tubules; a phenotype where the lumen of the canal forms properly but the basal surface of the canal does not extend, which causes the lumen to become convoluted within the smaller and now spherically shaped canal cell [51,57], (Fig. 8). If overexpression of EXC-5 in the mutant cystic strains causes a convoluted tubule phenotype, it may indicate that EXC-5 is working downstream of the mutant gene, as excess EXC-5 activity is epistatic to the other mutation and can override that mutant's cystic phenotype. If overexpression of EXC-5 in a mutant strain does not cause a convoluted tubule phenotype, then EXC-5 may work upstream of the mutation.

Materials and Methods

Strains Used

The *gk388*, *mu28*, and *gm38* alleles were provided by the *Caenorhabditis* Genetics Center. The *ced-10* (*n2993*), *exc-5* (*rh232*) double mutant was made by E. Struckhoff and was a gift from E. Lundquist. Animals containing the *cdc-42* DN or CA construct had an unstable transgenic array containing the gene. All strains except for those with the *gk388* allele also contained *qpIs11*.

DNA Constructs

Plasmids containing constructs expressing constitutively active (CA, G12V) and dominant-negative (DN, T17N) forms of nematode *cdc-42* were the gift of E. Lundquist. A 1.2kb NheI fragment was amplified from these plasmids containing *cdc-42* and re-cloned by use of standard molecular techniques into plasmid L3691 (gift from L. Timmons) which N-terminally labels the *cdc-42* gene with *gfp*.

To overexpress EXC-5, a plasmid containing the genomic copy of *exc-5* under its native promoter with a C-terminal GFP tag was injected into mutant strains (See Chapter 3 for construct details).

Measurement of Canals

Methods describing the measurement of the excretory canal cell can be found in the Materials and Methods section in Chapter 2, "Characterizing the Cystic Phenotype between Animals" and in Figure Legend 2.2.

Results

Injection of a *cdc-42* dominant-negative or constitutively active construct caused significant changes in canal morphology in a wild-type background (Table 5.1). The gain-of-function *cdc-42* (CA) transgene caused a high percentage (>80%) of animals to show a shortened and convoluted tubule phenotype. The *cdc-42* (DN) transgene caused over half the animals (56%) to develop cysts. These effects mimic *exc-5* gain-of-function and loss-of-function phenotypes in wild-type worms, and are consistent with the hypothesis that CDC-42 and EXC-5 function in the same pathway. Interestingly, the *cdc-42* (*gk388*) mutation does not produce cysts in the canal (Table 5.1, Fig. 5.1).

Expression of CDC-42 (CA) caused the same number of convoluted canals in an *exc-5* (*rh232*) mutant background as it did when expressed in a wild-type background (>80%)(Table 5.1). This convolution phenotype induced by CDC-42 (CA) appears to be independent of cyst formation and the length of the canal. Convolutions occurred near the cell body, but did not alter canal length, nor the number or sizes of cysts. This result indicates that excess CDC-42 activity is unable to compensate for the lack of EXC-5 activity in cyst formation, but can still cause convoluted lumen defects by itself.

Expression of the CDC-42 (DN) construct in the *exc-5*(*rh232*) background showed a small increase in the average number of cysts but did not increase cyst size. Similarly, the *gk388 cdc-42* mutant allele in combination with *exc-5*(*rh232*) also increased the average number of cysts. The *gk388* allele, however, did slightly increase cyst size in the *rh232* background (Table 5.1). Overall, expression of CDC-42 (DN) or the combination of the *gk388* allele did not have large effects on the *rh232* phenotype. The results from the loss-of-function CDC-42 mutations indicate that CDC-42 and EXC-5 may work in the same pathway, as the cystic phenotype does not get significantly worse in combination with *rh232*. In addition, the convoluting effect that expression of CDC-42 (CA) had even in the absence of EXC-5 activity would indicate that CDC-42 acts downstream of EXC-5. Contradicting this, however, is the result that CDC-42 (CA) does not have as severe a convoluted tubule phenotype and does not shorten canals like EXC-5 overexpression does. In addition, the CA activity of CDC-42 does not rescue the cystic phenotype of *rh232* animals. This last result indicates that EXC-5 may additionally function with another GTPase such as MIG-2.

mig-2 (*mu28*) and *ced-10* (*n2993*) mutations have not been reported to exhibit cystic phenotypes [96](personal observations). A *mig-2* (*mu28*); *exc-5* (*rh232*) double mutant animal shows a slight lengthening of the canal but no large differences in cyst formation from that of the *rh232* background (Table 5.1). The gain-of-function *mig-2* allele *gm38* does not show any large effects with *rh232* except in the number of canals that had cysts, reducing the normally 100% cystic phenotype to 93.6%. It should also be noted that 4% (4 out of 94) of the canals showed a complete rescue by being both full-length and having no cysts. This rescue was not observed in other strains tested. This indicates that although *mig-2* may not have a highly penetrant effect on *exc-5*, it is capable of fully rescuing *rh232* defects.

Table 5.1. Effects of other mutations on excretory canal phenotype[a]

Strain/Genotype	n[b]	Convoluted[c]	Canal Length[d]	Cystic[e]	# Cysts[f]	Size of Cysts[g]		
						Small	Medium	Large
N2 (Wild-type)	100	0	4.0	0				
VC898 *cdc-42* (*gk388*)	24	0	4.0	0				
Trans. Express.: *gfp*::CA *cdc-42*; N2	84	83.3	2.7	**1.2**	0	1.0	0	0
Trans. Express.: *gfp*::DN *cdc-42*; N2	48	0	3.1	**56.3**	**2.8**	**2.6**	**0.2**	0
NJ731 *exc-5* (*rh232*) mutants	96	0	1.2	100	8.6	7.5	1.7	1.1
cdc-42 (*gk388*); *exc-5* (*rh232*)	39	0	1.1	97.4	12.0	10.7	2.3	1.4
Trans. Express.: *gfp*::CA *cdc-42; exc-5 (rh232)*	54	81.5	1.6	100	8.0	6.7	1.0	0.3
Trans. Express.: *gfp*::DN *cdc-42; exc-5 (rh232)*	42	0	1.6	100	11.7	9.7	1.5	0.5
mig-2 (*mu28*); *exc-5* (*rh232*)	44	0	2.3	97.7	7.9	6.9	1.9	1.1
mig-2 (*gm38*); *exc-5* (*rh232*)	94	0	2.1	93.6	7.1	6.7	1.7	1.3
ced-10 (*n2993*) *exc-5* (*rh232*)	47	0	1.7	97.9	**22**	**20**	**3.2**	1.3

[a]Substantial increases in cyst number or size from those of controls are indicated in boldface. Increases in number of convoluted tubules and decreases in number of cysts are underlined.
[b]Number of canals examined.
[c]Percentage of canals that exhibited a lumen that traversed itself more than once.
[d]Average canal length relative to body length as described in Materials & Methods; 0 means no canal growth, 4 is full-length.
[e]Percentage of canals that exhibited any visible cysts at all.
[f]Average number of cysts observed for all animals
[g]Average number of large, medium, and small cysts (size determined as described in Materials & Methods) seen for animals exhibiting cysts.

Contrary to the other strains tested, a *ced-10* (*n2993*) *exc-5* (*rh232*) double mutant showed significant increases in the number of cysts formed in each canal. The double mutant roughly doubled the total number of cysts in these animals (Table 5.1). This doubling in cyst number was due to the increase in both small and medium sized cysts. These results indicate that in the excretory canal cell CED-10 and EXC-5 may have separate but overlapping roles in maintaining the integrity of the canal's tubular structure.

Injection of the *exc-5::gfp* construct at 20-25ng/µl into both *exc-1* (*rh26*) and *exc-9* (*n2669*) mutants resulted in >90% of transgenic animals showing a convoluted tubule phenotype [51], (personal observations). In contrast, injection of the *exc-5::gfp* construct into *exc-4* (*rh133*) and *exc-3* (*rh251*) animals resulted in transgenic animals that were still mutant for their respective phenotypes. Very few transgenic animals were obtained from both *exc-4* and *exc-3* mutant backgrounds, however (one animal per 30-40 animals injected), and injection of the *exc-5::gfp* construct into these strains may be causing a higher than normal toxic effect. This was most obvious in the *sma-1* (*ru18*) background where injecting *exc-5::gfp* at 25ng/µl into 27 animals resulted in 100% lethality in transgenic animals; 8 dead embryos and 24 animals died as L1's.

Discussion

Although *gk388* is a presumably null allele of *cdc-42* (it contains a 478bp deletion that includes a portion of upstream sequence as well as the first two exons [96]), animals homozygous for the deletion survive into adulthood. These animals are sterile, however, and the deletion must be maintained as a heterozygote. Because animals homozygous for the *cdc-42* deletion arise through a mother that had functional CDC-42 and are able to survive, it is likely that there is a significant maternal effect in the animals homozygous for the *cdc-42* deletion. This residual CDC-42 activity may be sufficient to allow normal development and maintenance of the excretory canals. Although there were cysts that appeared in these animals, they did not appear directly connected to the lumen of the canal (Fig. 5.1B). Canal-specific RNAi of *cdc-42* would be most useful here in order to avoid the lethality and gross body morphology defects associated with *cdc-42* loss-of-function in the entire animal, and to examine more closely what perturbations there would be on the canal when *cdc-42* activity is eliminated.

In lieu of such a system, expression of a DN CDC-42 only in the canal should be able to interfere with normal *cdc-42* activity and possibly mimic a *cdc-42* loss-of-function mutation. Indeed, expression of *cdc-42* DN in the canal caused a mild shortening of the canal, as well as cysts in slightly over half of the animals. Animals that did have cysts had only a few and none of them were very large (Table 5.1). These effects are much more mild than are the effects of an *exc-5* null mutation and may indicate that CDC-42 is not the only downstream target of EXC-5. Alternatively, the CDC-42 DN activity may not be as strong as a genuine null mutation of *cdc-42* would be, and the effects of the DN form are similarly less severe. Nevertheless, impairing CDC-42 activity did show a similar effect to that of knocking out EXC-5, which indicates that the proteins may be working together in the same

pathway. This conclusion is supported by the fact that introducing CDC-42 DN activity in animals already deleted for *exc-5* shows no significant change in the phenotype.

The result from introducing a CA *cdc-42* transgene into wild-type animals mimicked, but was not the same as, overexpressing *exc-5*. Canals showed convolutions, but these were not as severe or as shortened as they are in animals overexpressing a similar amount of EXC-5. These convolutions were present even in animals that had no EXC-5 activity, which does indicate that CDC-42 may be acting downstream of EXC-5. However, CDC-42 CA was unable to rescue the cystic phenotype of the *exc-5* null mutation. This result makes interpretation difficult. One reason for the apparent discrepancy may be due to the importance of CDC-42 cycling between its inactive GDP-bound state and its active GTP-bound state in order to maintain its wild-type effects [97,98]. Forcing a significant amount of CDC-42 into either a CA or DN state may not accurately reflect the wild-type activity of activated or inactivated CDC-42 when it is allowed to cycle between these two states.

If these constructs are accurately reflecting CDC-42 loss- and gain-of-function properties, and if CDC-42 were working downstream of EXC-5, then providing more CDC-42 activity would restore normal function of the canal. This is not the case. Instead, these data indicate that rather than working directly with EXC-5, CDC-42 is working only in part with EXC-5. They both function in the same pathway to create convolutions but work independently during cyst formation. This is partially supported by the genetic effects seen with *mig-2*.

Mutation of *mig-2* seems to have little or no synergistic effect with EXC-5, nor does it show any increase in the cystic phenotype of *rh232*. Taken together, these results indicate that these two proteins may act in the same pathway. Additionally, when a gain-of-function allele of *mig-2* (*gm38*) is present with the *exc-5* (*rh232*) null allele, a very low percentage of canals show full rescue. Though the effect is small, the ability to rescue *rh232* is not present in animals containing a CA copy of *cdc-42*. Consistent with EXC-5 acting with MIG-2 only partially, the *mig-2* loss-of-function *mu28* allele is not sufficient to cause cysts to form in the canal. This is similar to what is seen with the *cdc-42* (*gk388*) allele. It would be interesting to see whether a double mutant of *cdc-42* and *mig-2* would cause cysts to form in the canal.

Figure 5.1 – *cdc-42* (*gk388*) Mutants do Not form Cysts in the Canal

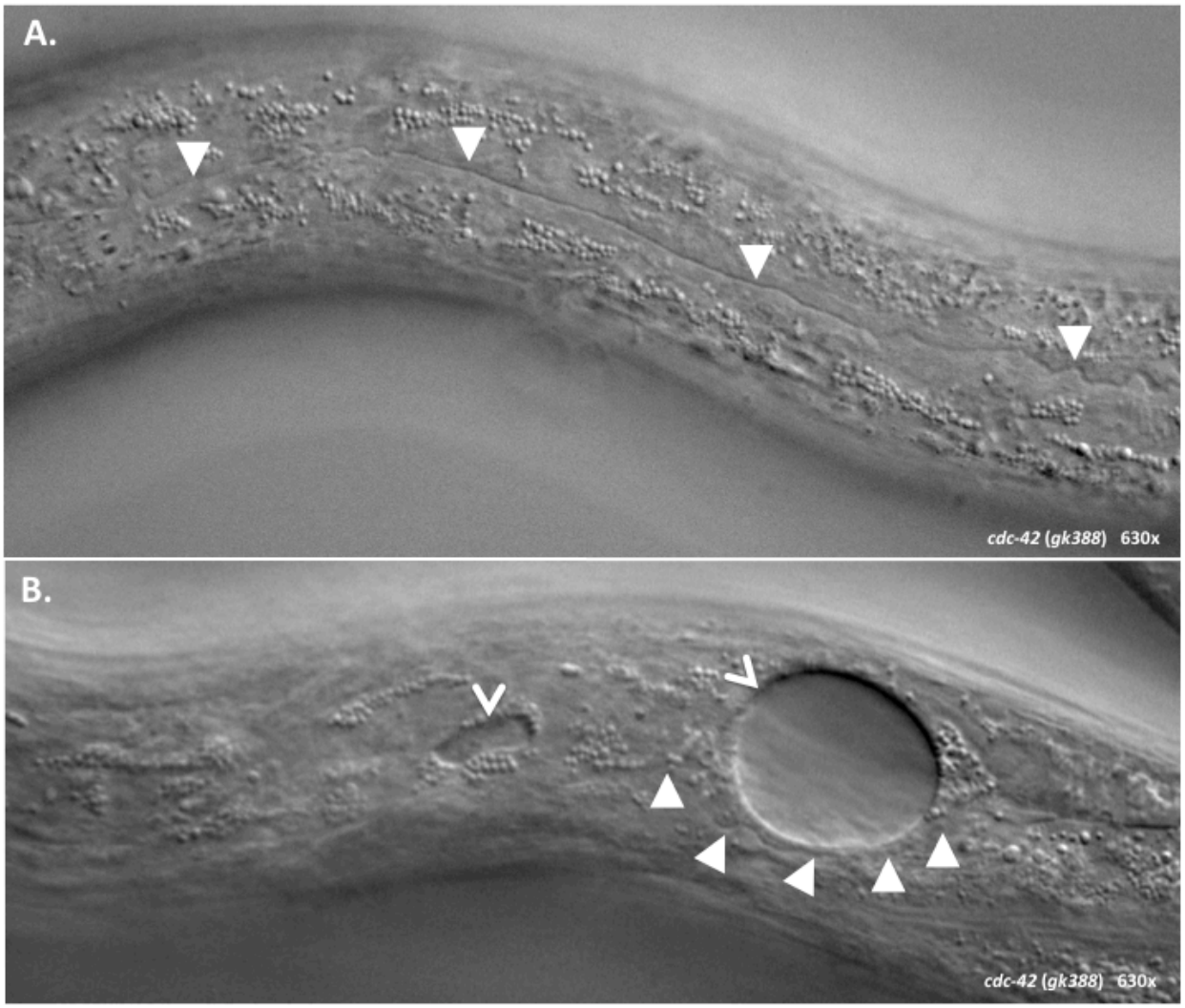

DIC images of young adult animals homozygous for the *cdc-42* (*gk388*) loss-of-function allele taken at 630x magnification. **(A)** Animals mutant for CDC-42 do not display significant canal defects (solid arrowheads). **(B)** Occasionally these animals develop cysts (open arrowheads; 2/24 animals observed). These cysts, however, do not appear to be connected to the excretory canal (solid arrowheads).

The *ced-10* (*n2993*) *exc-5* (*rh232*) strain showed a significant increase in cyst formation over that of the *rh232* background. The fact that knocking down CED-10 function in an animal that has no EXC-5 activity produces a different phenotype means that CED-10 is not dependent on EXC-5 activity in order to function. At the same time, it also indicates that CED-10 activity does help maintain the excretory canal shape in the absence of EXC-5. Since *ced-10* mutations alone have not been shown to cause cysts in the canal, CED-10 function must not be necessary to prevent cysts from developing. Its synergistic effect with *exc-5* however, shows that there must be a small amount of activity in maintaining the integrity of the canal lumen. One possible explanation is that EXC-5 and CED-10 work in different, but slightly overlapping pathways in that they both contribute to the lumen's structural integrity by maintaining the actin cytoskeleton. In the absence of CED-10's normal activity to help reinforce the integrity of the canal lumen, the *exc-5* mutation causes more cysts than normal to form in the canal due to its weakened state.

Injection of an *exc-5::gfp* construct into other *exc* mutants showed that EXC-5 activity is working downstream of both *exc-1* and *exc-9*. EXC-9 is a homologue of the intestinal protein CRIP whose specific biological function is unclear except for the fact that it is required to maintain the structure of the canal [51]. EXC-1 has recently been cloned by fellow lab member Kelly Grussendorf and shows highest homology to a part of the Ras GTPase domain of IIGP (personal communication). It is unclear how these three proteins interact and whether they are acting directly or indirectly with each other. Future plans include using a yeast two-hybrid assay to test whether EXC-5, EXC-9, and EXC-1 can bind to each other directly.

Our model of EXC-5 interacting with both CDC-42 and MIG-2 is consistent with previous work showing that FGD1 and Frabin (mammalian homologues of EXC-5) activity is mediated in both a CDC-42-dependent and -independent manner, and that their interaction with Rac proteins is indirect [77,78]. In the next chapter, I discuss how EXC-5 is involved in membrane trafficking. Interestingly, the intracellular trafficking of Rac has been shown to be involved in the actin dynamics that control cell morphology [18]. Providing an excess of MIG-2 activity may be able to compensate for the lack of its activation and transport to the apical surface in an *rh232* mutant. In addition to creating a double mutant of *cdc-42* and *mig-2* to see if there are any synergistic effects, future work could include using an antibody to activated MIG-2 and comparing its distribution in the canal cell in both wild-type and *rh232* animals. Activated MIG-2 should be enriched at the apical surface in wild-type animals in this model. In *rh232* mutants, MIG-2 may not be activated on the early endosomes as it normally should be, and therefore not be able to recycle back to the apical surface where it is needed to help reinforce the actin cytoskeleton in order to prevent cyst formation.

Chapter 6: Organization of Subcellular Organelles within the Excretory Canal and in *exc-5* Mutants

The bulk of this chapter has been submitted as a manuscript with the title "The FGD Homologue EXC-5 Regulates Apical Trafficking in *C. elegans* Tubules", authors B. Mattingly and M. Buechner.

Abstract

Due to the ability of EXC-5 to alter both the apical and basal surfaces of the canal as well as its interactions with CDC-42, we hypothesized that EXC-5 may direct trafficking inside the excretory canal cell. We examined the effects of altering expression levels of *exc-5* on the distribution of fluorescently-marked subcellular organelles. In *exc-5* mutants, early endosomes build up in the cell, especially in areas close to cysts, while recycling endosomes are depleted. Endosome morphology changes prior to cyst formation. Conversely, when *exc-5* is overexpressed, recycling endosomes are enriched. Since FGD proteins activate the small GTPases CDC42 and Rac, these results support the hypothesis that EXC-5 acts through small GTPases to move material from apical early endosomes to recycling endosomes, and that loss of such movement is likely the cause of tubule deformation both in nematodes and in tissues affected by FGD dysfunction such as Charcot-Marie-Tooth Syndrome type 4H.

Rationale

"How does EXC-5 affect the cellular processes of the canal in order to form cysts and convoluted tubules?"

By comparing the loss-of-function and gain-of-function phenotypes for EXC-5, it is clear that EXC-5 has complementary effects on the apical and basal surfaces of the canal. This characteristic immediately brings to mind cell polarization. In *exc-5* mutants, however, there appears to be no defects in the initial polarization of the cell. The excretory canal initially forms normally in *rh232* mutants, and in EXC-5-overexpressing animals there appears to be no defects in the differentiation between the apical and basal surfaces. Due to our observations that cell polarization does not seem to be grossly affected in the canal cell, that CDC-42 interacts with EXC-5 and that CDC-42 is closely associated with intracellular transport, and that other mutations that cause Charcot-Marie-Tooth-Syndrome type 4H are in transport proteins, we hypothesized that EXC-5 may be involved in directing intracellular transport.

Supporting this hypothesis are the effects seen with EXC-5 homologues. All FGD proteins contain a FYVE domain that binds to PI3P, a phospholipid characteristic of early endosomes [63]. In addition, FGD1 is associated with transport from the trans-Golgi network [72,99] as well as being located on the plasma membrane [72]. FGD2 is associated with early endosomes [100]. Even other proteins involved in Charcot-Marie-Tooth syndrome are necessary for proper membrane trafficking [101-103].

In order to understand the subcellular processes that underlie the cystic and convoluted tubule phenotypes we observe when EXC-5 activity is either lost or overexpressed, we created a set of excretory canal markers to label various subcellular compartments. We found that within the excretory canals, the number and distribution of several of the compartments depended heavily on normal levels of EXC-5. The most strongly affected compartments were the early endosomes and recycling endosomes. In addition, expression of a fragment of WSP-1 that binds to activated CDC-42 (the G-protein-binding domain) caused similar effects on canal structure as did expression of EXC-5. These results support the hypothesis that EXC-5 and other FGD proteins modulate small GTPase activity to move material from early endosomes to recycling endosomes, and this movement maintains the structure of the apical surface of these epithelia.

Materials and Methods

Nematode Genetics

C. elegans mutants were derived from the N2 Bristol strain background. All strains were grown on E. coli strain BK16 (a Streptomycin-resistant derivative of OP50) and maintained as described [43].

DNA Constructs

The *exc-5::gfp* construct was a gift from K. Matsumoto. It contains 12.6kb of genomic DNA comprised of 7.2kb of upstream sequence from *exc-5* and 5.3kb of *exc-5* coding region placed into pPD95.75 (gift from A. Fire) in front of the *gfp* gene and an *unc-54* 3' UTR.

Plasmid pCV01 is the generous gift of T. Oka and M. Futai, and contains the promoter for *vha-1* in front of *gfp* [104]; this construct is strongly expressed in the excretory canal cell and head mesodermal cell. Nematode lines BK30 and BK36 contain a stable integration (*qpIs11*) of pCVO1 together with the *unc-119* gene, transformed into *unc-119* animals that were either wild-type (BK36) or *exc-5*(*rh232*) (BK36) for canal morphology, via biolistic transformation by the method of [105]. Each integrant was outcrossed at least 5 times. For BK36, the site of integration was mapped to LG I.

Plasmids containing constructs expressing constitutively active (CA, G12V) and dominant-negative (DN, T17N) forms of nematode *cdc-42* were the gift of E. Lundquist. A 1.2kb NheI fragment was amplified from these plasmids containing *cdc-42* and re-cloned into L3691 (gift from L. Timmons), N-terminally labeling the *cdc-42* gene with GFP, by use of standard molecular techniques.

Subcellular marker Gateway® (Invitrogen Corporation) constructs were a generous gift from B. Grant. The *vit-2* promoter in the mCherry expression vector was excised as a 326bp SphI-KpnI fragment and replaced with a 1.4kb *exc-9* promoter by use of standard molecular techniques. The modified vector was then used in a series of nine Gateway® reactions with each of the donor vectors containing either the cDNA of nematode *rab-5, rab-7, rab-11, glo-1*, or *rme-1* (splice form d); or genomic copy of nematode *cdc-42, eea-1*, or *chc-1* genes; or the GRIP (Glutamate Receptor-Interacting Protein) domain of nematode

gene T05G5.9 (gift of B. Grant and S. Eimer). The result of each reaction was the *exc-9*-promoted *mCherry* cDNA fused N-terminally to the specific subcellular gene.

The G-protein-binding domain (GBD) of *wsp-1* [106] was PCR-amplified from constructs generously provided by Jayne Squirrel, Kraig Kumfer, and John White, and then cloned into a pENTR™/D-TOPO® vector (Invitrogen Corporation). This sub-clone was used as above to create *mCherry* cDNA fused N-terminally to *GBDwsp-1* expressed via the *exc-9* promoter.

Microinjection and Integration of Constructs

Subcellular constructs were injected into the rachis of young adult N2 animals at a concentration of 50 and 100ng/ml. Transgenic F_1 animals were isolated to separate plates and screened for array transmission.

A stable low-copy-number array of *exc-5*::*gfp* driven by the *exc-5* promoter was obtained via microinjection of the $P_{exc\text{-}5}$::*exc-5::gfp* construct at 15ng/ml mixed with 25ng/ml of N2 genomic DNA. Array transmission in this strain was 0.6% (n=300). Unstable low-copy transient arrays of altered *cdc-42* forms driven by the *vha-1* promoter were obtained via microinjection of the $P_{vha\text{-}1}$::*gfp::cdc-42* (DN or CA) construct at 10ng/ml.

Stable arrays were integrated into the nematode chromosome using 4,5',8-trimethylpsoralen (TMP) [79]. Nematodes were washed off plates with M9 buffer, pelleted, and resuspended in a minimal volume. TMP was added to a final concentration of 30μg/ml. Animals were soaked in the TMP solution for 15 minutes in the dark and washed twice in M9 buffer. Nematodes were then plated and irradiated by use of a Spectrolinker™ (Spectronics Corporation, New York) set to 350μJ at 360nm. F_2 progeny from the irradiated animals were isolated and screened for integrants. Plates containing all fluorescent transgenic progeny were identified as having the transgene homozygously integrated. Integrants were then outcrossed at least five times to create strain BK178.

Strains Used

Table 6.1 - Strains Used for Subcellular Marker Study

Strain	Genotype	Description	Reference
N2		wild-type	[43]
NJ731	*exc-5*(*rh232*)	*exc-5* deletion	[57]
BK36	*unc-119*(*ed3*); *qpIs11*[*unc-119*; *Pvha-1*::*gfp*] I	wild-type with integrated GFP marker expressed in excretory canals	This study
BK30	*exc-5*(*rh232*); *qpIs11*[*unc-119*; *Pvha-1*::*gfp*] I	NJ731 crossed to BK36 to express integrated GFP marker in an exc-5 mutant background	This study
BK179	N2; *qpIs78*[*exc-5*::*gfp*; N2 DNA] X	integrated low-copy-number EXC-5::GFP fusion	This study
Wild-type strains expressing mCherry-labeled marker genes		**mCherry Marker labels:**	
BK219	N2; *qpIs102*[*Pexc-9*::*mCherry*::*chc-1*]	CHC-1: clathrin-coated pits	This study
BK201	N2; *qpIs95*[*Pexc-9*::*mCherry*::*eea-1*] X	EEA-1: early endosomes	This study
BK209	N2; *qpIs99*[*Pexc-9*::*mCherry*::*rab-5*] IV	RAB-5: early endosomes	This study
BK210	N2; *qpIs100*[*Pexc-9*::*mCherry*::*rab-7*]	RAB-7: late endosomes	This study
BK206	N2; *qpIs98*[*Pexc-9*::*mCherry*::*glo-1*]	GLO-1: lysosomes	This study
BK211	N2; *qpIs101*[*Pexc-9*::*mCherry*::*rme-1*] X	RME-1: recycling endosomes	This study
BK205	N2; *qpIs97*[*Pexc-9*::*mCherry*::*rab-11*] V	RAB-11: recycling endosomes	This study
BK220	N2; *qpIs103*[*Pexc-9*::*mCherry*::*GRIP*]	GRIP: Golgi apparatus	This study
BK204	N2; *qpIs96*[*Pexc-9*::*mCherry*::*cdc-42*]	CDC-42: cytoplasm	This study
BK262	N2; *qpIs104*[*Pexc-9*::*mCherry*::*GBDwsp-1*]	GBD domain of WSP-1: cytoplasm	This study
exc-5 deletion strains with mCherry-labeled markers			
BK221	NJ731; *qpIs102*[*Pexc-9*::*mCherry*::*chc-1*]	CHC-1: clathrin-coated pits	This study
BK218	NJ731; *qpIs95*[*Pexc-9*::*mCherry*::*eea-1*] X	EEA-1: early endosomes	This study
BK217	NJ731; *qpIs99*[*Pexc-9*::*mCherry*::*rab-5*] IV	RAB-5: early endosomes	This study
BK216	NJ731; *qpIs100*[*Pexc-9*::*mCherry*::*rab-7*]	RAB-7: late endosomes	This study
BK213	NJ731; *qpIs98*[*Pexc-9*::*mCherry*::*glo-1*]	GLO-1: lysosomes	This study
BK214	NJ731; *qpIs101*[*Pexc-9*::*mCherry*::*rme-1*] X	RME-1: recycling endosomes	This study
BK215	NJ731; *qpIs97*[*Pexc-9*::*mCherry*::*rab-11*] V	RAB-11: recycling endosomes	This study
BK222	NJ731; *qpIs103*[*Pexc-9*::*mCherry*::*GRIP*]	GRIP: Golgi apparatus	This study
BK212	NJ731; *qpIs96*[*Pexc-9*::*mCherry*::*cdc-42*]	CDC-42: cytoplasm	This study
BK273	NJ731; *qpIs104*[*Pexc-9*::*mCherry*::*GBDwsp-1*]	GBD domain of WSP-1: cytoplasm	This study
Strains with slight overexpression of *exc-5* (labeled with GFP) containing mCherry-labeled markers			
BK227	BK179; *qpIs102*[*Pexc-9*::*mCherry*::*chc-1*]	CHC-1: clathrin-coated pits	This study
BK230	BK179; *qpIs95*[*Pexc-9*::*mCherry*::*eea-1*] X	EEA-1: early endosomes	This study
BK226	BK179; *qpIs99*[*Pexc-9*::*mCherry*::*rab-5*] IV	RAB-5: early endosomes	This study
BK224	BK179; *qpIs100*[*Pexc-9*::*mCherry*::*rab-7*]	RAB-7: late endosomes	This study
BK228	BK179; *qpIs98*[*Pexc-9*::*mCherry*::*glo-1*]	GLO-1: lysosomes	This study
BK223	BK179; *qpIs101*[*Pexc-9*::*mCherry*::*rme-1*] X	RME-1: recycling endosomes	This study
BK225	BK179; *qpIs97*[*Pexc-9*::*mCherry*::*rab-11*] V	RAB-11: recycling endosomes	This study
BK229	BK179; *qpIs103*[*Pexc-9*::*mCherry*::*GRIP*]	GRIP: Golgi apparatus	This study
BK231	BK179; *qpIs96*[*Pexc-9*::*mCherry*::*cdc-42*]	CDC-42: cytoplasm	This study
BK274	BK179; *qpIs104*[*Pexc-9*::*mCherry*::*GBDwsp-1*]	GBD domain of WSP-1: cytoplasm	This study

Microscopy

Nematodes were observed via a Zeiss Axioskop microscope with Nomarski optics and epifluorescence using 40x and 63x oil-immersion objectives. Animals were placed on 5% agarose pads in water or PBS containing 0.8% 1-phenoxy-2-propanol as anaesthetic. All images were taken with an Optronics MagnaFire Camera. Images were cropped and merged using the programs GIMP and Graphic Converter (Lemke Software, Peine, Germany).

Time-lapse images were taken by use of the same equipment, except that animals were anaesthetized with 10mM muscimol. Animals were kept at 20°C prior to microscopic observation. Cover slips were sealed with mineral oil to prevent desiccation of the animals.

Canal Measurements

Posterior excretory canal length was measured relative to the animal length as described in Chapter 2 and [51]. Animals were kept at 20°C and generally scored as L4 larvae. Canals that did not extend at all or remained near the cell body were scored as (0). Posterior canals that extended to between the cell body and the vulva were scored as (1), at the vulva (2), between the vulva and the tail (3), and full-length canals were scored as a (4). Cysts were counted and grouped according to size. Cysts with a diameter of over half the body width were labeled as large cysts; cysts larger than a quarter of the body diameter up to half the diameter were labeled as medium; cysts a quarter of the body diameter or smaller were labeled as small cysts. A canal that exhibited a lumen that traversed itself more than once was counted as a convoluted tubule.

Relative brightness of markers in cysts vs. non-cystic tubules was measured by use of the program NIH ImageJ. Micrographs showing the most anterior cyst of a posterior canal were used, and where possible, micrographs presenting a cyst not adjacent to other cysts were used, since two or more closely spaced cysts concentrated cytoplasm more than did a single cyst. A segmented line of width equal to the widest cyst to be measured was placed along the entire length of the canal, and plot profile was recorded. The average value of the plot profile of the same width of a dark section of the micrograph was subtracted as background. A section of non-cystic canal not overlapping out-of-focus fluorescence from other tissues or the opposite-side canal was normalized to relative brightness = 100. The brightest reading of cytoplasm at the junction of cyst and non-cystic canals was recorded as "peak brightness," while the lowest fluorescence along the center of the cyst was recorded as "trough brightness."

Results

EXC-5 dosage at the apical surface determines canal morphology

Previous work has shown that null mutation of *exc-5* in the excretory canal results in the formation of large fluid-filled cysts along the length of and especially at the distal tips of the canal (Fig. 6.1B), while strong overexpression of *exc-5* in the canal causes a "convoluted tubule" phenotype in which the apical surface and cytoskeleton maintain the correct diameter, but are wrapped inside a large cell body that fails to extend processes along the hypoderm (Fig. 6.1C) [57]. We found that microinjection of higher concentrations (>50 ng/ml) of an *exc-5*::*gfp* construct resulted in dead eggs and larvae that died at the L1 or L2 stage. Microinjection of varying concentrations of the *exc-5*::*gfp* construct at lower levels (5-25 ng/ml) resulted in progeny exhibiting tubule convolutions of severity proportionate to concentration of DNA injected (data not shown). In order to examine the subcellular location of EXC-5 within the canal, we integrated a stable low-copy-number *exc-5*::*gfp* transgene into the chromosome (integrant *qpIs78*). This integrated construct fluoresces very weakly (barely visible in a compound fluorescence microscope), and rescues the null mutant Exc-5 phenotype to create near-normal-length canals that each contain a normal-diameter lumen (data not shown). When the transgene is present homozygously in an N2 background (strain BK179), the canals are slightly shortened, and occasionally (8%) form highly convoluted tubules (Table 6.2). In addition, the diameter of the apical surface was occasionally irregular, with constricted areas (Fig. 6.1E). Examination at high magnification confirmed previous results demonstrating that the EXC-5 protein is expressed both in the cell body and throughout the length of the canal. The apical surface of the canal extends into the cell cytoplasm through a network of small vesicular tubules called canaliculi [107](Fig. 1.1C), so that apical expression generally appears as a thick layer surrounding the lumen when viewed via light microscopy. Nevertheless, we found that EXC-5 is enriched on the apical (luminal) side of the cytoplasm, but beneath the surface of the tubules (Fig. 6.1E-G). Apical clathrin (CHC-1) appears enriched in the same area of high expression as is EXC-5, which may indicate that clathrin-coated pits and EXC-5 are both found in the region of myriad tubulovesicular canaliculi that extend into the cytoplasm from the apical surface. Canal structure appears to provide a sensitive reflection of EXC-5 dosage, with the degree of shortening and convolution indicating higher levels of EXC-5 dosage at the apical surface.

Figure 6.1 – EXC-5 is Enriched at the Apical Surface and Regulates Canal Morphology

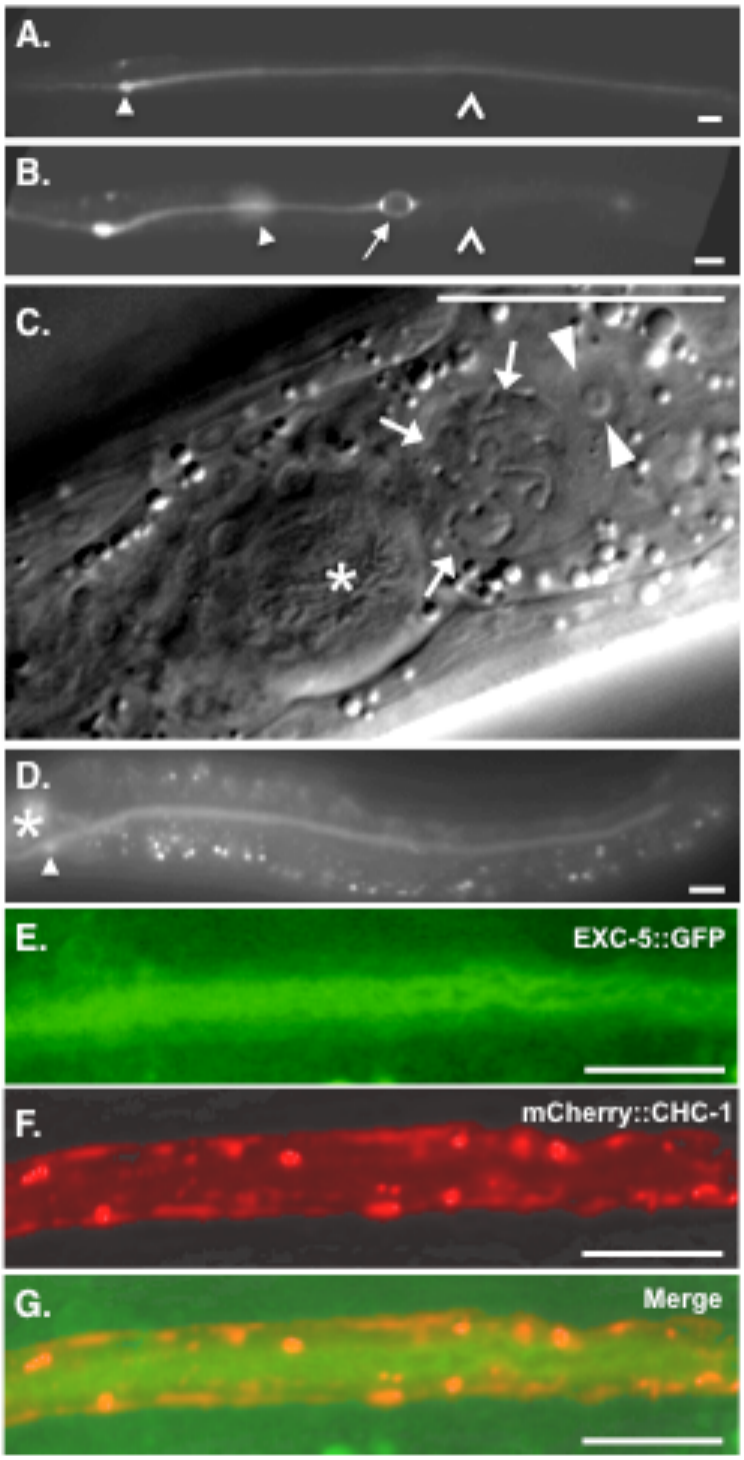

Varying expression of EXC-5 alters canal morphology. Animals in panels (A) and (B) contain the stable integrant *qpIs11*, which strongly expresses GFP driven by the *vha-1* promoter throughout the cytoplasm of the excretory canal cell and head mesodermal cell beginning in embryogenesis prior to canal extension [50]. **(A)** Fluorescence micrograph of animal wild-type for *exc-5* shows normal canal morphology. Left-hand anterior and posterior canals are shown (right-hand canal is out of plane of focus) branching from cell body (arrowhead). Open arrowhead marks position of vulva in center of animal. **(B)** Animal deleted for *exc-5* shows a posterior canal terminating in a large fluid-filled cyst (arrow) anterior to the vulva (open arrowhead). Cyst terminating opposing posterior canal is partially visible as a blur at even more anterior position (arrowhead). **(C)** DIC image of animal overexpressing *exc-5*::*gfp*. Excretory canal cell body, located just posterior of posterior pharyngeal bulb (asterisk) is filled with convoluted normal-diameter excretory tubule (arrows); nucleus of excretory cell is shown by arrowheads. **(D)** Homozygous expression of low-copy number integrant *qpIs78* (*exc-5*::*gfp*) in an N2 (wild-type) background (4 copies total of *exc-5*) caused shortening of the canals and moderate tubule convolution, but canal extension occurred, and cysts did not form. Asterisk indicates position of posterior pharyngeal bulb, arrowhead is canal cell body. **(E-G)** Higher magnification of posterior canal expressing integrated low-copy-number constructs of *exc-5*::*gfp* and membrane-delimited marker *mCherry*::*chc-1* (clathrin) indicates that EXC-5 is primarily expressed at apical (luminal) side of cytoplasm, but not on membrane surface where clathrin-coated pits form: (E) EXC-5, green; (F) CHC-1, red; (G) superimposed. Anterior is to the left in all figures, ventral to the bottom in all figures except C. All animals are either L4s or young adults. All fluorescence panels brightened and contrast-enhanced to show location of highest concentrations of weak GFP fluorescence. Bars, 100 μm in panels A and B, 50 μm in all others.

Table 6.2 - Effects of Subcellular Marker Expression on Excretory Canal Phenotype[a]

Strain/Genotype	n[b]	Convoluted[c]	Canal Length[d]	Cystic[e]	# Cysts[f]	Size of Cysts[g]		
						Small	Medium	Large
N2 (Wild-type) animals:	100	0	4.0	0				
expressing: *mCherry*::*cdc-42*	92	0	3.2	**20.7**	**0.4**	**2.0**	0	0
mCherry::*wsp-1GBD*	100	7.0	1.4	**2.0**	0	**1.0**	**1.0**	**1.0**
mCherry::*chc-1*	100	0	4.0	0				
mCherry::*eea-1*	99	0	3.3	0				
mCherry::*glo-1*	100	0	4.0	0				
mCherry::*GRIP*	100	0	3.4	0				
mCherry:*rab-5*	100	9.0	2.9	0				
mCherry::*rab-7*	100	0	2.5	0				
mCherry::*rab-11*	100	7.0	3.0	**2.0**	**0.1**	**2.5**	0	0
mCherry::*rme-1*	100	0	3.8	0				
trans. express: *gfp*::CA *cdc-42*	84	83.3	2.7	**1.2**	0	1.0	0	0
gfp::DN *cdc-42*	48	0	3.1	**56.3**	**2.8**	**2.6**	**0.2**	0
NJ731 *exc-5* (*rh232*) mutants	96	0	1.2	100	8.6	7.5	1.7	1.1
expressing: *mCherry*::*cdc-42*	100	0	1.3	100	9.8	6.9	2.3	**2.0**
mCherry::*wsp-1GBD*	104	20.2	0.5	50.0	1.8	3.8	1.1	1.0
mCherry::*chc-1*	92	0	1.4	98.9	6.4	4.4	2.2	1.2
mCherry::*eea-1*	100	0	1.6	97	5.6	4.4	2.0	1.3
mCherry::*glo-1*	100	0	1.3	98	7.8	6.0	2.2	1.2
mCherry::*GRIP*	100	0	1.1	98	8.7	6.6	2.4	1.3
mCherry:*rab-5*	99	0	1.1	100	9.0	7.6	1.9	1.3
mCherry::*rab-7*	100	0	1.2	100	**12.0**	**10.0**	2.5	1.4
mCherry::*rab-11*	100	0	1.3	99	8.3	7.3	1.9	1.2
mCherry::*rme-1*	99	0	1.3	89.9	3.8	3.4	1.8	1.4
trans. express: *gfp*::CA *cdc-42*	54	81.5	1.6	100	8.0	6.7	1.0	0.3
gfp::DN *cdc-42*	42	0	1.6	100	11.2	9.7	1.5	0.5
BK179 Low *exc-5* overexpress	100	8.0	1.5	0.0				
expressing: *mCherry*::*cdc-42*	100	84.0	0.5	**5.0**	**0.2**	**3.7**	**1.0**	**1.0**
mCherry::*wsp-1GBD*	102	14.7	1.1	0.0				
mCherry::*chc-1*	100		2.6	**1.0**	0	**3.0**	0.0	0.0
mCherry::*eea-1*	74		0.6	0.0				
mCherry::*glo-1*	100		1.3	0.0				
mCherry::*GRIP*	102		1.8	0.0				
mCherry::*rab-5*	99	13.1	1.1	**2.0**	0	**2.0**	0.0	0.0
mCherry::*rab-7*	99	37.4	0.9	0.0				
mCherry::*rab-11*	103	68.8	0.6	0.0				
mCherry::*rme-1*	100		2.1	0.0				

Table 6.2 - Effects of Subcellular Marker Expression on Excretory Canal Phenotype

[a]Substantial increases in cyst number or size from those of controls without mCherry constructs are indicated in boldface. Increases in number of convoluted tubules and decreases in number of cysts are underlined.
[b]Number of canals examined.
[c]Percentage of canals that exhibited a lumen that traversed itself more than once.
[d]Average canal length relative to body length as described in Materials & Methods; 0 means no canal growth, 4 is full-length.
[e]Percentage of canals that exhibited any visible cysts at all.
[f]Average number of cysts observed for all animals
[g]Average number of large, medium, and small cysts (size determined as described in Materials & Methods) seen for animals exhibiting cysts.

Subcellular Organelles Appear Throughout the Entire Length of the Excretory Canals

In *exc-5* mutants the canals initially form normally, but then develop large cysts predominantly at the growing tips of the tubules [48]. Since the majority of lumen initially forms with a normal diameter, it is likely that the defect in these mutants involves the continual reformation of components directed to maintain apical structure as the animal grows and moves, rather than the initial placement of cytoskeleton. During recycling, membrane-bound proteins are taken up either via clathrin-coated pits or via clathrin-independent pathways [15] (Fig. 6.2A). The material is transported via endocytic vesicles into early endosomes, where the material is either shuttled via late endosomes to lysosomes to be destroyed, or brought back to the surface by way of recycling endosomes (see Chapter 1 for more details). We examined the location of multiple components of the recycling machinery within the excretory canals by adapting a set of eight constructs expressing marker proteins specific to different subcellular organelles linked to the fluorescent tag mCherry for canal expression. We also made similar markers for the putative EXC-5 substrate protein CDC-42 (constructs generously provided by B. Grant) as well as the G-protein-binding domain of the WASP homologue WSP-1 that binds to activated CDC-42 (graciously provided by J. White, K. Kumfer, and J. Squirrell) [106], and transiently expressed constitutively-active (T17N) or dominant-negative (G12V) forms of CDC-42 (constructs generously provided by E. Lundquist). Stably integrated markers were expressed through the *exc-9* promoter in the excretory canal starting at the 3-fold stage, as well as in the uterine seam cell and several neurons [51]. The *exc-5* promoter was not used, in order to avoid the possibility that expression of the construct would deplete transcription factors specific to *exc-5* in the canal, and thereby decrease expression of EXC-5 in the cell. Under control of the *exc-9* promoter, some of the constructs did cause minor defects in canal morphology in a wild-type background (Fig. 6.2B-F) (Table 6.2). Expression of the wild-type form of the small GTPase CDC-42 linked to mCherry caused 21% of the animals to develop very small cysts near the distal tips of the canals. Expression of mCherry-linked WSP-1-GBD, which binds to GTP-bound CDC-42, greatly shortened the canals, with a widened (though only occasionally cystic) lumen diameter towards the distal end of the lumen, sometimes followed by a "tail" of cytoplasm containing no lumen (Fig. 6.2D). Transient expression of constitutively-active CDC-42 also caused formation of cytoplasmic "tails," while causing convolutions similar to those seen in animals overexpressing EXC-5. In contrast, the dominant-negative form of CDC-42 caused formation of cysts throughout the canal in a majority of animals examined, although the cysts were not quite as large or as frequent as in mutants of *exc-5*. These results are consistent with EXC-5 functioning at least in part through the activation of CDC-42 which in turn activates WSP-1.

Figure 6.2 – Expression of Subcellular Markers Has Mild Effects on Canal Morphology

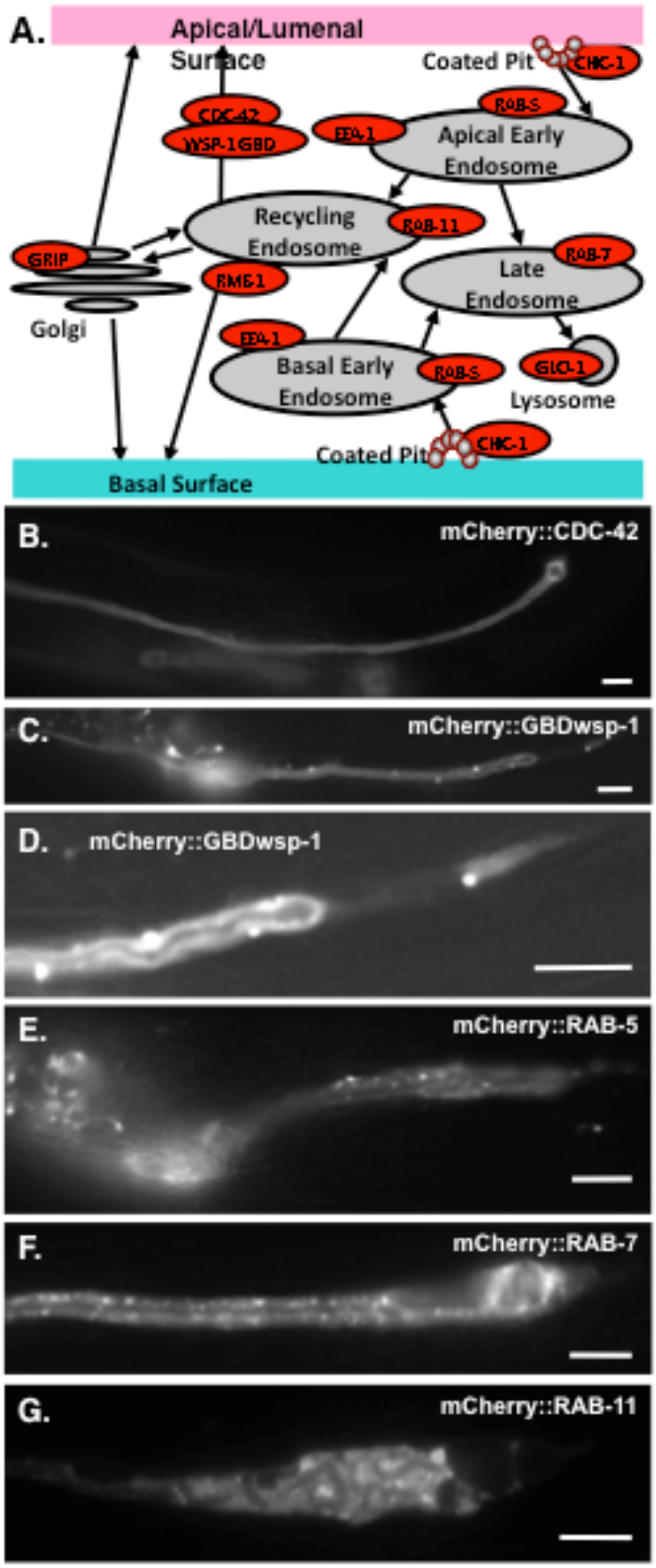

Expression of some subcellular markers within the excretory canals occasionally altered canal morphology. **(A)** Model of vesicular transport in the excretory canals, with markers used in this study to indicate various subcellular compartments. (B-J) Fluorescence micrographs of typical segments of posterior canal in young adult animals. All markers were expressed in constructs linked to mCherry and driven by the *exc-9* promoter. **(B)** Small GTPase CDC-42. **(C)** The domain of WSP-1 that binds to activated (GTP-bound) CDC-42. **(D)** Enlarged and brightened area C, of GBDwsp-1-labeled canal, shows "tail" of cytoplasm disconnected from lumen. **(E)** RAB-5; **(F)** RAB-7; **(G)** RAB-11. Bars, 50 µm. Micrographs were taken with Optronics camera either in black/white or RGB color mode, and are not altered, except for contrast enhancement of panel D and converting panel G from color to b/w.

Expression of markers labeling specific subcellular organelles had relatively smaller effects on canal morphology (Table 6.2). In 35% of canals examined, RAB-7 expression caused moderate shortening of the canal with neither cyst nor convoluted tubule formation. Expression of the endocytic vesicle marker RAB-5 had less of a canal-shortening effect (19% moderately affected), and caused a convoluted tubule in 9% of the animals. Finally, expression of the recycling endosome marker RAB-11 on occasion caused small cysts to form (2% of the animals), and also caused a convoluted tubule in 7% of the animals. In the great majority of animals expressing these constructs, however, the sensitive canal morphology was normal, consistent with marker expression not causing substantial changes in subcellular trafficking.

Expression of all 9 marker proteins was highest near the excretory canal cell body, and decreased along the length of the canals (Fig. 6.3). This distribution mirrors the placement of endoplasmic reticulum and Golgi bodies, which are also found throughout the canals as well as in the cell body [48,107]. Since cysts initially develop toward the tips of *exc-5* mutant animals during late embryogenesis [48], when the posterior canals have extended only halfway towards their full length [50], we examined expression primarily anterior to the vulva in order to compare the distribution of subcellular components in wild type and in cystic mutants. The canals are also wider closer to the excretory cell body [107,108], which facilitates determination of the apical/basal placement of vesicles in the canals.

The marker for clathrin-coated pits, CHC-1 (clathrin heavy chain), was expressed in a thin uniform layer on both the apical and basolateral surfaces of the canals, with frequent higher concentrations in discrete puncta (Figs. 6.1f-h, 6.4a). The bulk of EXC-5 expression did not overlap with the location of CHC-1.

Early endosomes, as marked by RAB-5 [109] and by EEA-1 [110], are distributed irregularly along the length of the canal (Fig. 6.4B, C). Occasional larger accumulations of EEA-1 were observed near the cell body at both the basal and apical surfaces of the canal.

Lysosomes and late endosomes were found in puncta spaced irregularly along the length of the canals (Fig. 6.4D, E). Late endosomes were marked with a RAB-7 [109] marker, while the marker GLO-1/Rab38 was used to detect lysosomes [111].

Figure 6.3 – Expression of Subcellular Markers is Highest at the Cell Body

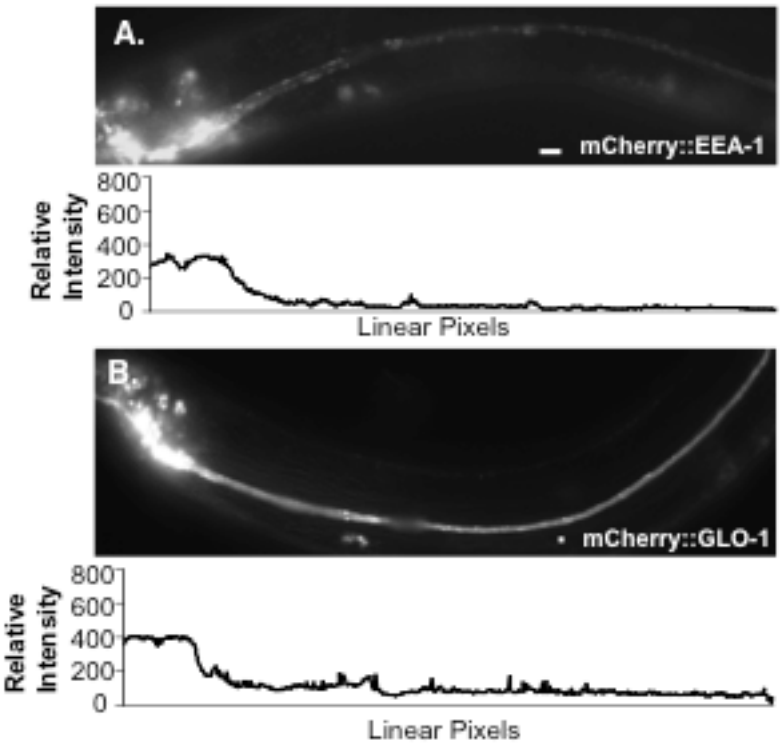

Expression of all subcellular markers is highest at the cell body, but proteins are apparent throughout the length of the canals. **(A)** Early endosome marker EEA-1. **(B)** Lysosomal marker GLO-1. Relative brightness along the length of the canals is shown beneath each panel, normalized to normal-diameter canals brightness midway along the posterior canal length. Micrographs were taken with Optronics camera either in black/white or RGB color mode, and are not altered, except that panel A was converted from color to b/w of equivalent brightness. Bars, 50 μm.

Figure 6.4 – Distribution of Subcellular Organelles in the Excretory Canal

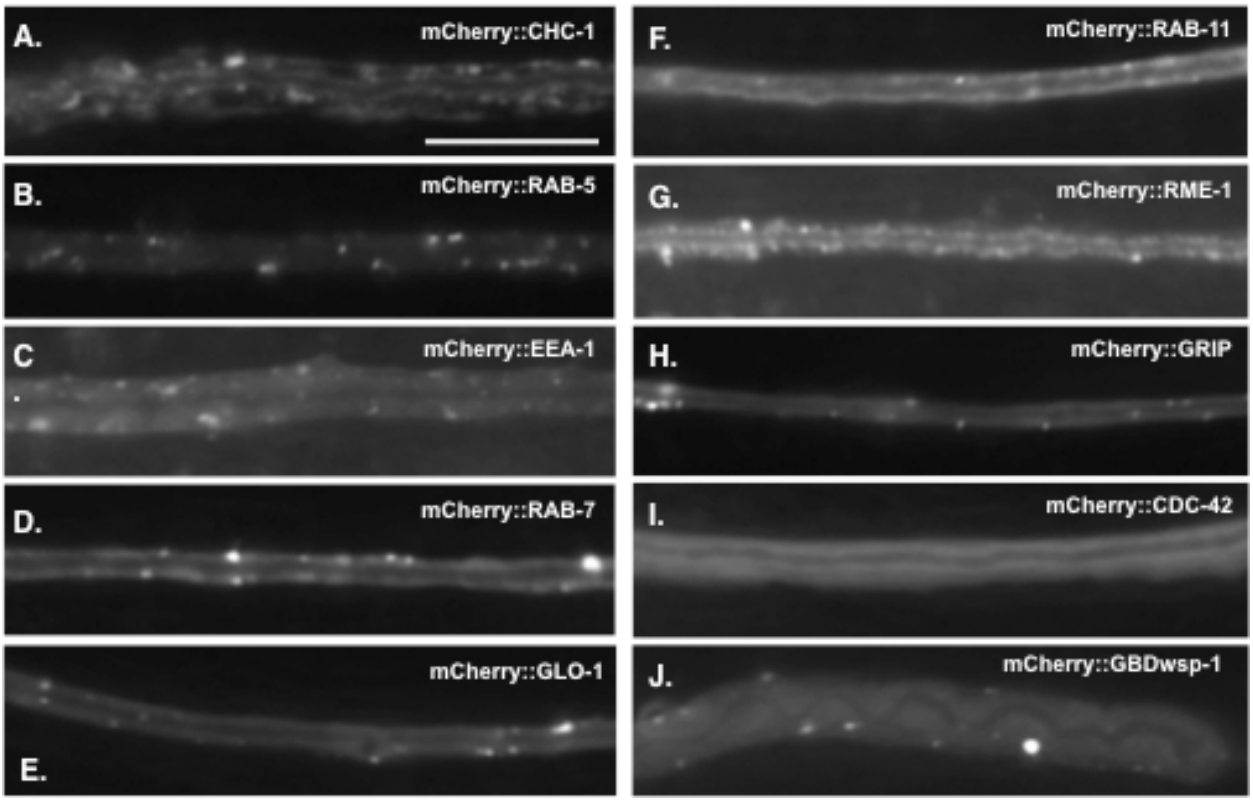

Expression of subcellular markers within the excretory canals in wild-type animals. Fluorescence micrographs of typical segments of posterior canal in young adult animals. All markers were expressed in constructs linked to mCherry and driven by the *exc-9* promoter. Bar, 50 µm. **(A)** CHC-1; **(B)** RAB-5; **(C)** EEA-1; **(D)** RAB-7; **(E)** GLO-1; **(F)** RAB-11; **(G)** RME-1; **(H)** GRIP; **(I)** CDC-42; **(J)** WSP-1 GTP-binding domain.

Recycling endosomes were marked by RAB-11 and RME-1 [112,113] (Fig. 6.4F, G). RAB-11 displayed mainly diffuse expression throughout the cell, with a few puncta irregularly placed along the canals. RME-1-marked vesicles were generally larger and far more numerous than were puncta labeled by RAB-11. In both cases, the number of puncta was highest near the cell body, but puncta were evident throughout the entire length of the canals.

Golgi bodies, marked by a Golgi-targeting GRIP domain [114,115] were also seen throughout the canals, though most prominently near the cell bodies (Fig. 6.4I). GRIP expression also was punctate throughout the distal canals. Finally, CDC-42, the presumptive target of EXC-5, was expressed diffusely throughout the cytoplasm of the excretory canals, with highest expression levels towards the apical surface of the canals. Expression of GBD-WSP-1 linked to mCherry, marking activated CDC-42, showed expression throughout the cytoplasm similar to that of CDC-42, but in addition appeared as occasional puncta throughout the canal (Fig. 6.4J).

All of the markers were evident throughout the length of both growing and adult full-grown canals, which suggests that material throughout the canals is steadily and continually being taken up from canal surfaces and recycled, while material from the Golgi bodies can be transported to the canals.

Loss of EXC-5 Activity Disrupts Endosome Morphology

In order to determine if EXC-5 mediates endocytic trafficking, as has been found for CDC-42 [38], the subcellular marker expression constructs were crossed into the *exc-5*(*rh232*) null allele strain. Cyst formation caused canal cytoplasm to accumulate at the point where the tubule widened, and between adjoining cysts, as seen via a cytoplasmic GFP marker (Fig. 6.5A). The distribution of labeled CHC-1, CDC-42, GBD-WSP-1, RAB-7, GLO-1, RAB-11, and GRIP was generally unaffected by loss of EXC-5 activity, as compared to the cytoplasmic GFP controls (Fig. 6.6) (Table 6.3). The placement, approximate number, and distribution of puncta in these mutants appeared quite similar to their expression in wild-type animals, with similar amounts of marked clathrin-coated pits, late endosomes, and lysosomes.

Loss of EXC-5 activity often caused a strong effect on the distribution of EEA-1 and RME-1 markers, however, as well as some infrequent but large effects on RAB-5 distribution (Table 6.3, Fig. 6.5). Early endosome marker EEA-1 was no longer seen in discrete puncta, but rather accumulated into large irregular shapes. These accumulations were often evident in the areas of the canals immediately adjacent to and surrounding the large cysts. In the majority of canals, the accumulation of labeled EEA-1 surrounding the cysts appeared substantially brighter than in the normal-diameter tubule anterior to the cyst. Labeled RAB-5 (marking early endosomes) was also sometimes enriched near cysts in *rh232* animals, but while these accumulations were much brighter than for most markers, the frequency of RAB-5 accumulations was similar to that of cytoplasm surrounding the cysts.

Figure 6.5 – *exc-5* lof Mutants Affect EEA-1 and RME-1 Distribution

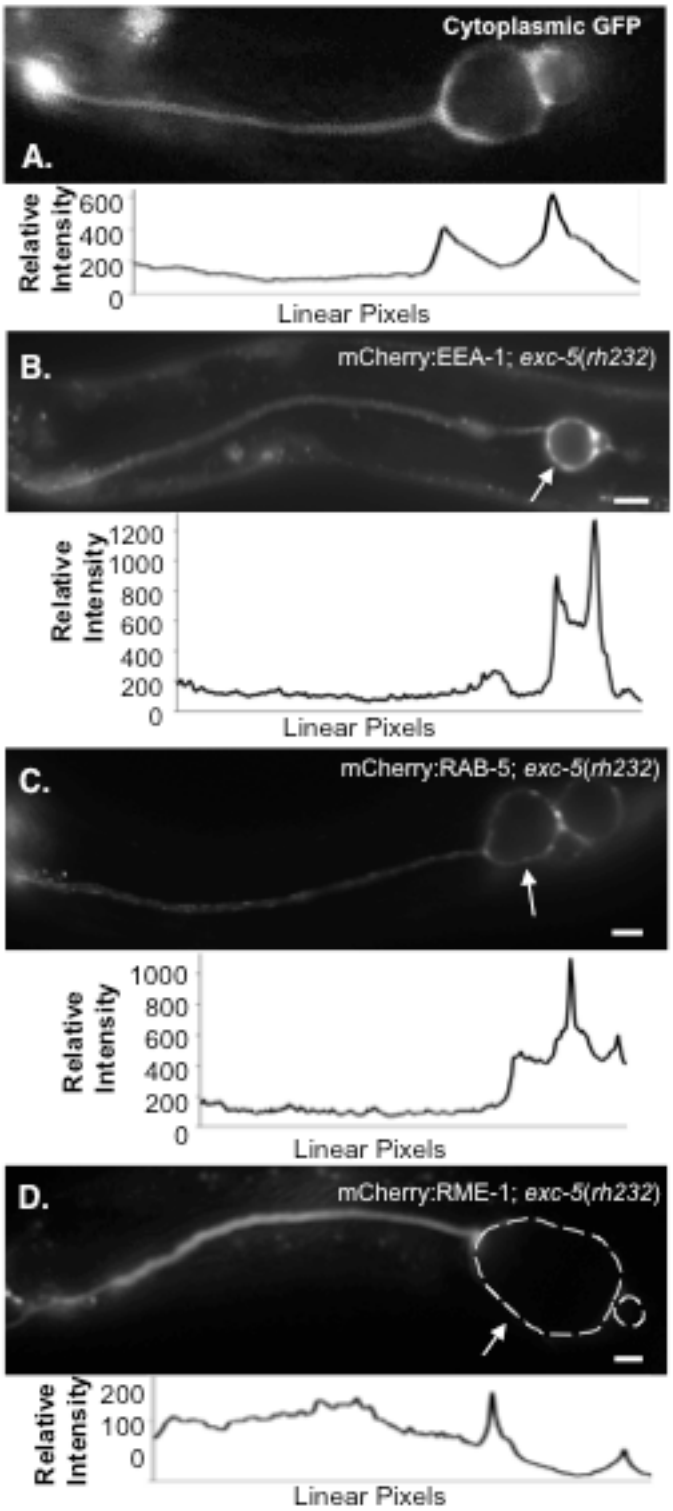

Effect of loss of EXC-5 on subcellular marker distribution. Young adult animals of *exc-5* (*rh232*) expressing integrated constructs containing subcellular markers. Relative brightness along the length of the canals is shown beneath each panel, normalized to normal-diameter canal brightness midway along the posterior canal length.
(A) Animal expresses cytoplasmic GFP driven by the strong canal-specific *vha-1* promoter. (B-D) Animals express subcellular markers linked to mCherry, and driven by the *exc-9* promoter; stronger expression altered canal morphology.
(B) EEA-1. Highest levels of expression surround area of fluid-filled cysts at canal terminus (arrow).
(C) RAB-5 shows higher levels of expression surrounding the cyst than in normal-diameter tubule.
(D) RME-1. Dashed grey circles outline lumen of large fluid-filled cysts (arrow) at canal terminus. Bars, 50 µm.

Figure 6.6 – *exc-5* lof Mutants do not Effect Most Subcellular Markers

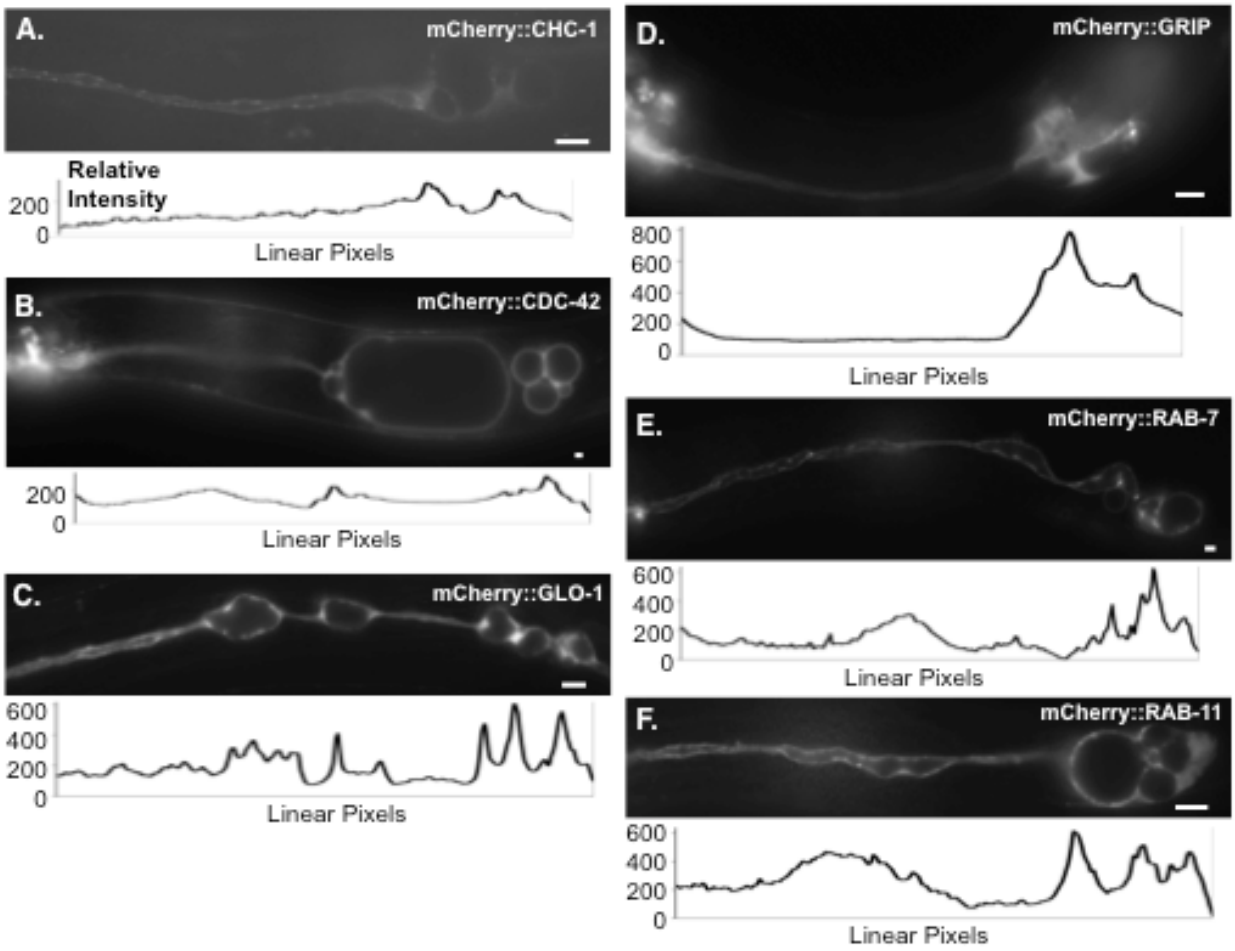

Loss of EXC-5 does not affect distribution of many subcellular markers (as compared to results in Fig. 6.4). Typical examples of young adult animals of *exc-5* (*rh232*) containing integrated constructs of subcellular markers linked to mCherry driven by the *exc-9* promoter. **(A)** CHC-1; **(B)** CDC-42; **(C)** GLO-1; **(D)** GRIP; **(E)** RAB-7; (F) RAB-11. Bars, 50 µm. Micrographs were taken with Optronics camera either in black/white or RGB color mode, and are not altered.

Table 6.3 - Effects of loss of EXC-5 on marker expression

Strain/Genotype	N[a]	% of animals with cysts noticeably brighter than in normal tubule[b]	% of animals with cysts noticeably fainter than in normal tubule
exc-5 mutants expressing:			
cytoplasmic GFP (P_{vha-1}::*gfp*)	250	28	0
mCherry::*cdc-42*	135	34	0
mCherry::*GBDwsp-1*	80	24	0
mCherry::*chc-1*	90	17	4
mCherry::*eea-1*	207	58	0
mCherry::*glo-1*	100	26	0
mCherry::*GRIP*	100	28	0
mCherry:*rab-5*	100	24	0
mCherry::*rab-7*	100	23	0
mCherry::*rab-11*	135	30	0
mCherry::*rme-1*	100	0	31

[a]Number of canals examined.
[b]Number of animals graded as "bright" was normalized to account for variations in brightness between wild-type animals viewed in different counting sessions.

Most strikingly, labeled RME-1 was the only marker to exhibit a strong and opposite phenotype: Other than near the excretory cell body, the amount of labeled RME-1 was severely depleted throughout the canals, and almost entirely absent in the cytoplasm surrounding large cysts. Taken together, these results suggest a defect in recycling endosome transport in *exc-5* mutants, similar to the defects previously reported in *C. elegans* coelomocytes upon depletion of CDC-42 via RNAi [116], in that material appears to be taken up normally into canal early endosomes, but is unable to be passed further into recycling endosomes.

Overexpressed EXC-5 Affects Recycling Endosomes

The subcellular markers were also crossed into strains containing the integrated *exc-5*::*gfp* construct. Overexpression of EXC-5 also showed little effect on most of the subcellular markers (Fig. 6.7), but showed strong interactions with RME-1 and EEA-1 (Fig. 6.8). Overexpression of *exc-5* together with the *rme-1* marker caused higher than normal accumulation of RME-1::mCherry puncta, whereas the level of labeled EXC-5 became depleted (Figs. 6.8a-c), consistent with a model in which EXC-5 ferried excess amounts of material from early endosomes to recycling endosomes. The effect of *exc-5* overexpression was even more striking when combined with the *mCherry::eea-1* marker. Expression of homozygous *mCherry*::*eea-1* was lethal in the homozygous *exc-5*::*gfp* strain; animals died during late embryogenesis, though no effects on canal morphology were obvious (Fig. 6.8D-F). Heterozygous expression of the *eea-1*::*mCherry* construct in animals homozygous for the *exc-5*::*gfp* integrated transgene allowed animals to survive, and showed somewhat fewer, but larger, puncta of mCherry::EEA-1 along the apical surface (Fig. 6.8G-I). Both loss and overexpression of EXC-5 activity therefore perturbed EAA-1- and RME-1-marked endosomes.

EXC-5 Interacts with the Rho GTPase CDC-42

The human EXC-5 homologue FGD1 activates the small Rho-GTPase CDC42 when overexpressed in 3T3 fibroblasts in tissue culture [75]. As noted above, in *C. elegans*, overexpression of *mCherry*::*cdc-42* increased the formation of small cysts along the length of shortened canals in wild-type, *exc-5* mutant, and *exc-5*-overexpressing animals (Table 6.2). Expression of *mCherry*::*cdc-42* in animals that overexpressed EXC-5 resulted in substantially shorter, more convoluted tubules. In those convoluted excretory cells, the location of CDC-42 expression is strongly concentrated around the area of the canals where the convoluted tubules and their associated canaliculi are located (Fig. 6.9A). This is the same area where EXC-5 is concentrated in these cells (Fig. 6.9B, C), consistent with the evidence from Table 6.2 that EXC-5 acts at least in part through activation of CDC-42.

Figure 6.7 – EXC-5 Overexpression does not Alter Most Subcellular Markers

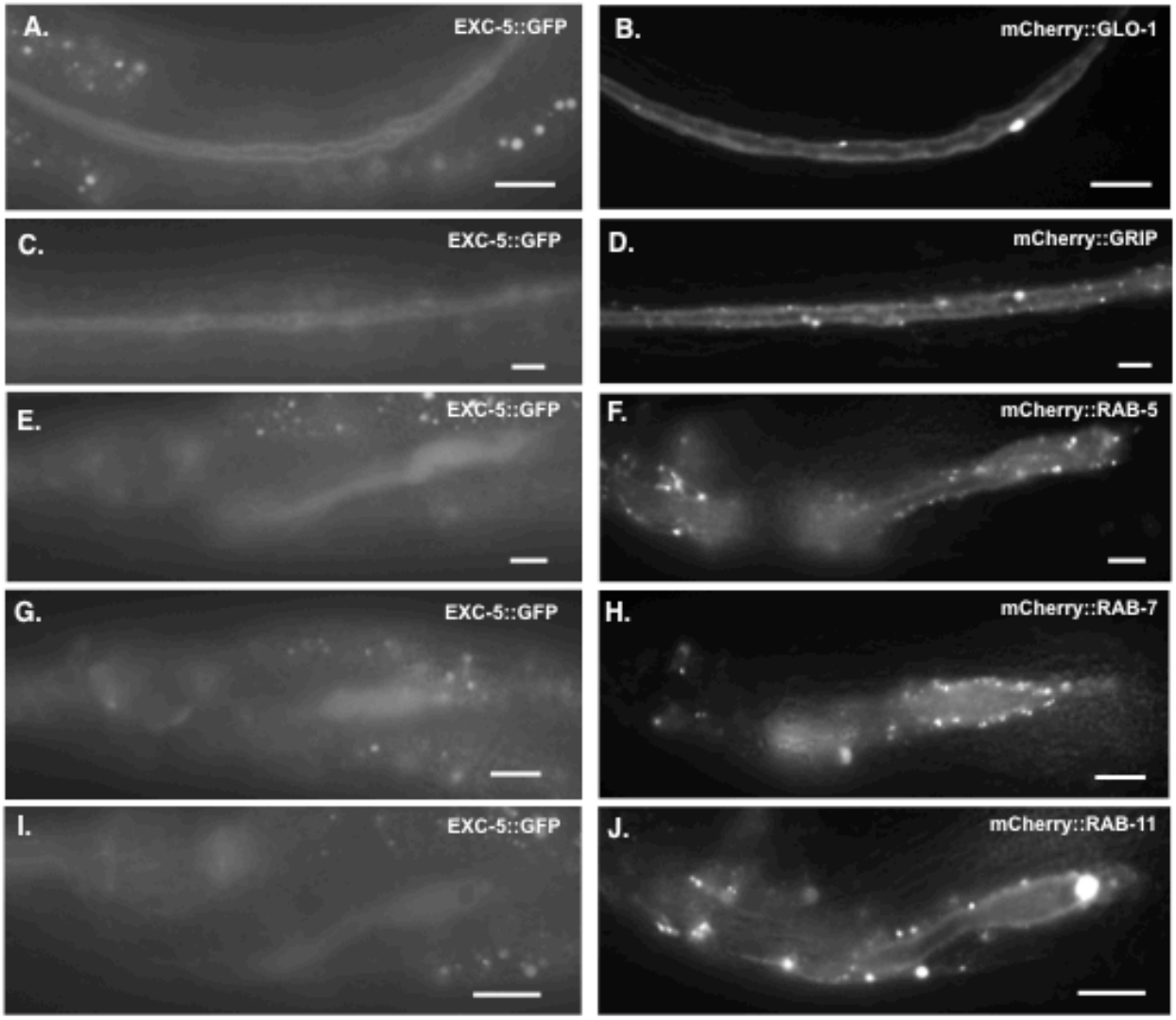

Overexpression of *exc-5* does not alter distribution of most subcellular markers. Excretory canal cells of young adult animals containing integrated homozygous *exc-5*::*gfp* constructs in addition to integrated constructs of subcellular markers linked to mCherry driven by the *exc-9* promoter. Left-hand panels show weak fluorescence of low overexpression of EXC-5::GFP as control, and right-hand panels show expression of mCherry-linked subcellular markers: **(A, B)** GLO-1; **(C, D)** GRIP; **(E, F)** RAB-5; **(G, H)** RAB-7; **(I, J)** RAB-11. Bars, 50 µm.

Figure 6.8 – EXC-5 Overexpression Alters RME-1 and EEA-1 Distribution

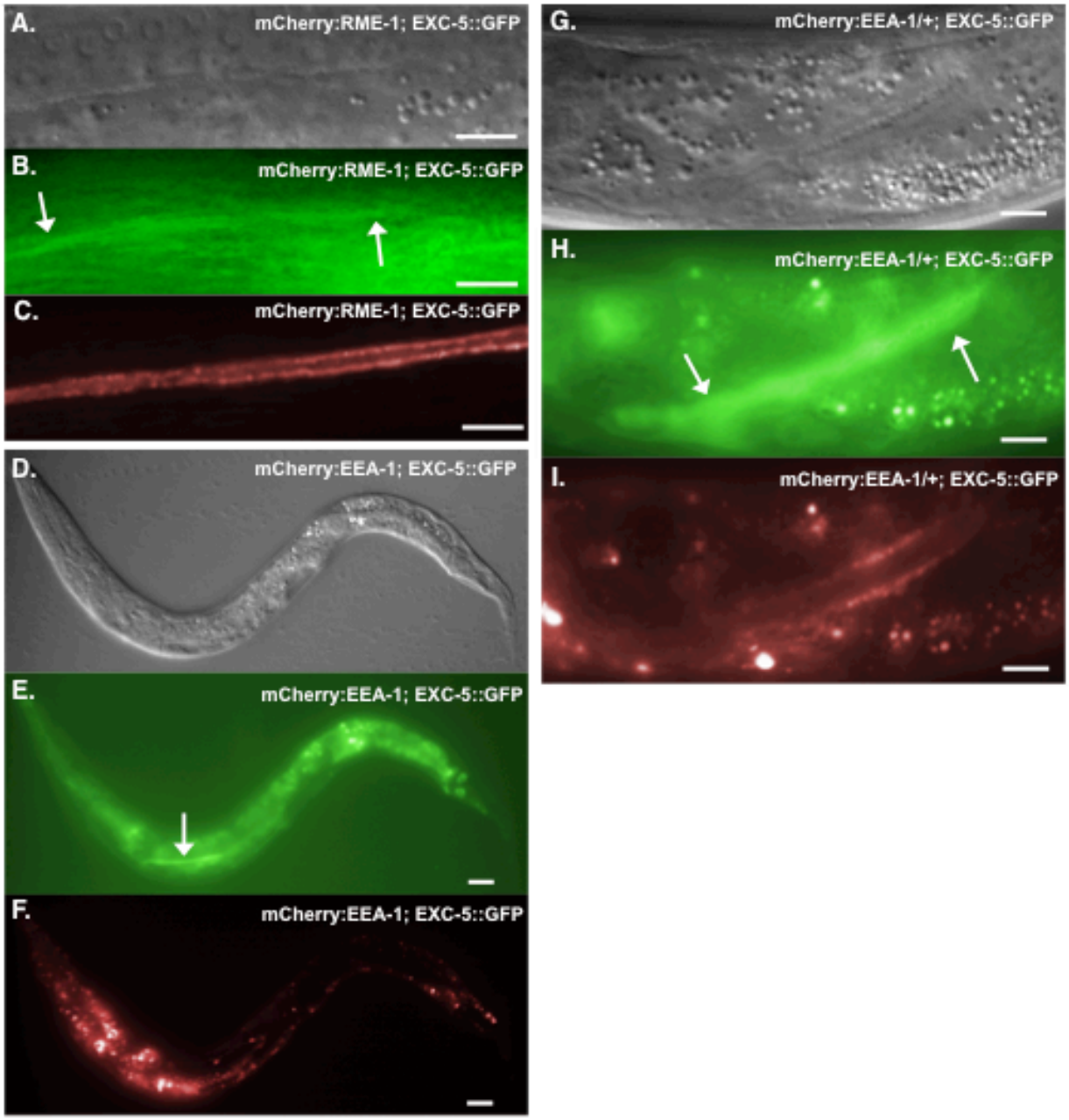

EXC-5 overexpression alters subcellular marker distribution. Excretory canal cells of young adult animals containing integrated homozygous *exc-5*::*gfp* constructs, in addition to integrated constructs of subcellular markers linked to mCherry driven by the *exc-9* promoter**. (A-C)** RME-1; **(D-F)** Dying L1 larva homozygous both for *mCherry*::*eea-1* and for *exc-5*::*gfp* (in a background wild-type for *exc-5*); **(G-I)** Young adult animal heterozygous for *mCherry*::*eea-1* and homozygous for *exc-5*::*gfp* (in a background wild-type for *exc-5*). Panels A, D, G, DIC image; panels B, E, H, expression of EXC-5::GFP; images contrast-enhanced to emphasize position of very weakly fluorescent GFP (especially in B, in which GFP expression was very low). Arrows indicate position of canal. Panels C, F, I, expression of markers linked to mCherry. Bars, 50 µm.

Figure 6.9 – CDC-42 and EXC-5 are Enriched at the Lumen

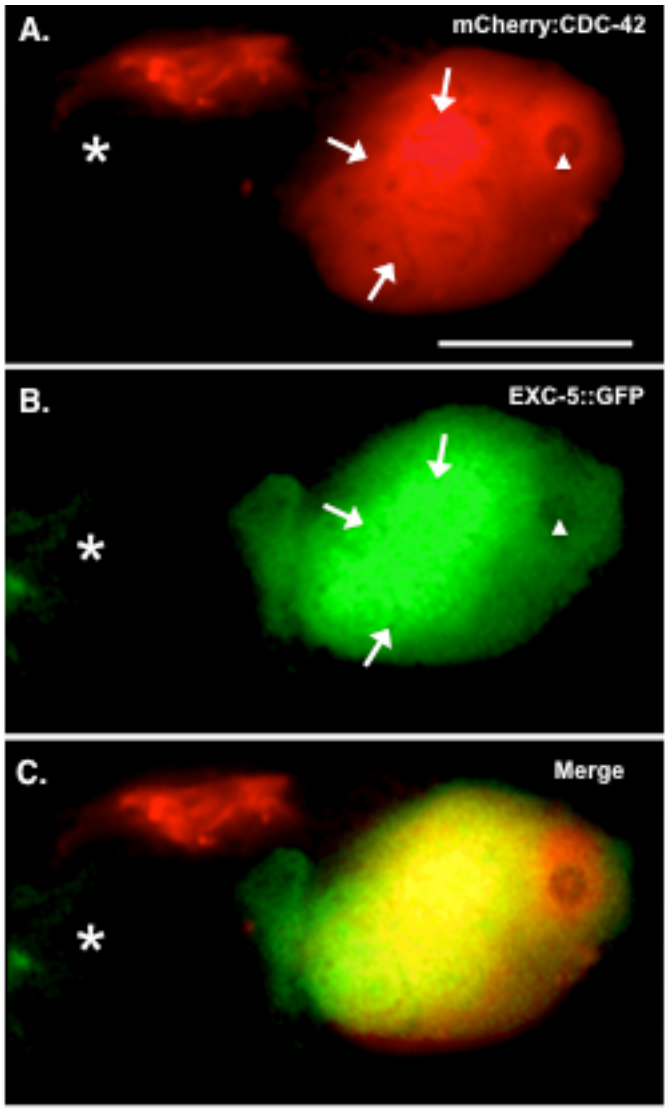

Subcellular location of EXC-5 and activated CDC-42 in convoluted excretory canal tubule of animal expressing both homozygous *mCherry*::*cdc-42* and functional *exc-5*::*gfp* constructs. DIC image of this animal's excretory canal cell body is shown in Fig. 6.1C. Arrows indicate area filled with convoluted tubule and associated canaliculi, arrowhead indicates cell nucleus, and asterisk indicates location of neighboring posterior pharyngeal bulb.
(A) mCherry::CDC-42 is concentrated around the convoluted tubular area, with some elevated expression also evident surrounding the nucleus (arrowheads).
(B) EXC-5::GFP is strongly concentrated in the subapical region surrounding the convoluted excretory canal tubule and canaliculi.
(C) Merged micrographs. All photographs false-colored and contrast-enhanced to show areas of highest expression. Bar, 50 μm.

Accumulation of Early Endosomes Precedes Cyst Formation

To test whether the accumulation of early endosomal material adjacent to cysts was the cause or a result of cyst formation, we examined the expression of early endosomal marker EEA-1 (Fig. 6.10) and recycling endosomal marker RME-1 in *rh232* animals prior to and during the formation of excretory canal cysts (data not shown). Other strains examined included BK30, BK36, BK209, BK204, BK221, BK217, BK215, BK212, and BK231; looking at CDC-42, CHC-1, RAB-5, and RAB-11 expression over time (data not shown). Cysts initially formed in the late stages of embryogenesis and early first larval stage. Cysts formed suddenly and were initially small in size. In *exc-5* mutants, these cysts formed at the end of both anterior and posterior canals, but occasionally developed in additional isolated areas along the length of the canal.

The EEA-1 marker showed altered expression during the process of cyst formation. In animals containing only the *mCherry*::*eea-1* integrant, there was little visible EEA-1 accumulation along the length of the canal even after the animal hatched. When expressed in *rh232* animals, however, there appeared strong build-ups of mCherry::EEA-1 during embryogenesis in regions of the canal prior to cyst formation (Fig. 6.10). Continuous observation of these canals showed the rapid development of cysts at the locations where EEA-1::mCherry had accumulated. Since expression of EEA-1 precedes the appearance of cysts, we conclude that the abnormal buildup of apical early endosomes in *exc-5* mutants causes weakening of the apical cytoskeleton that allows collapse of the tubule into fluid-filled cysts. We conclude that disruption of EXC-5-mediated endosome regulation precedes and is likely the cause of failure of the apical surface leading to cyst formation.

Figure 6.10 – Accumulation of EEA-1 Precedes Cyst Formation

.

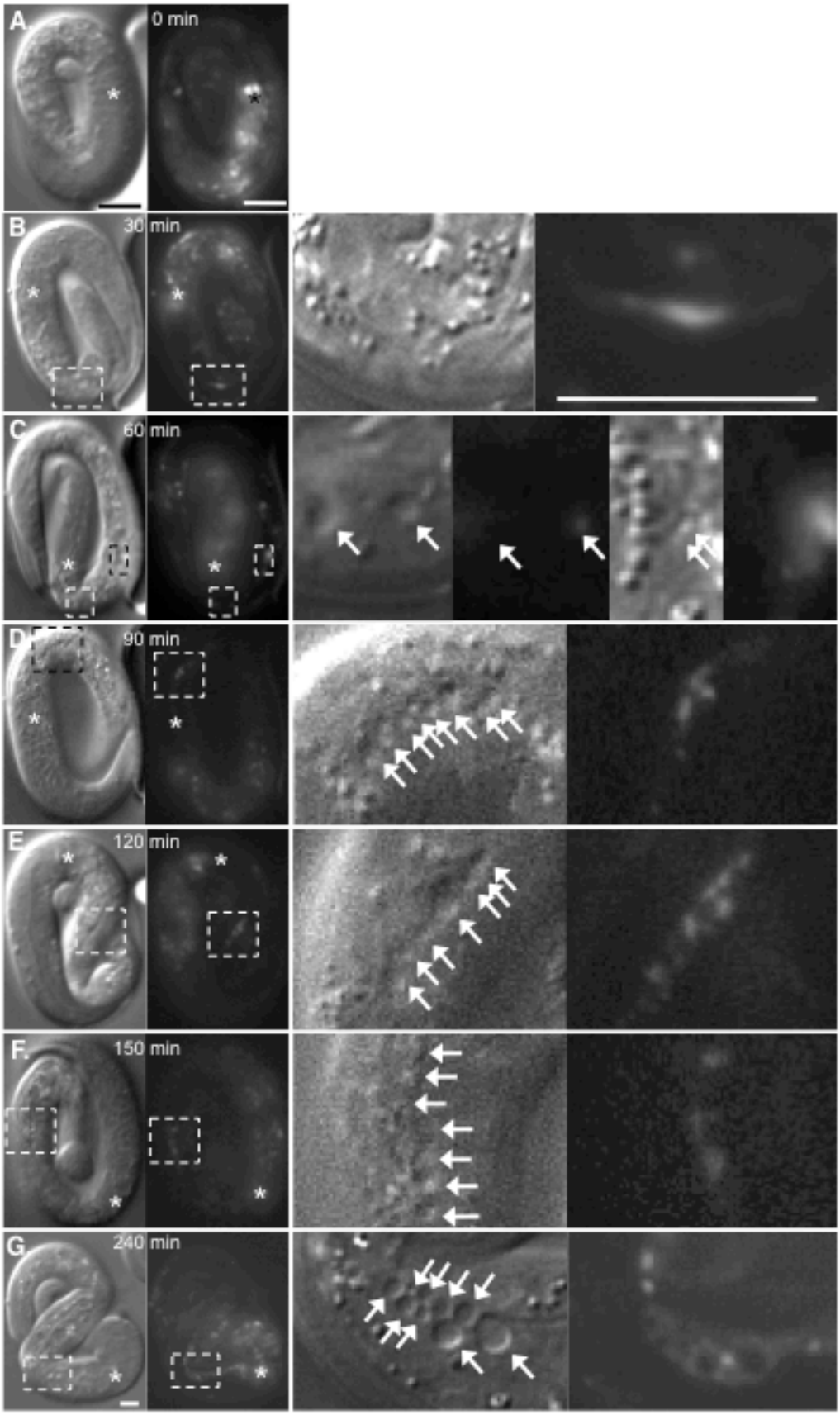

Figure 6.10 – Accumulation of EEA-1 Precedes Cyst Formation

Alteration of subcellular marker expression precedes cyst formation in *exc-5* (*rh232*) animals. **(A-G)** DIC and fluorescence micrographs of a single animal expressing *mCherry*::*eea-1* driven by the *exc-9* promoter, beginning at the 3-fold stage of embryogenesis. Expression is evident in many head neurons at this stage as well as in the excretory canal cell. Images were taken at the times indicated, starting at the point at which observation of the animal began. Wild-type embryos hatch within 2 hours of the 3-fold stage at 20°C [45]. Cysts appear in DIC micrographs with DIC "shadow" to the upper left of the cyst. Gut granules and other subcellular organelles show a DIC "shadow" to the lower right of the object. Animal was moving inside the embryo; DIC and fluorescence micrographs show similar positions, but cannot always be directly overlaid. Boxed areas indicate the same areas of the animal, and are enlarged in panels to the right. An asterisk designates the posterior pharyngeal bulb. Arrows in enlarged DIC micrographs show cysts. **(A)** No cysts were evident in the canals, and *eea-1* expression was barely detectable in the left-hand posterior canal. **(B)** Localized *eea-1* accumulation is evident in the canal, while no cysts have formed. **(C)** The area expressing *eea-1* in panel B now shows small cysts (right-hand enlarged panels), while *eea-1* expression is now evident in a new area near the cell body (left-hand enlarged panels). **(D-F)** *eea-1* expression persists throughout this area of the posterior canal as cysts become evident. **(G)** By the time of hatching, *eea-1* expression has spread and intensified, many new cysts have formed, and cysts have greatly enlarged. Brightness and contrast was enhanced in DIC micrographs only to show cysts more clearly. Fluorescence micrographs were brightened and contrast increased to show areas of greatest canal fluorescence. In enlarged panels, DIC micrographs only were digitally sharpened. Bars, 50 μm.

Discussion

EXC-5 mediates movement of material from apical early endosomes to recycling endosomes

All cells must constantly recycle and move material in order to accommodate growth and movement of the animal. For narrow single-celled tubules, recycling is especially important. Osmotic pressure constantly exerts force to expand the tubule. Nematodes continuously bend back and forth, additionally stressing the narrow excretory canals. In the excretory canals, loss of proteins at the basolateral surface causes misdirection and shortening of tubule outgrowth, but does not affect lumen diameter [67,117]. Failure of the apical surface allows osmotic pressure to form fluid-filled cysts rapidly. EXC proteins thus prevent loss or weakening of the apical canal surface [48]. As seen here and in previous work, overexpression of EXC-5, EXC-9, or constitutively-active CDC-42 proteins allows the tubule to form and maintain a normal diameter, but prevents extension of the canals along the basal surface, which results in a convoluted tubule [51,57]. Similar results have been seen in *C. elegans* mosaic animals deficient in basolateral or basement membrane proteins (integrin, laminin) [66,67], as well as in the narrow single-celled tubular termini of *Drosophila* trachea deficient in talin or integrin [6]. We infer that EXC proteins that mediate intracellular trafficking primarily exert their effects on movement of vesicles to or from the apical surface, but that overexpression of these proteins can prevent normal basolateral trafficking as well.

Expression of multiple labeled markers for subcellular compartments found that all of these compartments are at greatest concentration near the excretory cell body, but are all present throughout the length of the canals. These results confirm previous electron micrographic studies that showed endoplasmic reticulum, Golgi, multivesicular bodies, lysosomes, and a myriad of tubulovesicular structures throughout the excretory canals, especially near the apical (luminal) surface [48,107].

The results presented in this chapter show that EXC-5 plays a critical role in returning material to the apical surface in the canals. When *exc-5* is deleted, most of the mCherry-labeled markers retained the position and intensity observed in wild-type animals, with the exception of labeled EEA-1 and RME-1. Without EXC-5 present, RME-1/EHD, found on labeled recycling endosomes [31,112,118], appeared gradually depleted, while EEA-1, a marker for early endosomes, abnormally accumulated. EEA-1 formed large irregular accretions especially surrounding cysts. Such enlarged endosomes are a hallmark of blocked recycling [119,120]. Most strikingly, progressive studies showed that the accumulations of EEA-1 formed at these locations prior to the formation of cysts, and could in fact be used to predict the sites of cyst formation. We infer that EXC-5 is needed for the transport of material from apical early endosomes to recycling endosomes. In this model (Fig. 6.11), when EXC-5 is missing, apical surface proteins that guide reformation and strengthening of the cytoskeleton are taken up into endocytic vesicles, but cannot pass further into recycling endosomes to be returned to the surface, so that the apical cytoskeleton is not maintained, ultimately to collapse (Fig. 6.11B). When *exc-5* is overexpressed, the apical surface is maintained or in severe cases constricted; we hypothesize that so much material is passed

to the apical surface that traffic to the basal surface is slowed and eventually depleted, leading to inability of the canal to extend properly, so that the cell forms convoluted tubules of normal diameter inside an enlarged cell body (Fig. 6.11C). Such a balance of apical to basal endocytic trafficking mediated by Rho proteins such as Cdc42 has been found to be important for the maintenance of polarity in mammalian epithelial cells [38,121].

The Excretory Canals Are a Sensitive Indicator of Endosomal Movement and Structure

The labeled markers used here have previously been found to label distinct structures in nematode intestinal cells and coelomocytes [15,122,123]. Although the distance from apical to basal surface is much smaller in the canals vs. wide intestinal cells, the markers labeled distinct locations within the canals. In addition, the great length of the canals (the longest cell in the organism) provides a sensitive indicator of the effects of trafficking on cell structure. The distance from nucleus to distal cell surfaces is magnified, so that differences in endosome concentration along the length of the canals are easily apparent. As a result, mild changes in the dose of EXC-5 produced rapid formation of easily detectable cysts, or of convolutions in the path of the canals.

Expression of a few of the markers by themselves occasionally showed effects on canal structure. In some cases, this expression caused the luminal surface of the canal cell to dissociate from the basal surface, which resulted in formation of a narrow "tail" of cytoplasm without a lumen (Fig. 6.2D). This 'tailing' effect was seen consistently in animals overexpressing EXC-5 in conjunction with any of the subcellular markers. Expression of marked RAB-5 or RAB-11 at low but significant penetrance (7-9%, Table 6.2) caused the canals to exhibit the convoluted canal structure caused by overexpression of functional EXC-5 or EXC-9 [51], in which the apical tubule is maintained at its proper diameter and length, but the basal surface fails to extend. One possible explanation is that overexpression of any of these proteins increases the rate of turnover of material from the apical surface, which then monopolizes the recycling pathways such that membrane proteins from the basal surface are not efficiently recycled. Overexpression of RAB proteins can alter the ratio of material passed through different pathways; e.g. in mammalian cells, RAB-11 overexpression forced material away from movement into lysosomes towards greater amounts of recycling [124,125]. Expression of constitutively activated RAB-5 causes the formation of enlarged endosomes [126,127], but that effect was not seen here in canals with wild-type levels of EXC-5. In canals overexpressing EXC-5, surprisingly, expression of labeled EEA-1 did cause enlargement of endosomes. It will be interesting to observe the effects on canal structure caused by manipulation of other proteins that regulate trafficking.

Figure 6.11 – A Model for EXC-5 Function in Membrane Trafficking

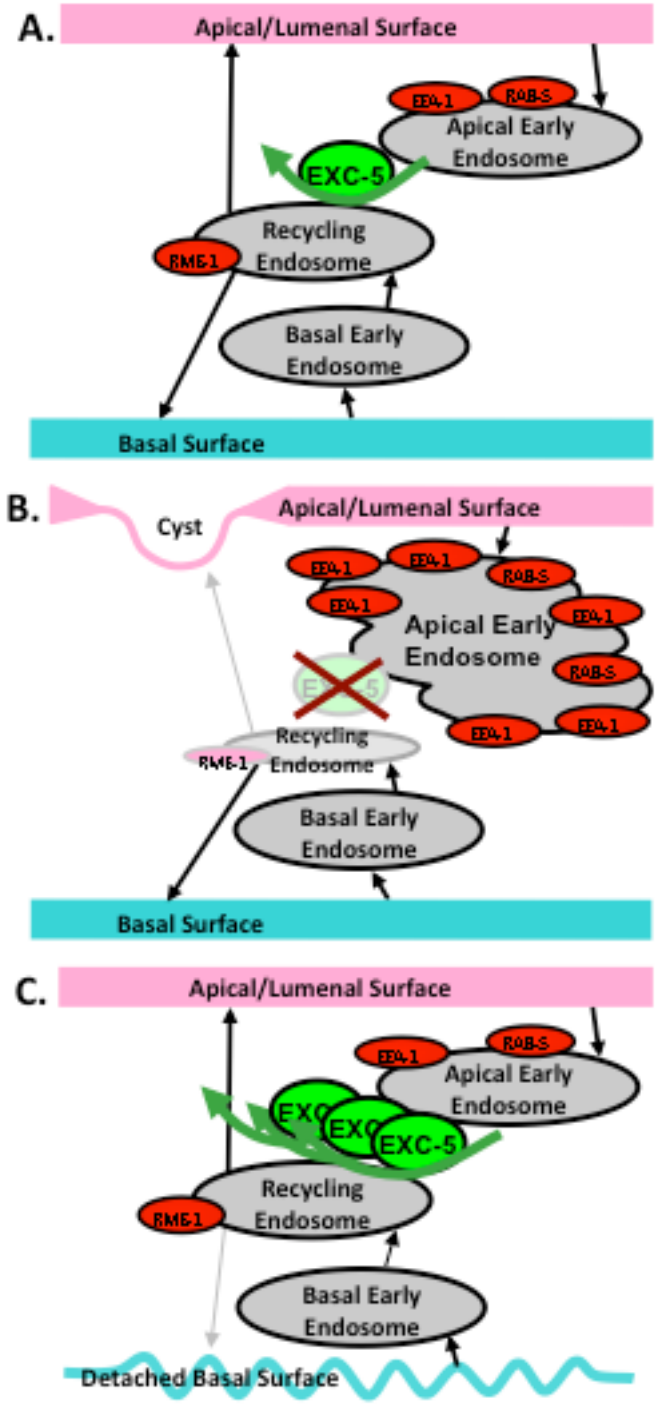

Model for effects of EXC-5 on organelle movement. **(A)** EXC-5 mediates the passage of early endosomes to recycling endosomes, presumably through activation of CDC-42 as well as other small GTPases. **(B)** Loss of EXC-5 through mutation prevents movement of apical early endosomes, marked by RAB-5 and especially by EEA-1, which then accumulate. As less material is moved into the recycling endosome, the expression of the recycling endosome marker RME-1 is depleted. Loss of membrane-bound proteins at the apical surface cause weakening of this surface, eventually to break under osmotic pressure from the canal lumen, to form a fluid-filled cyst.
(C) Overexpression of EXC-5 enhances apical recycling, so that the apical surface is maintained and lumen diameter remains narrow. The large amount of apical material passing through the recycling endosome prevents efficient passage of material from the basal early endosome, presumably including membrane proteins such as integrins that bind to the basement membrane. Slow recycling of these proteins to the basal surface allows delamination of these cells to occur, as seen in animals overexpressing *exc-5* [57], and extension of the canals is halted.

EXC-5 as a Model for FGD Activity

EXC-5 is homologous to the FGD family of four mammalian guanine exchange factors [56,57]. These genes include FGD1, which is defective in Aarskog-Scott Syndrome, a developmental syndrome in which the skeleton of the jaws and limbs are malformed [58]; and FGD4, the locus of Charcot-Marie-Tooth Syndrome Type 4H (CMT4H), a muscular dystrophy [59]. FGD1 has been shown in 3T3 cells to activate the Rho-GTPase CDC42, but also had other effects not mediated through CDC42 [77,78]. We found similar effects here. Transient expression of constitutively active CDC-42, as well as stable expression of the small GBD-WSP-1 (which binds to activated CDC-42 [106], both exerted effects on the canal similar to that of EXC-5 overexpression. Both in wild-type animals and mutants lacking EXC-5 function, expression of WSP-1 GBD caused shortening of the canals and formation of convoluted tubules, similar to the effects of EXC-5 overexpression (Table 6.2). Transient expression of constitutively active CDC-42 had the same effect in wild-type animals. In addition, when the *exc-5* gene was overexpressed, expression of WSP-1 GBD had little further effect on canal morphology, consistent with EXC-5 overexpression having already activated CDC-42. Finally, transient expression of dominant-negative CDC-42 in wild-type worms caused defects in canal morphology similar to that caused through loss of EXC-5 activity. We infer that EXC-5 and WSP-1 GBD may cause similar effects on CDC-42 by causing an increase in the amount of this GTPase present in the activated, phosphorylated, form.

On the other hand, we saw no obvious differences in the location of labeled GBD-WSP-1 in the canals when EXC-5 was present or deleted. GBD-WSP-1 labeled some puncta, but most of the expression of both GBD-WSP-1 and CDC-42 was cytoplasmic, so it is not clear if activated CDC-42 would have been easily evident in these animals. While constitutively-active CDC-42 did not rescue the cystic phenotype in *exc-5* mutants, it is worth noting that overexpression of GBD-WSP-1 had the strongest rescuing effects of any gene tested. As mentioned above, expression of GBD-WSP-1 in an *rh232* mutant shortened the canal length but it also prevented cysts from forming in 50% of the canals examined. Even those canals that did develop cysts, showed a reduced number of them (Table 6.2). This suggests that the length of the canal and cyst formation are separable events, and that EXC-5 may function through multiple pathways, not all of which are directly mediated by interaction with CDC-42. EXC-5 does exhibit some genetic interactions with MIG-2, a Rac homologue [57] (Chapter 5), and with EXC-9, a homologue of the mammalian LIM-domain protein CRIP [51]. It will be important to determine if these other proteins similarly affect endosome morphology in the excretory canals and other cells where they are expressed.

In patients with CMT4H, the Schwann cells of the peripheral nervous system develop properly to wrap around neurons to form single-celled tubular insulation. Over the course of years, however, tubules in CMT4H patients develop structural defects strikingly similar in morphology to those of the excretory canals in *exc-5*-deficient mutants, with apparently normal tubules juxtaposed next to myelin outfoldings that no longer insulate the nerves [65]. While FGD1 is associated with transport from the trans-Golgi network [99], FGD proteins all contain a FYVE domain that associates with phosphatidylinositol 3-phosphate characteristic of early endosomes [63]. Mammalian FGD1 and FGD2 as well as fungal FGD have all been found associated with early endosomes or plasma membrane [64,72,100]. Based

on the results presented here, we suggest that EXC-5 functions similarly to other FGD proteins in the regulation of endosomes and membrane trafficking. The results also suggest that the narrow single-celled tubules of the mammalian Schwann cells, like those of the nematode excretory canals, are a difficult cell structure to maintain, and that endosomal traffic must be delicately balanced in order to accommodate the movement and growth of these polarized cells over the lifespan of the individual.

Chapter 7: Intein Incorporation into *C. elegans* Genes to Generate Temperature-Sensitive Proteins

Abstract

In order to take a more directed approach to finding conditional alleles of EXC-5, we have incorporated self-excising sequences of amino acids, called inteins, into EXC-9 and EXC-5. The inteins used, 208-S18 and 103-S36, are temperature-sensitive variants whose excision depends on their permissive temperatures. Incorporation of the 208-S18 intein into EXC-9 was able to rescue the Exc-9 mutant phenotype, but this activity has not shown a temperature-dependent effect.

Rationale

"When during development is EXC-5 required?"

Although we were unable to isolate a temperature-sensitive (ts) allele of EXC-5 itself (see Chapter 2), we were still interested in creating a conditional version of the protein. Creating a conditional form of EXC-5 would allow us to understand at what point in the formation of the canal cell is EXC-5 activity required and at what point can EXC-5 activity stop cyst formation.

Inteins are self-excising sequences of amino acids that remove themselves post-translationally from the proteins in which they exist[128]. Once spliced out of the protein, the inteins leave no residual amino acid sequence to interfere with the final protein product. Mutations in yeast-derived inteins have led to the development of a wide range of TS variants, allowing conditional control of their splicing [129,130]. By engineering these TS inteins into a particular gene, it is possible to create a TS allele of that gene. At permissive temperatures, these inteins will splice themselves out, leading to a non-mutant protein sequence. At non-permissive temperatures, the inteins will remain in the protein product and disrupt the normal protein sequence, to yield a non-functional protein.

We used two different TS intein: 103-S36, which is permissive at 18° but mutant at higher temperatures; 208-S18, which is permissive at 22° but nonfunctional at higher temperatures, and engineered them into *exc-9* and *exc-5* in order to create TS alleles of both genes.

Materials and Methods

Strains Used

exc-5 (*rh232*) and *exc-9* (*n2669*) were used to test the ability of the intein transgenes to rescue the mutant phenotypes.

DNA Constructs

An *exc-5* cDNA was created from mRNA prepared from wild-type (N2) animals with a Magnetic mRNA Isolation kit and Phusion®RT-PCR Kit (New England Biolabs). The resultant 2481 bp *exc-5* cDNA was amplified and sub-cloned into a pENTR™/D-TOPO® vector (Invitrogen Corporation). The sequence of this cDNA encodes the shorter and more prevalent isoform of EXC-5 [56]

The 208-S18 and 108-S36 intein constructs were a generous gift from Change Tan. In order to make a clean excision of the intein, the intein sequence must be placed just before a naturally occurring cysteine in the protein of interest. For *exc-9,* we chose an insertion site roughly in the middle of the protein, in front of Cys-36. For *exc-5* the sequence was placed in the last half of the DH domain, in front of Cys-434. This was done to ensure that unspliced intein sequence left in the protein would disrupt a major functional domain of EXC-5. Incorporation of the intein sequence into the genes was accomplished via a fusion PCR method [131]. Two fragments of the gene to be used were amplified, one fragment containing the sequence upstream of the cysteine and one fragment containing the cysteine and all downstream sequence. For *exc-9*, which was amplified from genomic DNA, the upstream fragment was amplified using a forward primer in the 5' UTR and a reverse primer containing the 21bp of sequence prior to the cysteine as well as the first 21bp of the intein sequence (for a total primer size of 42bp). The downstream fragment was amplified using a forward primer that contained 21bp of intein sequence followed by 21bp of *exc-9* sequence starting at the cysteine and a reverse primer in the 3'UTR. DNA fragments of *exc-5* were amplified in a similar manner, but due to amplification from a cDNA in pENTR™ instead of a genomic copy, the M13F and M13R primers were used in place of the 5'UTR and 3'UTR primers used for *exc-9*. The intein sequences were re-amplified as linear PCR products with primers specific for the first and last 21bp of the intein. These three fragments: the upstream gene fragment, the intein fragment, and the downstream fragment, were all placed in the same PCR reaction and amplified using primers specific to the beginning and end of each gene. The resultant product was a fusion of all three fragments and contained the intein sequence directly in front of the chosen cysteine. These products were then sub-cloned into a pENTR™ vector and subsequently used in a Gateway® reaction with an expression vector containing the 1.4kb promoter of *exc-9* linked to mCherry. The resultant product was a construct that contained an N-terminal mCherry-tagged *exc-9* or *exc-5* intein-containing gene under the direction of the *exc-9* promoter. As a control, both the *exc-5* cDNA and a genomic copy of *exc-9* that did not contain the intein sequence were placed into the mCherry expression vector and tested for activity.

Microinjection

Injection of the *exc-9* control plasmid and the *exc-9* intein construct was at 100ng/µl into *exc-9* (*n2669*) animals.

Injection of the *exc-9* construct containing the 208-S18 (22°) intein at 100ng/µl into *exc-9* (*n2669*) animals resulted in a worm line containing a stable array of the transgene. Animals were placed at 15° and 25° and allowed to grow for three or more days and produce progeny. Second generation animals were then examined to see if the canals were rescued or mutant. At the same time, second generation animals were picked from each temperature and placed at the opposite temperature. Animals were allowed to grow for three or more days and produce progeny. Second generation animals were examined again to see if the canals were rescued or mutant. Temperature was monitored in order to verify that incubator temperatures had not exceeded the permissive temperatures.

Injection of the *exc-9* construct containing the 103-S36 (18°) intein at 100ng/µl into *exc-9* (*n2669*) animals resulted in a worm line containing an unstable array of the transgene. Animals were placed at 15° or 25° and allowed to grow for three days. Animals were then examined for their canal phenotypes.

Results

EXC-9 Intein does not show Temperature-Dependent Rescue

Injection of the *exc-9* control plasmid (lacking an inserted intein) into *exc-9* (*n2669*) animals rescued the mutant phenotype and in some cases cause convoluted tubules. This result indicates that the expression vector as well as the *exc-9* sequence used in the production of the intein-containing version was functional and able to rescue the *exc-9* mutant animals.

Some animals expressing the EXC-9::208-S18 intein did display almost complete rescue (Fig. 7.1). Unfortunately, this effect was infrequent and not temperature-dependent. Only 5% of the canals at 15° (n=82) showed a rescued or partially rescued phenotype. Similarly, at 25° only 6.5% of canals (n=124) showed a rescued or partially rescued phenotype. These results indicate that the EXC-9::203-S18 intein is able to create enough EXC-9 activity to restore the wild-type phenotype at a low frequency, but this activity is independent of temperature. These results indicate that intein splicing is occurring randomly and inefficiently.

Interestingly, animals expressing the EXC-9::103-S36 intein could not be rescued. At all temperatures, all animals examined showed a mutant phenotype.

EXC-5 Intein does not Produce Transgenic Progeny

Injection of the *exc-5* control plasmid into *exc-5* (*rh232*) animals at 50ng/µl and at 10ng/µl (for a total of 120 animals) produced almost no transgenic animals.

Injection of the *exc-5* construct containing the 103-S36 intein at 50, 15, and 5ng/µl into *exc-5* (*rh232*) animals (for a total of 95 animals) resulted in no transgenic animals.

Figure 7.1 – EXC-9::208-S118 Functions Independently of Temperature

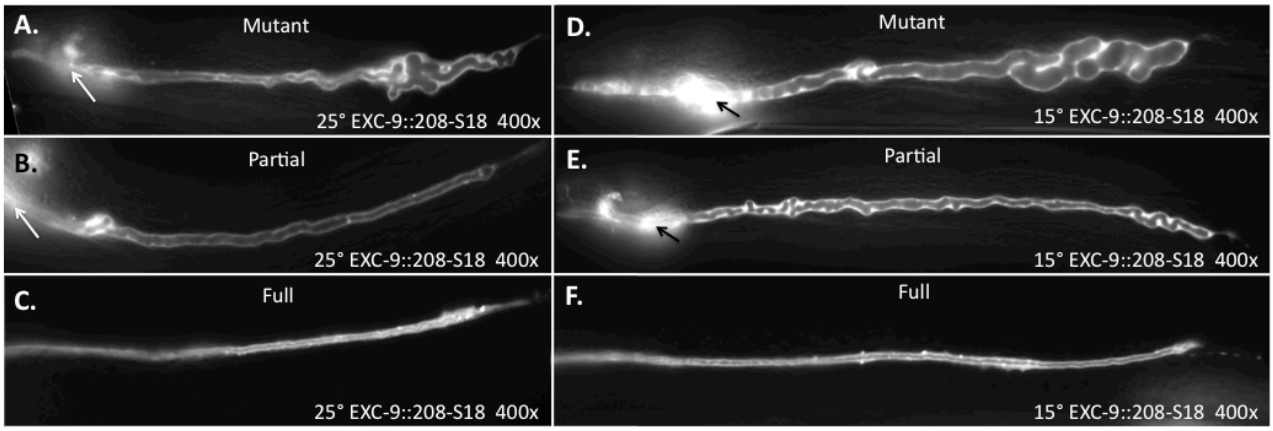

The EXC-9::208-S18 protein fusion rescues the *exc-9* (*n2669*) phenotype at low frequencies independent of temperature. Fluorescent images of L4 animals expressing the EXC-9::208-S18 fusion protein. **(A-C)** Animals were grown at 25°. (A) The majority of the animals had a mutant phenotype. (B) Infrequently (6.4%) the animals showed either partial or (C) full rescue of the canal. Similarly to animals grown at 25°, **(D-F)** animals grown at 15° (D) were mostly mutant. (E) Animals showed either partial, or (F) full rescue at the same frequency (5%) as animals grown at 25°. Arrows indicate the cell body. C and F show only the ends of canals that reached full length in the animal.

Discussion

If the EXC-9::208-S18 intein were working as expected, all or almost all of the animals kept at 15° should be rescued. The intein should excise itself from the EXC-9 protein and leave behind a fully functional protein. At 25° the ability of the inteins to remove themselves should be destroyed, leaving only non-functional EXC-9 protein being produced. Our data did not show this. Instead, it appears that in the majority of the animals the intein is not being excised, even in animals grown at 15°.

The EXC-9::103-S36 protein did even worse. None of the animals expressing this intein construct showed any reduction of the mutant phenotype. It is worth noting that the 103-S36 intein had two silent mutations present in the constructs sent by Change Tan as compared to the sequences we were provided. At basepair 1190, there is a C→A transverion causing the codon to change from GTC to GTA, both of which code for valine. The second mutation is at basepair 1394 and has a T→C transition causing the codon to change from CGT to CGC, both of which code for arginine. It is possible that these mutations are affecting the ability of the intein to be excised although it is unclear how. In addition, the phenotype of *exc-9* (*n2669*) animals injected with the *exc-9*:: *103-S36* construct appear to be more mutant than those animals injected with *exc-9::208-S18*. Canals were consistently shorter and more cystic than animals expressing EXC-9::208-S18 (personal observations).

Currently, the *exc-5* intein-containing construct uses the 103-S36 intein. Although no transgenic lines have been created using this construct, work on creating an EXC-5::208-S18 intein is underway as the results from using 103-S36 in the *exc-9* background were unproductive.

To date, there has not been any significant transgenic progeny generated from the injection of the *exc-5* constructs. There are several reasons why these may be failing. The first is that isolating transgenic progeny from *exc-5* (*rh232*) animals can be difficult. The animals are sensitive to osmotic stress and have lower survival rates from the injection process (personal observations) than do N2 animals. In addition, *rh232* animals produce less progeny than do wild-type animals and become egg-laying-defective as they become older. Although injection of *rh232* animals can work, previous more successful methods of permanently introducing transgenes into the *rh232* background have been accomplished through use of genetic crossing from a worm strain that already contains the integrated array. It may be easiest to inject these constructs into N2 animals first, integrate the resulting array, and then cross them into *exc-5* (*rh232*) animals.

The second problem may be related to the construct itself. Previous work with microinjecting *exc-5* has shown the animals to be sensitive to the amount of EXC-5 being expressed in the animal when *exc-5* is being expressed under its native promoter (see Chapter 3 and Chapter 6). The 1.4kb *exc-9* promoter is significantly stronger than the *exc-5* promoter is, and expressing EXC-5 at higher levels may be lethal even when the injections are done at low concentrations. This could be solved two ways. The first is injecting carrier DNA with the $P_{exc\text{-}9}$*::mCherry::exc-5* cDNA constructs as was done with N2 DNA and the *exc-5::gfp* construct when creating BK157 in order to reduce the repetitive copy number of the

transgene in the extra-chromosomal arrays that are built in the animals. The second is to change the promoter being used in the constructs to the native *exc-5* promoter. Although more technically involved, this method would ensure that EXC-5 is expressed in exactly the right tissues, in exactly the right time, and at less deleterious levels than is expressed from the *exc-9* promoter.

The third problem may be the protein sequence on either side of the intein insertion site. Previous studies have shown that excision efficiency of inteins either *in vitro* or *in vivo* can be altered by the sequences upstream and downstream of the intein[132]. Although we are limited on the possible insertion sites, it is possible that alternative insertion sites may be more effective and have more temperature-sensitive activity.

Even if the *exc-5* constructs were successfully expressed, it is unclear whether intein splicing is a viable strategy in *C. elegans*. To date, using temperature-sensitive inteins have been successful in bacteria, yeast, *D. melanogaster*, and zebrafish [130](C. Tan, personal communication). To our knowledge this is the first time that intein splicing has been attempted in *C. elegans*. Although there is no specific aspect of *C. elegans* biology that would lead us to believe that intein splicing would not work (the inteins are self-excising), it is possible that this type of approach is not effective in nematodes.

Chapter 8: Generating Antibodies to EXC-5

Abstract

We chose four different amino acid sequences from EXC-5 as antigens for the production of EXC-5 antibodies. The antibodies did not show specific banding patterns for the expected mass of the EXC-5 protein. Antibodies from animals 656 and 658 did label the excretory canal but this labeling was also observed in *rh232* animals. In addition, GFP-labeled EXC-5 derived from worm protein lysates was not detectable using commercially produced GFP antibodies.

Rationale

"How can we identify and manipulate EXC-5?"

In order to perform a host of biochemical experiments, the most simple of which would be to detect the presence or absence of EXC-5 protein in animals and more complex ones such as co-immunoprecipitations to identify EXC-5 binding partners, we required an antibody that could bind and recognize EXC-5.

We chose four amino acid sequences from different parts of the EXC-5 protein to be used as antigenic peptides and then tested the resultant eight polyclonal antibodies for their specificity to the EXC-5 protein by means of western blot and *in situ* labeling.

None of the antibodies showed strong specificity for the EXC-5 protein, so an alternate strategy was used. Antibodies for GFP were used to try and isolate GFP-labeled EXC-5 protein for the purposes of using the EXC-5::GFP protein in co-immunoprecipitation reactions.

Material and Methods

<u>Strains Used</u>

N2 and *exc-5* (*rh232*) animals were used for protein lysates in testing the rabbit-derived antibodies to EXC-5. *exc-5* (*rh232*) animals were also used to prepare an acetone powder for purifying the antibodies. N2, BK36, and BK157 were used to generate protein lysates for experiments using the GFP antibodies. BK157 contains the *exc-5::gfp* insertion and was used to identify GFP-labeled EXC-5 protein. BK36 animals contain the $P_{vha\text{-}1}$*::gfp* transgene, which expresses GFP at a very high level in the excretory canals, and were used as a positive control for the GFP antibody. N2 animals have no GFP expression and were used as a negative control.

Antibody Production

Four peptides corresponding to different regions of the EXC-5 were chosen based on their location within the domain structure of EXC-5 and their predicted antigenic properties. One peptide was designed at aa's 107-120 in the N-terminal region of EXC-5 (ISGDIKGMKPIEFSN), two peptides were designed for the end of the first PH domain at aa's 525-539 and 598-612 (KTEERFIFLFNDLVI, QKEKNDWVDSIFSII), and a fourth peptide was designed between the FYVE and last PH domain at aa's 695-709 (GIPRSFSTQSNMRRN). Synthetic peptides were made and antibody production was done by Sigma-Genosys (The Woodlands, Texas). Two rabbits were used for each peptide, resulting in eight different antibodies: 653, 654 – (ISGDIKGMKPIEFSN); 655, 656 – (KTEERFIFLFNDLVI); 657, 658 – (QKEKNDWVDSIFSII); 659, 660 – (GIPRSFSTQSNMRRN). To reduce nonspecific background, immune sera were treated with an acetone powder made from *exc-5* (*rh232*) animals to remove antibodies that bound to anything other than EXC-5.

The antibodies used against GFP were commercially produced by Roche Applied Science™ (Mannheim, Germany) as 'Anti-GFP' and is a mixture of two monoclonal antibodies.

Western Blotting

Whole animal protein lysates were made from both N2 and *exc-5* animals. Animals were suspended in RIPA buffer containing both 'cOmplete Mini' protease inhibitor tablets and 'PhosSTOP' phosphatase inhibitor tablets (Roche Applied Science, Mannheim, Germany), frozen in liquid nitrogen, and then ground into a powder. The powder was collected and frozen at -80°C. Protein samples were taken from these stocks and allowed to thaw. Samples were prepared for loading by adding 61.5µg of protien with sample buffer containing 1% SDS, 10% glycerol, 1% TRIS ph6.8, and bromophenol blue and then boiled for 10 minutes. Samples were then run via SDS-PAGE on 10% polyacrylamide gels. The separated proteins were then transferred to Immobilon™-P transfer membrane (Millipore, MA). Blots were blocked with 5% milk/PBST. The blots were cut into strips and then treated with either pre-immune serum as a control or primary antibody from the immune serum of one of the eight antibodies. Anti-sera dilutions were 1:250 for the lower affinity sera (653, 654, 655, and 657) and 1:500 for the higher affinity sera (656 and 658). Peroxidase-labeled affinity-purified antibodies to rabbit IgG were used as secondary antibodies (Kirkegaard & Perry Laboratories, Inc., Gaithersburg, Maryland) in a 1:5000 dilution. Blots were developed by use of ECL ™ Western Blotting Detection Reagents (Amersham Biosciences, Buckinghamshire, England) and imaged on X-ray film.

Blots labeled for GFP were done similarly using protein lysates for N2, BK36, and BK157 animals. Whole blots were blocked with 5% milk/PBST; incubated with Anti-GFP antibodies at a 1:1000 dilution in 1% BSA/PBST; then labeled using peroxidase-conjugated affinity-purified antibodies to mouse IgG (Kirkegaard & Perry Laboratories, Inc., Gaithersburg, Maryland) at a dilution of 1:2000 in 1% BSA/PBST. Blots were imaged using a KODAK™ 4000R Image Station, the use time of which was generously provided by E. Lundquist.

In situ Labeling

Glass slides were prepared by adding one drop of N2 animals and one drop of *exc-5* (*rh232*) animals on opposite ends. Cover slips were placed over the drops and then the slides were submerged in liquid N_2. The slides were then removed, the cover slips cracked off the frozen worm samples, and then placed into ice-cold methanol for two minutes. The slides were then removed and placed in ice-cold acetone for four minutes. Slides were then taken out of the acetone and allowed to dry. Drops of primary antibody were applied to the N2 and *exc-5* worm samples and allowed to incubate overnight. Slides were washed with PBS and then treated with GFP-labeled affinity-purified secondary antibodies to rabbit IgG (Kirkegaard & Perry Laboratories, Inc., Gaithersburg, Maryland), and 10µl of a 1mg/ml solution of p-Phenylenediamine was added to preserve fluorescence.

Results

EXC-5 Antibodies Do Not Show Expected EXC-5-Specific Binding on Blots or in Worms

The expected mass for EXC-5 is 97 kDa for the longer isoform and 95 kDa for the shorter isoform. Preliminary tests with all the antibodies on both N2 and *rh232* lysates showed no single band at this size that was both present in the N2 animals and absent in the *rh232* animals (Fig. 8.1). Immune serum from animal 656 showed an extreme amount of background sensitivity as did serum from animal 658. In addition to adjusting antibody concentrations and exposure times, the antibodies were then cleared with an acetone powder made from crushed *exc-5* (*rh232*) animals. This was done to eliminate any antibodies that would bind to proteins other than EXC-5. Since *rh232* animals should have no EXC-5 protein, antibodies binding to any background protein present in the animals should adhere to the acetone powder and be removed from the solution, presumably leaving only the antibodies that can't bind to the proteins in an *exc-5* mutant animal. After these adjustments, background signal from the antibodies was greatly reduced (Fig. 8.2). Unfortunately, these changes did not show a band corresponding to the expected ~100 kDa EXC-5 protein in N2 lysates, but missing in the *rh232* lysates. On the contrary, antibodies 654, 655, 657, 659 and 660 all showed a strong bands at ~50 kDa in the *rh232* lysate and not in the N2 lysate. This is counter-intuitive to what we were expecting, especially considering the *rh232*-acetone-powder-treated antibodies, which should have removed or reduced all binding of the antibody with the *exc-5* lysate. The *exc-5* (*rh232*) strain was checked to make sure that the animals being used contained the *rh232* deletion, and it was confirmed that the strain was missing the *exc-5* coding region (see Chapter 2 for methods).

In parallel to the blots, we also examined the staining of worms with these antibodies after treatment with the *rh232* acetone powder. Based on the expression pattern of GFP-labeled EXC-5, we would expect to see the excretory canal, pharynx, and some other neurons being labeled by an antibody specific to EXC-5. Similarly to the blots, this labeling should be present in N2 animals and not in the *exc-5*-null strain *rh232*. Antibodies 656 and 658 both labeled the canal as well as the pharynx. In addition, 658 appeared also to label the duct cell (Fig. 8.3). Labeling of the canal between N2 and *exc-5* worms was inconsistent and had a high amount of background fluorescence, commonly seen for antibody staining of worms. Labeling of the canal was seen in both backgrounds with both antibodies, although the canal was labeled more prevalently in N2 animals (data not shown).

Figure 8.1 – Immune Sera do not Show EXC-5 Specificity

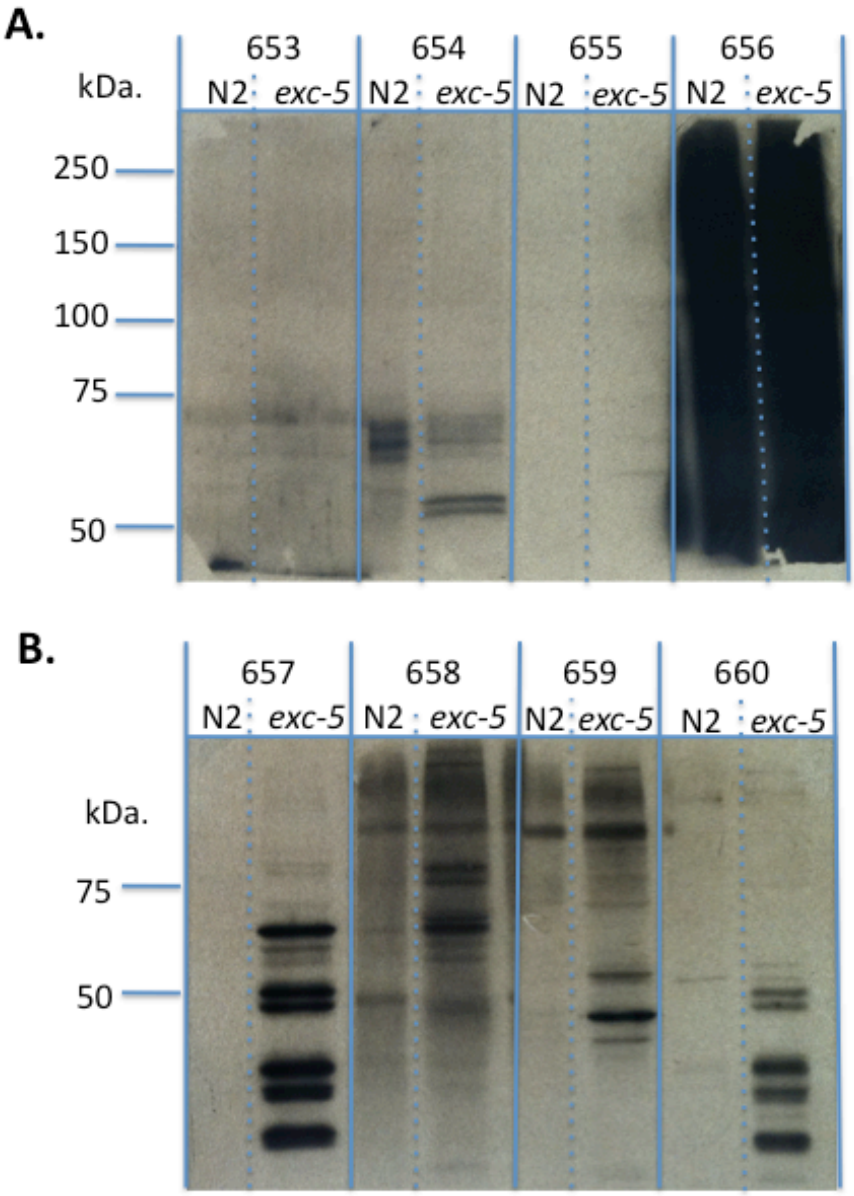

Images of Western blots exposed to X-ray film for 1 minute. Immune serum from eight rabbits (653-660), each inoculated with one of four different antigenic peptides, were tested against N2 and *exc-5* (*rh232*) protein lysates. None of the sera identified a ~100kDa band (the expected size of EXC-5) in the N2 lysate and not in the *exc-5* (*rh232*) lysate.
(A) Sera from animals 653-656. 656 showed extremely high reactivity with worm proteins.
(B) Sera from animals 657-660. 658 also shows high reactivity with worm proteins. Although there are bands present at ~100kDa, these bands are not specific to the N2 lysate.

Figure 8.2 – Preadsorbed Sera do not Show EXC-5 Specificity

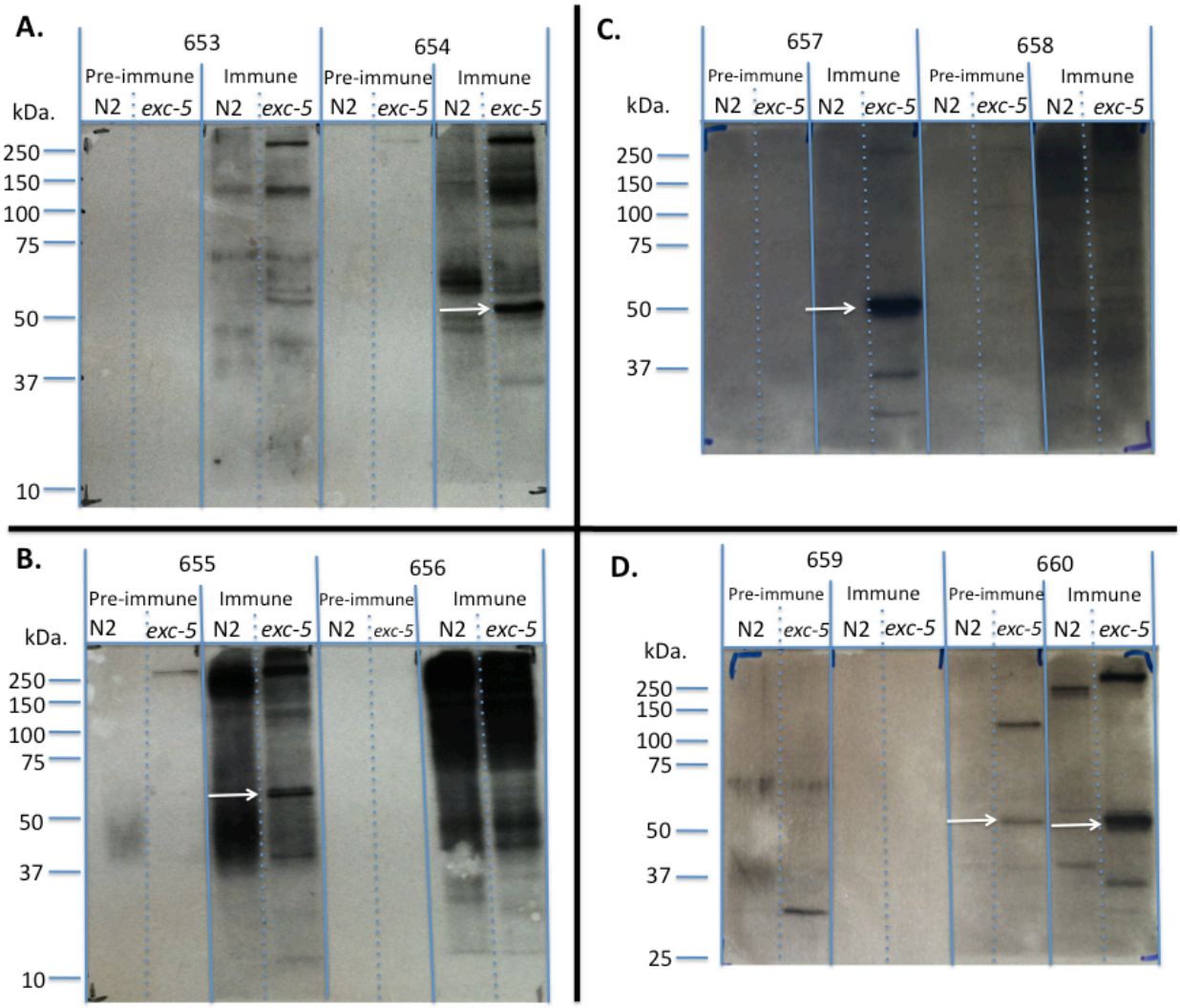

Images of Western blots exposed to X-ray film. Immune sera were treated with an acetone powder composed of *exc-5* (*rh232*) animals and tested against protein lysates from both N2 and *exc-5* (*rh232*) animals along with the pre-immune sera (PRE) controls. No ~100kDa bands were seen that were specific to the N2 lysate. **(A)** 653, 654. **(B)** 655, 656. **(C)** 657, 658. **(D)** 659, 660. 656 and 658 still have high reactivity to both the N2 and *exc-5* (*rh232*) protein lysate. Interestingly, the banding pattern between the *exc-5* (*rh232*) and N2 protein lysate differ. Frequently the immune sera identified a ~50kDa band(arrow)(654, 655, 657, in both the pre-immune and immune serum from 660) that was not present in N2 animals.

Figure 8.3 – *In situ* labeling of *C. elegans* using 656 and 658

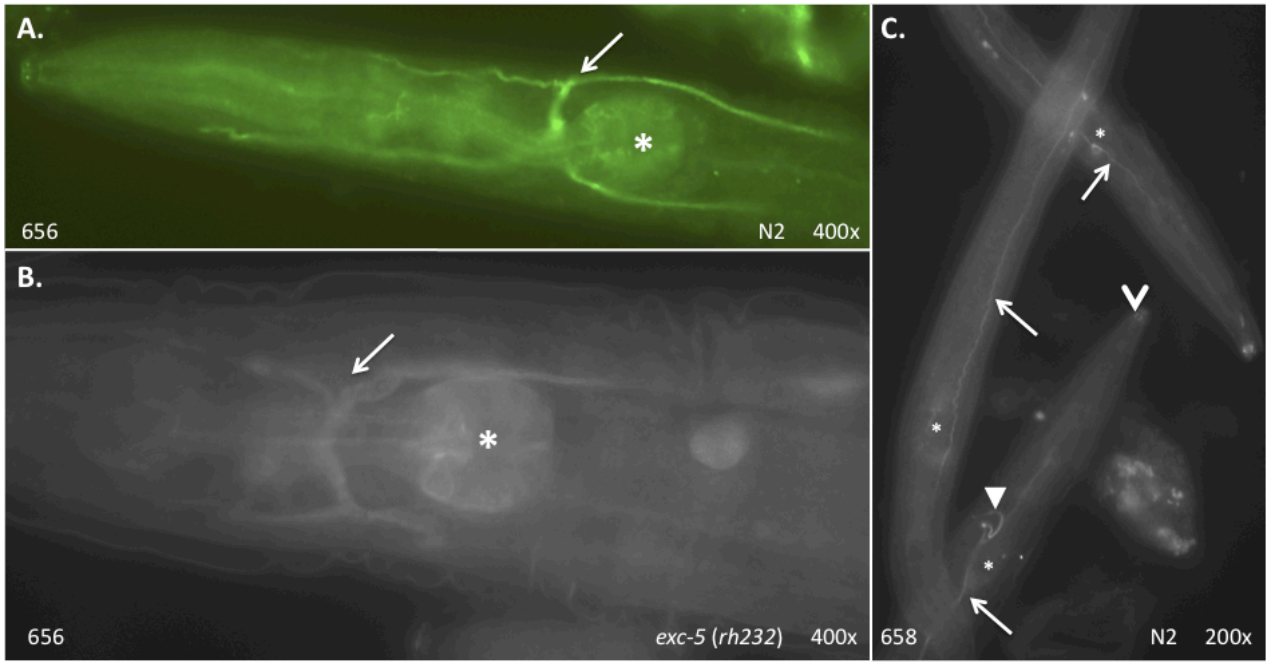

Fluorescent micrographs of animals labeled with either immune serum from 656 or 658. Arrows indicated the labeled excretory canal. Asterisks indicate the posterior bulb of the pharynx. **(A)** 656 brightly labels the excretory canal as well as the pharynx of N2 animals. **(B)** 656 also brightly labels the excretory canal and pharynx of *exc-5* (*rh232*) animals. **(C)** 658 brightly labels the excretory canal as well as the duct cell (solid arrowhead) and the mouth of the animal (open arrowhead). The pharynx is also faintly labeled. This labeling was seen in both N2 and *exc-5* (*rh232*) animals. Magnifications are as indicated.

EXC-5::GFP Protein is Undetectable in BK157 Animals

The molecular mass of GFP is roughly 30 kDa. The predicted mass of EXC-5 fused to GFP is approximately 126 kDa (121 kDa for the shorter isoform). Blots using N2, BK36, and BK157 protein lysates showed a clear band in the BK36 animals at about 30 kDa, corresponding to the GFP protein (Fig. 8.4). In addition, there was no GFP detected in the N2 protein lysates, as we expected. Although both controls for the detection of GFP worked, we did not observe the ~120 kDa band size for EXC-5:: GFP (or any other band) in the BK157 lysate.

Figure 8.4 – Identifying GFP-labeled EXC-5 Protein

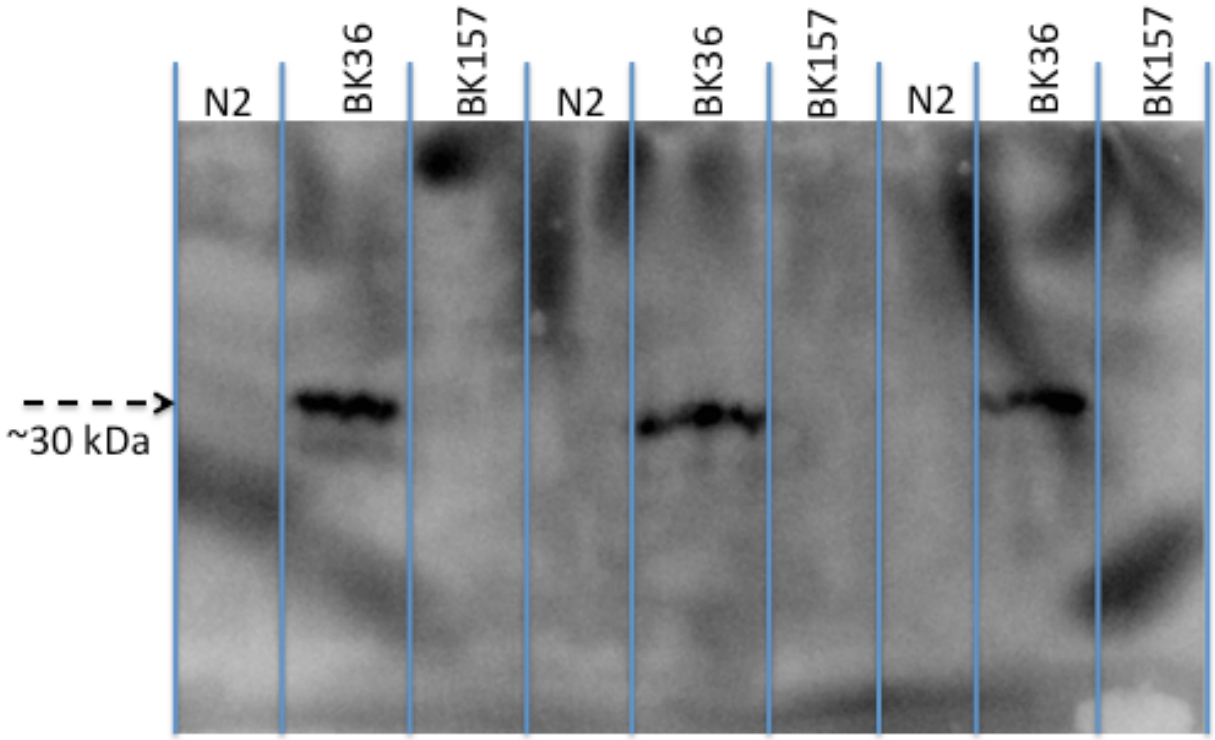

Image of a western blot labeled with Anti-GFP antibodies. Three different protein lysates were used. GFP has a molecular mass of ~30 kDa. N2 animals do not express GFP and were used as a negative control. BK36 animals contain the *qpIs11* insertion and express GFP at high levels in the canal (Fig. 1.10A, 6.1A) and were used as a positive control. BK157 animals contain the *qpIs78* insertion and express EXC-5::GFP. Expression of GFP was easily detected in BK36 animals but not in BK157. BK157 lanes have increasing amounts of protein. The last lane contains as much undiluted protein lysate as possible in the well.

Discussion

It is unclear what the antibodies designed for EXC-5 are binding to, but it is very unlikely to include the EXC-5 protein. After confirming the deletion in the *rh232* strain used for the experiments, only sequence in the genome for antibody binding sites 659 and 660 still exist. Clearing the antibodies with an acetone powder was ultimately ineffective, although it did alter the banding patterns for both N2 and *exc-5* animals. It should be noted that the banding pattern between N2 and *exc-5* animals are different, which indicates that the population of proteins within each preparation differ significantly. This result may be due to some sort of contamination, although the strains were grown and prepared in parallel to minimize the amount of discrepancy between the two preparations. In addition, this effect persisted using a second preparation of a protein lysate from *exc-5* animals. Alternatively, the *exc-5* mutation may be having a tremendous effect on the protein expression pattern of the animals. As we know now, EXC-5 controls recycling and transport in the canal cell. If these defects are occurring in the pharynx and other nerves that *exc-5* is expressed in, the effects on the animal could be large. The physiology of *exc-5*(*rh232*) animals is clearly altered from that of N2 animals. *exc-5* animals must compensate for not only the morphological defects caused by large cyst formation interfering with normal organ architecture/placement within the animal, but also less efficient growth. *exc-5* mutants are noticeably less healthy than are N2 animals (slower growth, lower number of progeny, and often egg-laying-defective as young adults). What the strong 50 kDa protein is that several antibodies are recognizing in the *exc-5* lysate but not in the N2 lysate is unclear.

Interestingly, antibody staining within the animals did show canal labeling for antibodies 656 and 658, though this labeling was seen in both N2 and *exc-5* animals. These two antibodies also show the highest background staining and therefore may be more reactive to worm proteins overall rather than to EXC-5 specifically. It is possible that the rabbits being used for the generation of these antibodies had nematode infections either actively or at one point in their lives. This would explain why they had such broad-spectrum reactivity on the western blots, and labeled tissues that are directly exposed to the external environment in the animals (Fig. 8.2).

In retrospect, the immune sera received from Sigma-Genosys could have been handled much better. The sera were never specifically purified for IgG polyclonal antibodies and purification with a Protein A column would have been relatively simple. An even more effective way to prepare the sera (but more complex) would have been by immunoaffinity purification. By linking either the peptides or the EXC-5 protein to activated beads, the polyclonal serum could be purified specifically for antibodies that recognize EXC-5 or a peptide of EXC-5 sequence by use of an antigen-linked column. Relatively large quantities of sera still exist and have been kept frozen for six years. Future work would require testing these sera to see if they still retain activity using a more rigorous purification step, as mentioned above, before they could be used for other biochemical experiments.

The antibodies designed to GFP worked quite well. Unfortunately, we were not able to detect EXC-5::GFP protein in the BK157 strain. This is likely due to the less detectable nature of GFP in the BK157 strain despite efforts to concentrate the amount of protein present in the samples as much as possible. The difference in relative levels of GFP between these two strains can easily be seen in the microscope (Fig. 6.1). In comparison to BK36, BK157 has extremely low fluorescence levels. To create enough GFP-labeled EXC-5 protein to use for other experiments, we would need to switch from native expression in *C. elegans* to a bacterial-based expression system. GFP would no longer be needed, and a more purification-friendly tag such as GST could be added instead to facilitate purification. Future plans do include the production of such a GST-labeled EXC-5 protein as well as other proteins to be used for co-immunoprecipitation experiments as well as for identifying direct binding partners.

Chapter 9: Conclusions

The primary purpose of this thesis is to describe how EXC-5 functions in order to maintain tubular structures. Very little was known about the role of EXC-5 before this work was done. The mutant phenotypes of *exc-5* had been characterized, the tissues in which EXC-5 is expressed had been identified, and the gene had been mapped and identified as a homologue of FGD1 [48,56,57]. Our simplistic starting model supposed that EXC-5 worked with CDC-42 at the apical surface to maintain the structural integrity of the lumen (Fig. 9.1). Through my investigations we have affirmed the basics of our starting model but more importantly we have significantly increased our understanding of how EXC-5 works within the excretory canal and the cellular processes involved in tubule formation and maintenance (Fig 9.2).

The first approach was to determine when during cyst formation and excretory canal cell growth EXC-5 is required. In Chapter One I describe the general characteristics of the canal and its formation, as well as provide a detailed description of EXC-5 and its mutant phenotypes. We know that EXC-5 is not necessary for the birth, differentiation, polarization, or even formation of the excretory canal. In the *rh232* null allele, all these processes are unaffected. Based on our observations on the development of cysts, EXC-5 is required only at certain points along the canal, most importantly at the terminus of the canal where outgrowth occurs. If EXC-5 were required along the entire length of the canal to maintain tubule diameter, the entire canal would be affected, and uniformly disrupted. This is not what is observed in *rh232* animals. In *exc-5* null mutants, cysts are confined to distinct points along the canal and are bounded by lengths of canal that retain their wild-type diameter (Figs. 1.10, 6.5, 6.6). In addition, the canals do not extend past the vulva, and maintain this relative length as the animals grows larger. The canal must be growing in length to maintain this proportional body length. EXC-5 must not be absolutely required for the lengthening of pre-existing tubules as *rh232* mutants have canals that still reach the vulva. EXC-5 activity is, however, important in this process as cysts do form in these areas and become progressively larger. This again indicates that EXC-5 function is required at certain points to maintain the tubule diameter as the canal grows and the animal ages.

Figure 9.1 – Starting Model of EXC Proteins in the Canal

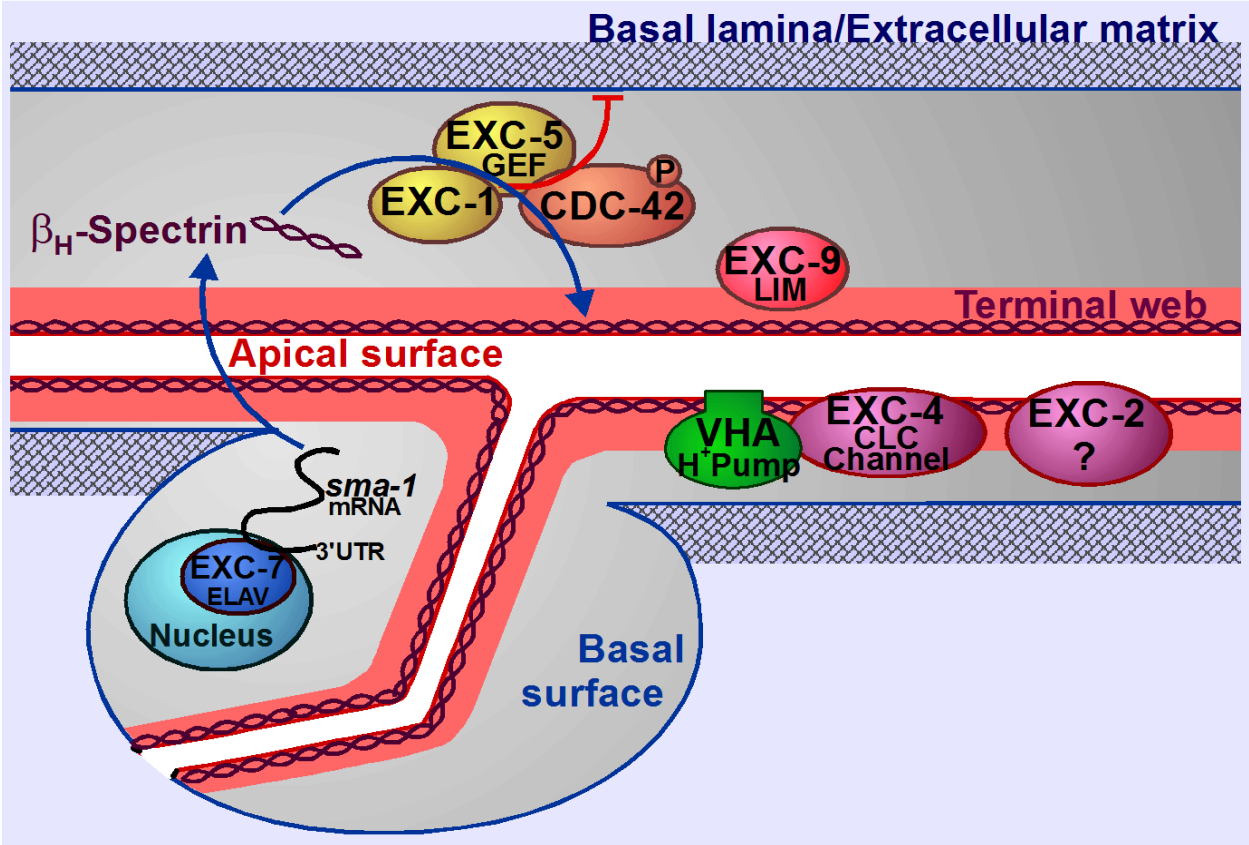

A previous model of how EXC proteins function to maintain the canal included EXC-1 acting upstream of EXC-5 to promote apical structure formation and inhibit the growth of the basal surface through CDC-42. EXC-9 was hypothesized to work downstream of EXC-5 at the apical surface. EXC-4 is a CLIC family member of chloride ion channels that is required for normal canal morphology [49]. EXC-7 is an ELAV homologue and RNA transport protein that binds to *sma-1* mRNA [50] and may help to transport it out of the nucleus at the cell body to be translated closer to its product's, β_H-spectrin, destination at the apical surface of the canal. VHA is a vacuolar ATPase proton pump that lines the apical surface of the canal. The promoter for one of its subunits, VHA-1, is expressed only in the canal and head mesodermal cell. Image courtesy of M. Buechner.

Figure 9.2 – Current Model of EXC-5 Function in the Canal

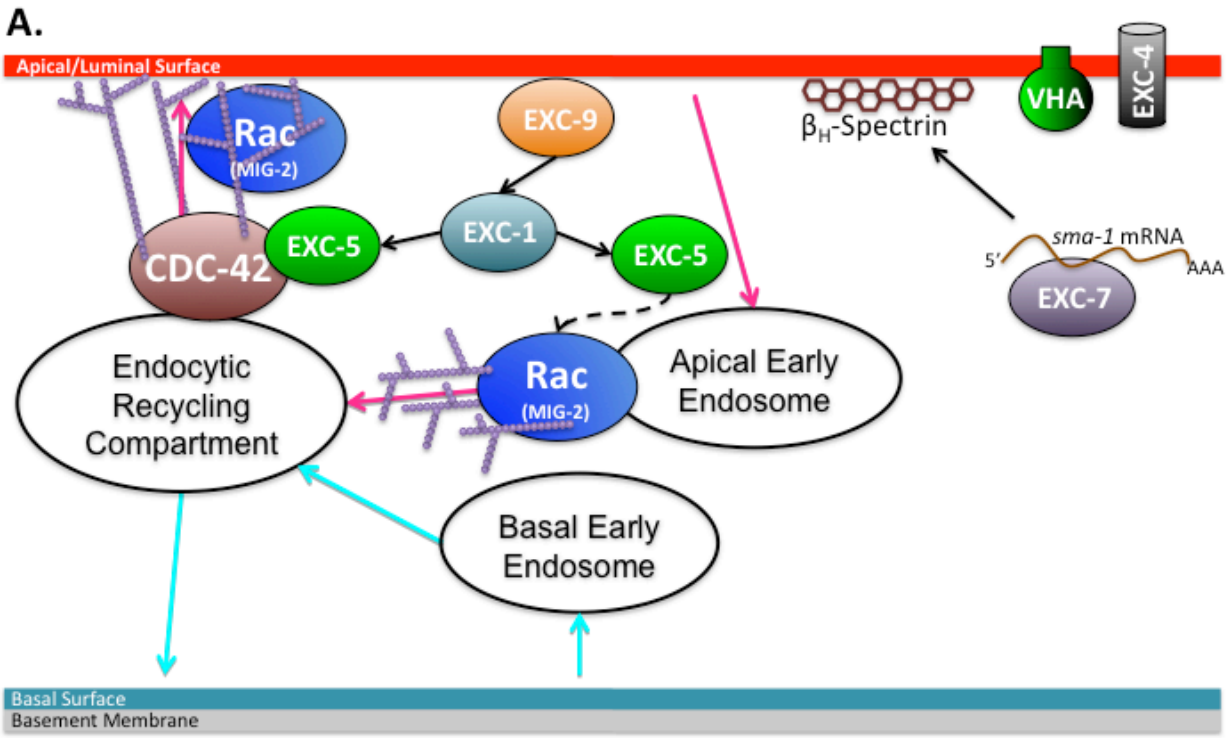

(A) EXC-9 recognizes or is recruited to points of growth or damage along the canal. It then recruits EXC-1, which in turn promotes EXC-5 activity at the apical surface. EXC-5 indirectly activates Rac on the early endosome. This activation may promote actin filament formation and the movement of cargo from early endosomes to recycling endosomes. EXC-5 directly activates CDC-42 to promote recycling of material back to the apical surface, including activated Rac and other membrane associated proteins like spectrin, where they can reinforce the apical surface through actin filament formation and anchoring to the plasma membrane.

Figure 9.2 B – Current Model of EXC-5 Function in the Canal

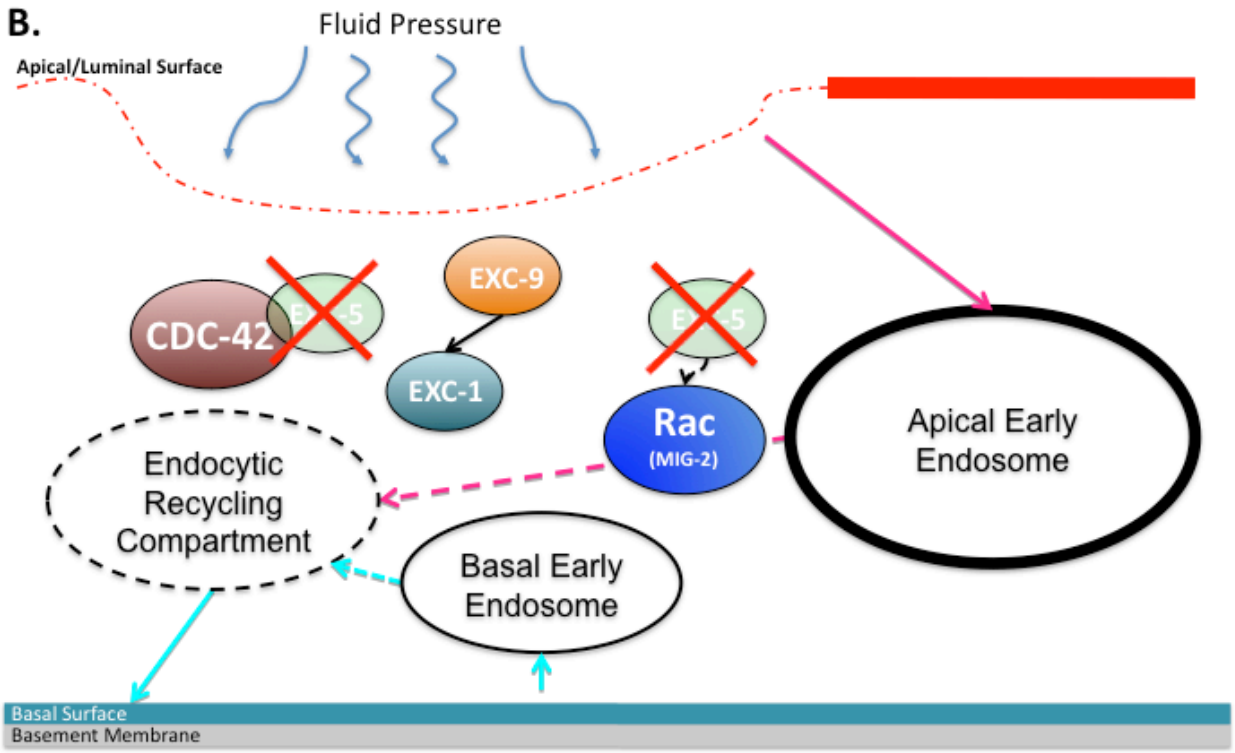

(B) When EXC-5 is not present in the cell, material builds up in the early endosome and is unable to be recycled back to the apical surface. RME-1-labeled recycling endosomes are depleted, and the apical surface of the canal is weakened. This weakening allows pressure from the fluids being transported through the lumen to exert more pressure on the canal cell. In response, the canal cell forms cysts that continue to grow in size as the animal ages.

Figure 9.2 C – Current Model of EXC-5 Function in the Canal

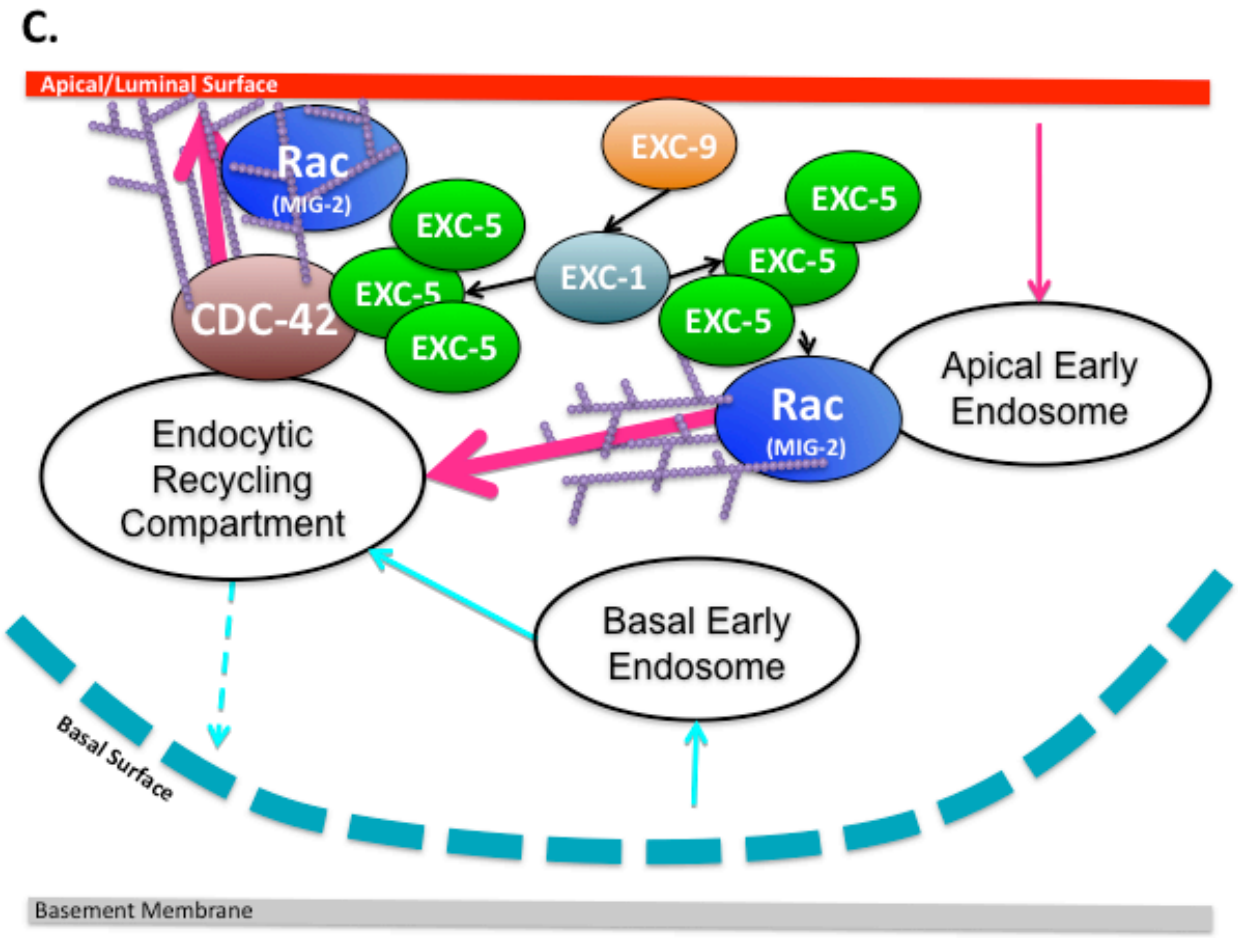

(C) When EXC-5 is overexpressed, recycling to the apical surface is enhanced at the expense of sorting to the basal surface. The abundance of activated CDC-42 and Rac may indirectly inhibit sorting to the basal surface and prevent integral membrane proteins such as integrin from being incorporated into the membrane. As a result, the basal surface is unable to maintain its connection to the basement membrane and is unable to grow and extend normally, causing a convoluted tubule phenotype.

In order to be able to control EXC-5 activity during the growth of the canal and therefore learn more about the developmental time requirements of EXC-5, I attempted to create conditional alleles of the gene (as described in Chapters Two and Seven). While several new alleles were isolated and provided us with new insight into the protein, these attempts were ultimately unsuccessful in generating the type of conditional allele that would have been useful in developmental time-course studies. As such, large questions still remain about the timing and specific requirements of EXC-5 activity in the excretory canal. Is supplying EXC-5 activity only in the early stages of cyst formation enough to prevent cysts from forming later in the animal's life? My prediction is that the answer is no. In my model for EXC-5 function, its activity is continuously required to maintain the apical surface and prevent the cysts from forming. What if you supplied EXC-5 activity after cysts have formed? Would delayed activity reduce or repair cyst formation? It is unlikely that supplying EXC-5 activity after a cyst has formed will cause the canal to return to normal. In my model, cyst formation occurs because of a failure in the apical surface. This failure then becomes progressively worse as the canal compensates for the continued osmotic pressure against the cell by growing in size. There is no evidence that cyst formation is a reversible process and it is unlikely that adding EXC-5 activity after they have formed would return the canal back to a normal diameter. It is more likely that supplying EXC-5 activity after cysts have already formed will prevent them from becoming more severe and prevent new cysts from forming. Adding back EXC-5 activity may allow the cell to repair the apical surface and prevent further damage or expansion. Future work will require alternative methods to generate the kind of conditional expression of EXC-5 that is required to investigate these hypotheses.

The second approach to identify how EXC-5 functions to maintain the excretory canal was to identify other genes or proteins that interact with EXC-5. By identifying interacting genes or proteins, we can implicate EXC-5 in the same pathways that those genes or proteins are involved. In Chapters Two and Three, I discuss the isolation of three different mutations that affect the EXC-5 phenotype. One of these mutations, *qp49*, showed subtle temperature-sensitive suppression effects. The other mutations contained in strains BK188 and BK190 act as genetic enhancers of EXC-5. These results show that it is relatively easy to isolate extragenic interactions with *exc-5*. In order for these mutations to be informative on the role EXC-5 plays in the excretory canal cell, these mutations need to be mapped and identified. Future studies could accomplish this by continuing to use traditional mapping, which is laborious and time consuming, or through the relatively new approach of whole-genome sequencing, which was not available when these alleles were isolated and has its own limitations on sensitivity.

In Chapter Four, I discuss methods that were used to try to create a canal-specific RNAi strain. The creation of such a strain would allow us to selectively knock down genes in the canal that would otherwise be deleterious to the worm. We could then manipulate these genes in *exc-5* (or other) mutants through RNAi and observe the effects on the phenotype. Currently such a canal-specific RNAi screen is being set up based on the effects of cell-specific expression of *sid-1*. Although I was unsuccessful in creating a functional canal-specific RNAi strain, we did discover that RDE-1 has significant effects on the canal and that, like neurons, the canal is resistant to RNAi.

In Chapter Five, I discuss the effects of several genes on the EXC-5 phenotype and show that CDC-42 and MIG-2 both interact with EXC-5. Although the exact nature of this interaction is unclear, it is likely that EXC-5 acts primarily as a GEF for CDC-42 and that EXC-5's interactions with the Rac family member MIG-2 may be indirect. In addition, EXC-9 and EXC-1 both show genetic interactions with EXC-5, and these interactions place EXC-5 downstream of both proteins. The specific functions of both EXC-1 and EXC-9 are unknown and it will be interesting to find out how they work with EXC-5 in order to prevent cysts from forming in the excretory canal.

In Chapter Six, the GBD of WSP-1 shows the most efficient rescue of *rh232* of all the constructs tested. WSP-1 is the sole homologue of N-WASP in *C. elegans* [133]. It is a downstream target of both CDC-42 and Rac, and interacts with the Arp2/3 complex to stimulate actin filament formation [134,135]. Although it is unclear how only the GBD of WSP-1 can cause this effect in the canal cell, it is consistent with the model that EXC-5 acts in the same pathway as both CDC-42 and Rac, and that activation of these proteins is crucial to maintain the apical surface.

Investigations into the interactions of EXC-5 with other proteins is ongoing. Current studies include yeast two-hybrid assays to test direct interactions between EXC-5 and other candidate proteins such as EXC-1 and CDC-42. In addition, the generation of a GST-labeled EXC-5 protein for use in pulldown assays is being undertaken to identify more EXC-5 binding partners.

The third approach was to investigate how EXC-5 functioned in the canal cell. In combination with our observations and previous work, we hypothesized that EXC-5 was involved in directing material to the apical surface of the canal. In Chapter Six, we examined a set of ten markers labeling various subcellular compartments and EXC-5-related proteins in both *exc-5* (*rh232*) mutants and animals mildly overexpressing EXC-5::GFP. We show that in both *rh232* mutants and EXC-5 overexpressors, the distribution of EEA-1 and RME-1 is disrupted. These results indicate that EXC-5 function is essential in the movement of material from early endosomes to recycling endosomes and then back to the plasma membrane. In addition, mild-overexpression of the markers CDC-42, RAB-5, RAB-11, and GBD:WSP-1 all caused mild convoluted and cystic phenotypes in a low percentage of canals (Table 6.2). This is consistent with the model that disruption of intracellular trafficking leads to convolution and cyst formation in the canal. Although we believe that EXC-5 is interrupting intracellular transport, it is difficult to delineate where cell polarization and intracellular membrane trafficking diverge. To help elucidate this distinction, it would be helpful to view the movement of cargo through the excretory canal in real time. The creation of labeled cargoes that are recycled to either the apical or basal surface would allow us to see accumulation of material in certain compartments or if they were being missorted due to local disruption of cell polarity.

In addition, the actin network has been understudied in the canal. Based on our model, EXC-5 is exerting its effects (indirectly) through modulation of the actin cytoskeleton. Interestingly, recent studies have shown that the formation of actin filaments is essential for the proper sorting of material out of endosomes [136]. Although not described in detail in this thesis, the creation of a GFP-labeled amino acid sequence that labels F-actin, termed

Lifeact [137], and expressed only in the canal has not shown a distinct actin filament network within the canal (Fig. 9.3). The excretory canal is sensitive to expression of Lifeact, and overexpression of Lifeact causes defects including shortening of the length of the canal, widening of the lumen, occasional cysts, small cytoplasmic 'tails', and accumulations of material at the canal termini. Regardless of the morphological defects, actin appears enriched on the luminal surface and in accumulations where the canals prematurely end. It is interesting to note that both CDC-42 and EXC-5 are enriched on the luminal surface as well. Unfortunately, the small size of the excretory canal makes resolution of the observed structures and distinct locations of the all of these proteins difficult using standard differential interference contrast light microscopy. In the future, it may be useful to turn to more elaborate light microscopy techniques such as 3D structured illumination microscopy (3D-SIM)[138] or more traditional electron microscopy.

The central question of this dissertation is 'How does EXC-5 function in order to maintain tubular structure?' Taken together, my investigations support a new model of tubular maintenance that includes membrane trafficking within the canal cell (compare Figs. 9.1, 9.2). These observations show that EXC-5 functions with CDC-42 and Rac to direct recycling of proteins to the apical surface of the canal. This direction of material to the apical surface is not required universally along the canal tubule; it is required only at certain points along the canal. Presumably, these points are where the canal is undergoing significant restructuring because of growth or physical damage. The activity of EXC-5 is related to but downstream of both EXC-1 and EXC-9. Although it is unclear how EXC-1 and EXC-9 interact with EXC-5, it is possible that they help recruit and direct the remodeling machinery necessary to maintain the apical structure at the points of growth or damage where the cysts form. EXC-5 is part of this machinery and may indirectly activate Rac on the early endosomes. The activation of Rac may help to remodel the actin cytoskeleton and form the actin filaments necessary for the sorting of early endosomal material into recycling endosomes. EXC-5 then directly activates CDC-42 to transport materials such as activated Rac and spectrin back to the apical surface. These proteins, in addition to activated CDC-42, can reinforce the apical surface through actin filament formation and anchoring to the plasma membrane. When *exc-5* is mutant, materials are not efficiently sorted to the apical surface and the actin cytoskeleton is not remodeled or reinforced to maintain the structure of the lumen. The weakening of the apical matrix causes failure of the lumen under the osmotic pressure from fluid within the excretory canal. This increased pressure causes the canal cell to respond by growing and forming a cyst. As the animal ages, the constant pressure causes the cysts to continue to increase in size. When EXC-5 is overexpressed, sorting to the apical surface is enhanced. This increased rate of transport to the apical surface is at the expense of sorting to the basal surface. The abundance of activated CDC-42 and Rac due to the enhanced EXC-5 activity may indirectly inhibit sorting to the basal surface and prevent integral membrane proteins such as integrin from being incorporated into the membrane. This leads to an inability of the basal surface to adhere to the extracellular matrix of the basement membrane and consequently its inability to extend along the length of the animal, causing a convoluted tubule phenotype.

Figure 9.3 – Actin is Enriched on the Apical Surface of the Canal

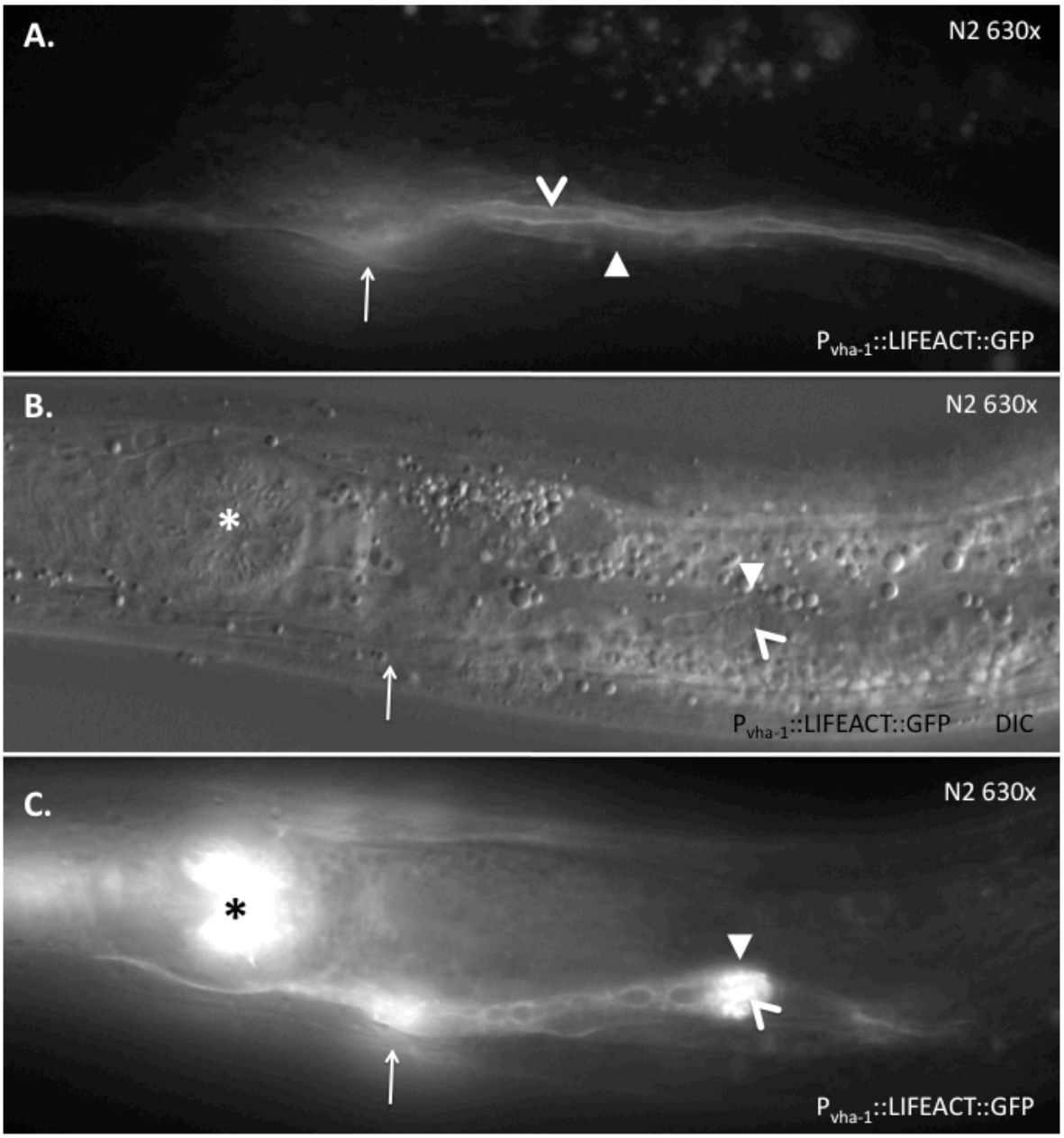

F-actin-binding peptide Lifeact fused to GFP and expressed under the *vha-1* promoter in wild-type (N2) animals. Arrows indicate the excretory cell body. Solid arrowheads indicate the basal surface of the canal. Open arrowheads indicate the apical surface of the canal. Asterisks indicate the posterior bulb of the pharynx. All images are of L4 animals taken at 630x magnification. **(A)** Actin is enriched on the luminal surface of the canal. **(B)** Expression of Lifeact causes defects in canal structure. The canals are short and have a defective lumen. This animal has a mass at the end of the canal filled with small vesicles. **(C)** Fluorescence micrograph of the same animal shown in panel B shows that Lifeact accumulates at the ends of these short canals where actin filament formation may be most active. Lifeact may be over-stabilizing these dynamic actin filaments and disrupting normal morphology.

Many questions still remain about how this process works. What activities do EXC-9 and EXC-1 have in this pathway? They both seem to be working upstream of EXC-5. Are they regulating growth or repair? How does EXC-5's interaction with CDC-42 cause sorting to the apical surface? Is it directly related to actin cytoskeleton remodeling? How does the cycling of CDC-42 between its active and inactive state control trafficking? Our work with DN and CA forms of the protein indicate that the ability of CDC-42 to switch between the two states is essential in wild-type activity. What role does Rac play in these processes either directly or indirectly? How does the function of EXC-5 compare with that of the other FGD proteins? Does the family of FGD proteins work to control membrane trafficking in all cells and their specific effects are dependent on the cells they are expressed?

These questions and many more like them are the driving force of scientific discovery. If they are to be answered, we must encourage and foster the innate curiosity we have as humans about the world we live in. We must share our enthusiasm and appreciation of science with the people around us. We must educate and inform others on the value of continuous learning, the desire to know more, and of the scientific process. Education and scientific research must remain a priority in our national identity if we are to continue to be a successful country. We must continue to support our scientific institutions and our research funding agencies. In this dissertation, I have only touched on a small fragment of the knowledge we have accumulated due to our continued support of the sciences. For us to continue to improve our quality of life and to be able to understand the world in which we live, it is imperative that we do not forget some of the naïve wonder we have all felt at one point in our lives and use that to fuel our curiosity to discover more about the world around, and in the case of this dissertation, the world flowing through us.

References:

1 Lubarsky, B. & Krasnow, M. A. Tube morphogenesis: making and shaping biological tubes. *Cell* **112**, 19-28 (2003).

2 Bryant, D. M. & Mostov, K. E. From cells to organs: building polarized tissue. *Nat Rev Mol Cell Biol* **9**, 887-901, doi:10.1038/nrm2523 (2008).

3 Martin-Belmonte, F. & Mostov, K. Regulation of cell polarity during epithelial morphogenesis. *Curr Opin Cell Biol* **20**, 227-234, doi:10.1016/j.ceb.2008.01.001 (2008).

4 Martin-Belmonte, F. *et al.* PTEN-mediated apical segregation of phosphoinositides controls epithelial morphogenesis through Cdc42. *Cell* **128**, 383-397, doi:10.1016/j.cell.2006.11.051 (2007).

5 Gassama-Diagne, A. *et al.* Phosphatidylinositol-3,4,5-trisphosphate regulates the formation of the basolateral plasma membrane in epithelial cells. *Nat Cell Biol* **8**, 963-970, doi:10.1038/ncb1461 (2006).

6 Levi, B. P., Ghabrial, A. S. & Krasnow, M. A. *Drosophila* talin and integrin genes are required for maintenance of tracheal terminal branches and luminal organization. *Development* **133**, 2383-2393, doi:10.1242/dev.02404 (2006).

7 Luschnig, S., Batz, T., Armbruster, K. & Krasnow, M. A. *serpentine* and *vermiform* encode matrix proteins with chitin binding and deacetylation domains that limit tracheal tube length in *Drosophila*. *Curr Biol* **16**, 186-194, doi:10.1016/j.cub.2005.11.072 (2006).

8 Hogan, B. L. & Kolodziej, P. A. Organogenesis: molecular mechanisms of tubulogenesis. *Nat Rev Genet* **3**, 513-523, doi:10.1038/nrg840 (2002).

9 Jazwinska, A., Ribeiro, C. & Affolter, M. Epithelial tube morphogenesis during *Drosophila* tracheal development requires Piopio, a luminal ZP protein. *Nat Cell Biol* **5**, 895-901, doi:10.1038/ncb1049 (2003).

10 Nauli, S. M. *et al.* Polycystins 1 and 2 mediate mechanosensation in the primary cilium of kidney cells. *Nat Genet* **33**, 129-137, doi:10.1038/ng1076 (2003).

11 Barr, M. M. *et al.* The Caenorhabditis elegans autosomal dominant polycystic kidney disease gene homologs lov-1 and pkd-2 act in the same pathway. *Curr Biol* **11**, 1341-1346 (2001).

12 Yoder, B. K., Hou, X. & Guay-Woodford, L. M. The polycystic kidney disease proteins, polycystin-1, polycystin-2, polaris, and cystin, are co-localized in renal cilia. *J Am Soc Nephrol* **13**, 2508-2516 (2002).

13 Fliegauf, M., Benzing, T. & Omran, H. When cilia go bad: cilia defects and ciliopathies. *Nat Rev Mol Cell Biol* **8**, 880-893, doi:10.1038/nrm2278 (2007).

14 Mellman, I. Endocytosis and molecular sorting. *Annu Rev Cell Dev Biol* **12**, 575-625, doi:10.1146/annurev.cellbio.12.1.575 (1996).

15 Grant, B. D. & Donaldson, J. G. Pathways and mechanisms of endocytic recycling. *Nat Rev Mol Cell Biol* **10**, 597-608, doi:10.1038/nrm2755 (2009).

16 Jordens, I., Marsman, M., Kuijl, C. & Neefjes, J. Rab proteins, connecting transport and vesicle fusion. *Traffic* **6**, 1070-1077, doi:10.1111/j.1600-0854.2005.00336.x (2005).

17 Apodaca, G. Endocytic traffic in polarized epithelial cells: role of the actin and microtubule cytoskeleton. *Traffic* **2**, 149-159 (2001).

18 Palamidessi, A. *et al.* Endocytic trafficking of Rac is required for the spatial restriction of signaling in cell migration. *Cell* **134**, 135-147, doi:10.1016/j.cell.2008.05.034 (2008).
19 Rodriguez-Boulan, E., Kreitzer, G. & Musch, A. Organization of vesicular trafficking in epithelia. *Nat Rev Mol Cell Biol* **6**, 233-247, doi:10.1038/nrm1593 (2005).
20 Simonsen, A. *et al.* EEA1 links PI(3)K function to Rab5 regulation of endosome fusion. *Nature* **394**, 494-498, doi:10.1038/28879 (1998).
21 Christoforidis, S., McBride, H. M., Burgoyne, R. D. & Zerial, M. The Rab5 effector EEA1 is a core component of endosome docking. *Nature* **397**, 621-625, doi:10.1038/17618 (1999).
22 Hoekstra, D., Tyteca, D. & van, I. S. C. The subapical compartment: a traffic center in membrane polarity development. *J Cell Sci* **117**, 2183-2192, doi:10.1242/jcs.01217 (2004).
23 Maxfield, F. R. & McGraw, T. E. Endocytic recycling. *Nat Rev Mol Cell Biol* **5**, 121-132, doi:10.1038/nrm1315 (2004).
24 Rink, J., Ghigo, E., Kalaidzidis, Y. & Zerial, M. Rab conversion as a mechanism of progression from early to late endosomes. *Cell* **122**, 735-749, doi:10.1016/j.cell.2005.06.043 (2005).
25 Wang, T., Ming, Z., Xiaochun, W. & Hong, W. Rab7: role of its protein interaction cascades in endo-lysosomal traffic. *Cell Signal* **23**, 516-521, doi:10.1016/j.cellsig.2010.09.012 (2011).
26 Vanlandingham, P. A. & Ceresa, B. P. Rab7 regulates late endocytic trafficking downstream of multivesicular body biogenesis and cargo sequestration. *J Biol Chem* **284**, 12110-12124, doi:10.1074/jbc.M809277200 (2009).
27 Sun, Y., Buki, K. G., Ettala, O., Vaaraniemi, J. P. & Vaananen, H. K. Possible role of direct Rac1-Rab7 interaction in ruffled border formation of osteoclasts. *J Biol Chem* **280**, 32356-32361, doi:10.1074/jbc.M414213200 (2005).
28 Cogli, L., Piro, F. & Bucci, C. Rab7 and the CMT2B disease. *Biochem Soc Trans* **37**, 1027-1031, doi:10.1042/BST0371027 (2009).
29 Weisz, O. A. & Rodriguez-Boulan, E. Apical trafficking in epithelial cells: signals, clusters and motors. *J Cell Sci* **122**, 4253-4266, doi:10.1242/jcs.032615 (2009).
30 Mellman, I. & Nelson, W. J. Coordinated protein sorting, targeting and distribution in polarized cells. *Nat Rev Mol Cell Biol* **9**, 833-845, doi:10.1038/nrm2525 (2008).
31 Grant, B. *et al.* Evidence that RME-1, a conserved C. elegans EH-domain protein, functions in endocytic recycling. *Nat Cell Biol* **3**, 573-579, doi:10.1038/35078549 (2001).
32 Grant, B. D. & Caplan, S. Mechanisms of EHD/RME-1 protein function in endocytic transport. *Traffic* **9**, 2043-2052, doi:10.1111/j.1600-0854.2008.00834.x (2008).
33 Donaldson, J. G., Porat-Shliom, N. & Cohen, L. A. Clathrin-independent endocytosis: a unique platform for cell signaling and PM remodeling. *Cell Signal* **21**, 1-6, doi:10.1016/j.cellsig.2008.06.020 (2009).
34 Harris, K. P. & Tepass, U. Cdc42 and vesicle trafficking in polarized cells. *Traffic* **11**, 1272-1279, doi:10.1111/j.1600-0854.2010.01102.x (2010).
35 Etienne-Manneville, S. Cdc42--the centre of polarity. *J Cell Sci* **117**, 1291-1300, doi:10.1242/jcs.01115 (2004).

36 Cerione, R. A. Cdc42: new roads to travel. *Trends Cell Biol* **14**, 127-132, doi:10.1016/j.tcb.2004.01.008 (2004).
37 Wissler, F. & Labouesse, M. PARtners for endocytosis. *Nat Cell Biol* **9**, 1027-1029, doi:10.1038/ncb0907-1027 (2007).
38 Rojas, R., Ruiz, W. G., Leung, S. M., Jou, T. S. & Apodaca, G. Cdc42-dependent modulation of tight junctions and membrane protein traffic in polarized Madin-Darby canine kidney cells. *Mol Biol Cell* **12**, 2257-2274 (2001).
39 Cohen, D., Musch, A. & Rodriguez-Boulan, E. Selective control of basolateral membrane protein polarity by cdc42. *Traffic* **2**, 556-564 (2001).
40 Kroschewski, R., Hall, A. & Mellman, I. Cdc42 controls secretory and endocytic transport to the basolateral plasma membrane of MDCK cells. *Nat Cell Biol* **1**, 8-13, doi:10.1038/8977 (1999).
41 Harris, K. P. & Tepass, U. Cdc42 and Par proteins stabilize dynamic adherens junctions in the *Drosophila* neuroectoderm through regulation of apical endocytosis. *J Cell Biol* **183**, 1129-1143, doi:10.1083/jcb.200807020 (2008).
42 Zhang, X. *et al.* Cdc42 interacts with the exocyst and regulates polarized secretion. *J Biol Chem* **276**, 46745-46750, doi:10.1074/jbc.M107464200 (2001).
43 Brenner, S. The genetics of Caenorhabditis elegans. *Genetics* **77**, 71-94 (1974).
44 Riddle, D. L., Blumenthal, T., Meyer, B. J. & Priess, J. R. *C. elegans II*. 2nd edn, (Cold Spring Harbor Laboratory Press, 1997).
45 Sulston, J. E., Schierenberg, E., White, J. G. & Thomson, J. N. The embryonic cell lineage of the nematode Caenorhabditis elegans. *Dev Biol* **100**, 64-119 (1983).
46 Nelson, F. K. & Riddle, D. L. Functional study of the Caenorhabditis elegans secretory-excretory system using laser microsurgery. *J Exp Zool* **231**, 45-56, doi:10.1002/jez.1402310107 (1984).
47 Altun, Z. F., Herndon, L. A., Crocker, C., Lints, R. & Hall, D. H. *WormAtlas*, <http://www.wormatlas.org> (2002-2011.).
48 Buechner, M., Hall, D. H., Bhatt, H. & Hedgecock, E. M. Cystic canal mutants in Caenorhabditis elegans are defective in the apical membrane domain of the renal (excretory) cell. *Dev Biol* **214**, 227-241, doi:10.1006/dbio.1999.9398 (1999).
49 Berry, K. L., Bulow, H. E., Hall, D. H. & Hobert, O. A C. elegans CLIC-like protein required for intracellular tube formation and maintenance. *Science* **302**, 2134-2137, doi:10.1126/science.1087667 (2003).
50 Fujita, M. *et al.* The role of the ELAV homologue EXC-7 in the development of the Caenorhabditis elegans excretory canals. *Dev Biol* **256**, 290-301 (2003).
51 Tong, X. & Buechner, M. CRIP homologues maintain apical cytoskeleton to regulate tubule size in C. elegans. *Dev Biol* **317**, 225-233, doi:10.1016/j.ydbio.2008.02.040 (2008).
52 Praitis, V., Ciccone, E. & Austin, J. SMA-1 spectrin has essential roles in epithelial cell sheet morphogenesis in C. elegans. *Dev Biol* **283**, 157-170, doi:10.1016/j.ydbio.2005.04.002 (2005).
53 Jones, S. J. & Baillie, D. L. Characterization of the let-653 gene in Caenorhabditis elegans. *Mol Gen Genet* **248**, 719-726 (1995).
54 Stone, C. E., Hall, D. H. & Sundaram, M. V. Lipocalin signaling controls unicellular tube development in the Caenorhabditis elegans excretory system. *Dev Biol* **329**, 201-211, doi:10.1016/j.ydbio.2009.02.030 (2009).

55 Gobel, V., Barrett, P. L., Hall, D. H. & Fleming, J. T. Lumen morphogenesis in C. elegans requires the membrane-cytoskeleton linker erm-1. *Dev Cell* **6**, 865-873, doi:10.1016/j.devcel.2004.05.018 (2004).
56 Gao, J., Estrada, L., Cho, S., Ellis, R. E. & Gorski, J. L. The Caenorhabditis elegans homolog of FGD1, the human Cdc42 GEF gene responsible for faciogenital dysplasia, is critical for excretory cell morphogenesis. *Hum Mol Genet* **10**, 3049-3062 (2001).
57 Suzuki, N. *et al.* A putative GDP-GTP exchange factor is required for development of the excretory cell in Caenorhabditis elegans. *EMBO Rep* **2**, 530-535, doi:10.1093/embo-reports/kve110 (2001).
58 Pasteris, N. G. *et al.* Isolation and characterization of the faciogenital dysplasia (Aarskog-Scott syndrome) gene: a putative Rho/Rac guanine nucleotide exchange factor. *Cell* **79**, 669-678 (1994).
59 Delague, V. *et al.* Mutations in FGD4 encoding the Rho GDP/GTP exchange factor FRABIN cause autosomal recessive Charcot-Marie-Tooth type 4H. *Am J Hum Genet* **81**, 1-16, doi:10.1086/518428 (2007).
60 Carter, G. T. *et al.* Neuropathic pain in Charcot-Marie-Tooth disease. *Arch Phys Med Rehabil* **79**, 1560-1564 (1998).
61 Aghazadeh, B. *et al.* Structure and mutagenesis of the Dbl homology domain. *Nat Struct Biol* **5**, 1098-1107, doi:10.1038/4209 (1998).
62 Harlan, J. E., Hajduk, P. J., Yoon, H. S. & Fesik, S. W. Pleckstrin homology domains bind to phosphatidylinositol-4,5-bisphosphate. *Nature* **371**, 168-170, doi:10.1038/371168a0 (1994).
63 Gaullier, J. M. *et al.* FYVE fingers bind PtdIns(3)P. *Nature* **394**, 432-433, doi:10.1038/28767 (1998).
64 Schink, K. O. & Bolker, M. Coordination of cytokinesis and cell separation by endosomal targeting of a Cdc42-specific guanine nucleotide exchange factor in Ustilago maydis. *Mol Biol Cell* **20**, 1081-1088, doi:10.1091/mbc.E08-03-0280 (2009).
65 Stendel, C. *et al.* Peripheral nerve demyelination caused by a mutant Rho GTPase guanine nucleotide exchange factor, frabin/FGD4. *Am J Hum Genet* **81**, 158-164, doi:10.1086/518770 (2007).
66 Gettner, S. N., Kenyon, C. & Reichardt, L. F. Characterization of beta pat-3 heterodimers, a family of essential integrin receptors in C. elegans. *J Cell Biol* **129**, 1127-1141 (1995).
67 Hedgecock, E. M., Culotti, J. G., Hall, D. H. & Stern, B. D. Genetics of cell and axon migrations in Caenorhabditis elegans. *Development* **100**, 365-382 (1987).
68 Flibotte, S. *et al.* Whole-genome profiling of mutagenesis in Caenorhabditis elegans. *Genetics* **185**, 431-441, doi:10.1534/genetics.110.116616 (2010).
69 Orrico, A. *et al.* A mutation in the pleckstrin homology (PH) domain of the FGD1 gene in an Italian family with faciogenital dysplasia (Aarskog-Scott syndrome). *FEBS Lett* **478**, 216-220 (2000).
70 Lopez-Lago, M., Lee, H., Cruz, C., Movilla, N. & Bustelo, X. R. Tyrosine phosphorylation mediates both activation and downmodulation of the biological activity of Vav. *Mol Cell Biol* **20**, 1678-1691 (2000).
71 Kuhne, M. R., Ku, G. & Weiss, A. A guanine nucleotide exchange factor-independent function of Vav1 in transcriptional activation. *J Biol Chem* **275**, 2185-2190 (2000).

72 Estrada, L., Caron, E. & Gorski, J. L. Fgd1, the Cdc42 guanine nucleotide exchange factor responsible for faciogenital dysplasia, is localized to the subcortical actin cytoskeleton and Golgi membrane. *Hum Mol Genet* **10**, 485-495 (2001).
73 Hou, P. *et al.* Fgd1, the Cdc42 GEF responsible for Faciogenital Dysplasia, directly interacts with cortactin and mAbp1 to modulate cell shape. *Hum Mol Genet* **12**, 1981-1993 (2003).
74 Stalder, L. & Muhlemann, O. The meaning of nonsense. *Trends Cell Biol* **18**, 315-321, doi:10.1016/j.tcb.2008.04.005 (2008).
75 Olson, M. F., Pasteris, N. G., Gorski, J. L. & Hall, A. Faciogenital dysplasia protein (FGD1) and Vav, two related proteins required for normal embryonic development, are upstream regulators of Rho GTPases. *Curr Biol* **6**, 1628-1633 (1996).
76 Nakanishi, H. & Takai, Y. Frabin and other related Cdc42-specific guanine nucleotide exchange factors couple the actin cytoskeleton with the plasma membrane. *J Cell Mol Med* **12**, 1169-1176, doi:10.1111/j.1582-4934.2008.00345.x (2008).
77 Ono, Y. *et al.* Two actions of frabin: direct activation of Cdc42 and indirect activation of Rac. *Oncogene* **19**, 3050-3058, doi:10.1038/sj.onc.1203631 (2000).
78 Whitehead, I. P., Abe, K., Gorski, J. L. & Der, C. J. CDC42 and FGD1 cause distinct signaling and transforming activities. *Mol Cell Biol* **18**, 4689-4697 (1998).
79 Yandell, M. D., Edgar, L. G. & Wood, W. B. Trimethylpsoralen induces small deletion mutations in Caenorhabditis elegans. *Proc Natl Acad Sci U S A* **91**, 1381-1385 (1994).
80 Fire, A. *et al.* Potent and specific genetic interference by double-stranded RNA in Caenorhabditis elegans. *Nature* **391**, 806-811, doi:10.1038/35888 (1998).
81 Parrish, S. & Fire, A. Distinct roles for RDE-1 and RDE-4 during RNA interference in Caenorhabditis elegans. *Rna* **7**, 1397-1402 (2001).
82 Tabara, H. *et al.* The rde-1 gene, RNA interference, and transposon silencing in C. elegans. *Cell* **99**, 123-132 (1999).
83 Kramer, J. M., French, R. P., Park, E. C. & Johnson, J. J. The Caenorhabditis elegans rol-6 gene, which interacts with the sqt-1 collagen gene to determine organismal morphology, encodes a collagen. *Mol Cell Biol* **10**, 2081-2089 (1990).
84 Steiner, F. A., Okihara, K. L., Hoogstrate, S. W., Sijen, T. & Ketting, R. F. RDE-1 slicer activity is required only for passenger-strand cleavage during RNAi in Caenorhabditis elegans. *Nat Struct Mol Biol* **16**, 207-211, doi:10.1038/nsmb.1541 (2009).
85 Farazi, T. A., Juranek, S. A. & Tuschl, T. The growing catalog of small RNAs and their association with distinct Argonaute/Piwi family members. *Development* **135**, 1201-1214, doi:10.1242/dev.005629 (2008).
86 Djuranovic, S., Nahvi, A. & Green, R. A parsimonious model for gene regulation by miRNAs. *Science* **331**, 550-553, doi:10.1126/science.1191138 (2011).
87 Tavernarakis, N., Wang, S. L., Dorovkov, M., Ryazanov, A. & Driscoll, M. Heritable and inducible genetic interference by double-stranded RNA encoded by transgenes. *Nat Genet* **24**, 180-183, doi:10.1038/72850 (2000).
88 Qadota, H. *et al.* Establishment of a tissue-specific RNAi system in C. elegans. *Gene* **400**, 166-173, doi:10.1016/j.gene.2007.06.020 (2007).
89 Esposito, G., Di Schiavi, E., Bergamasco, C. & Bazzicalupo, P. Efficient and cell specific knock-down of gene function in targeted C. elegans neurons. *Gene* **395**, 170-176, doi:10.1016/j.gene.2007.03.002 (2007).

90 Winston, W. M., Molodowitch, C. & Hunter, C. P. Systemic RNAi in C. elegans requires the putative transmembrane protein SID-1. *Science* **295**, 2456-2459, doi:10.1126/science.1068836 (2002).
91 Feinberg, E. H. & Hunter, C. P. Transport of dsRNA into cells by the transmembrane protein SID-1. *Science* **301**, 1545-1547, doi:10.1126/science.1087117 (2003).
92 Calixto, A., Chelur, D., Topalidou, I., Chen, X. & Chalfie, M. Enhanced neuronal RNAi in C. elegans using SID-1. *Nat Methods* **7**, 554-559, doi:10.1038/nmeth.1463 (2010).
93 Jenna, S. *et al.* Regulation of membrane trafficking by a novel Cdc42-related protein in Caenorhabditis elegans epithelial cells. *Mol Biol Cell* **16**, 1629-1639, doi:10.1091/mbc.E04-08-0760 (2005).
94 Lundquist, E. A. Small GTPases. *WormBook*, 1-18, doi:10.1895/wormbook.1.67.1 (2006).
95 Lundquist, E. A., Reddien, P. W., Hartwieg, E., Horvitz, H. R. & Bargmann, C. I. Three C. elegans Rac proteins and several alternative Rac regulators control axon guidance, cell migration and apoptotic cell phagocytosis. *Development* **128**, 4475-4488 (2001).
96 WormBase. *WormBase: The Biology and Genome of C. elegans*, <www.wormbase.org> (2011).
97 Fidyk, N., Wang, J. B. & Cerione, R. A. Influencing cellular transformation by modulating the rates of GTP hydrolysis by Cdc42. *Biochemistry* **45**, 7750-7762, doi:10.1021/bi060365h (2006).
98 Irazoqui, J. E., Gladfelter, A. S. & Lew, D. J. Cdc42p, GTP hydrolysis, and the cell's sense of direction. *Cell Cycle* **3**, 861-864 (2004).
99 Egorov, M. V. *et al.* Faciogenital dysplasia protein (FGD1) regulates export of cargo proteins from the golgi complex via Cdc42 activation. *Mol Biol Cell* **20**, 2413-2427, doi:10.1091/mbc.E08-11-1136 (2009).
100 Huber, C., Martensson, A., Bokoch, G. M., Nemazee, D. & Gavin, A. L. FGD2, a CDC42-specific exchange factor expressed by antigen-presenting cells, localizes to early endosomes and active membrane ruffles. *J Biol Chem* **283**, 34002-34012, doi:10.1074/jbc.M803957200 (2008).
101 Roberts, R. C. *et al.* Mistargeting of SH3TC2 away from the recycling endosome causes Charcot-Marie-Tooth disease type 4C. *Hum Mol Genet* **19**, 1009-1018, doi:10.1093/hmg/ddp565 (2010).
102 Bolino, A. *et al.* Charcot-Marie-Tooth type 4B is caused by mutations in the gene encoding myotubularin-related protein-2. *Nat Genet* **25**, 17-19, doi:10.1038/75542 (2000).
103 Dang, H., Li, Z., Skolnik, E. Y. & Fares, H. Disease-related myotubularins function in endocytic traffic in Caenorhabditis elegans. *Mol Biol Cell* **15**, 189-196, doi:10.1091/mbc.E03-08-0605 (2004).
104 Oka, T., Toyomura, T., Honjo, K., Wada, Y. & Futai, M. Four subunit a isoforms of Caenorhabditis elegans vacuolar H+-ATPase. Cell-specific expression during development. *J Biol Chem* **276**, 33079-33085, doi:10.1074/jbc.M101652200 (2001).
105 Praitis, V., Casey, E., Collar, D. & Austin, J. Creation of low-copy integrated transgenic lines in Caenorhabditis elegans. *Genetics* **157**, 1217-1226 (2001).
106 Kumfer, K. T. *et al.* CGEF-1 and CHIN-1 regulate CDC-42 activity during asymmetric division in the Caenorhabditis elegans embryo. *Mol Biol Cell* **21**, 266-277, doi:10.1091/mbc.E09-01-0060 (2010).

107 Nelson, F. K., Albert, P. S. & Riddle, D. L. Fine structure of the Caenorhabditis elegans secretory-excretory system. *J Ultrastruct Res* **82**, 156-171 (1983).
108 Chitwood, B. G., Chitwood, M. B. H. & Christenson, R. O. *Introduction to Nematology*. Consolidated edn, (University Park Press, 1974).
109 Chavrier, P., Parton, R. G., Hauri, H. P., Simons, K. & Zerial, M. Localization of low molecular weight GTP binding proteins to exocytic and endocytic compartments. *Cell* **62**, 317-329 (1990).
110 Mu, F. T. *et al.* EEA1, an early endosome-associated protein. EEA1 is a conserved alpha-helical peripheral membrane protein flanked by cysteine "fingers" and contains a calmodulin-binding IQ motif. *J Biol Chem* **270**, 13503-13511 (1995).
111 Hermann, G. J. *et al.* Genetic analysis of lysosomal trafficking in Caenorhabditis elegans. *Mol Biol Cell* **16**, 3273-3288, doi:10.1091/mbc.E05-01-0060 (2005).
112 Lin, S. X., Grant, B., Hirsh, D. & Maxfield, F. R. Rme-1 regulates the distribution and function of the endocytic recycling compartment in mammalian cells. *Nat Cell Biol* **3**, 567-572, doi:10.1038/35078543 (2001).
113 Ullrich, O., Reinsch, S., Urbe, S., Zerial, M. & Parton, R. G. Rab11 regulates recycling through the pericentriolar recycling endosome. *J Cell Biol* **135**, 913-924 (1996).
114 Kjer-Nielsen, L., Teasdale, R. D., van Vliet, C. & Gleeson, P. A. A novel Golgi-localisation domain shared by a class of coiled-coil peripheral membrane proteins. *Curr Biol* **9**, 385-388 (1999).
115 Munro, S. & Nichols, B. J. The GRIP domain - a novel Golgi-targeting domain found in several coiled-coil proteins. *Curr Biol* **9**, 377-380 (1999).
116 Balklava, Z., Pant, S., Fares, H. & Grant, B. D. Genome-wide analysis identifies a general requirement for polarity proteins in endocytic traffic. *Nat Cell Biol* **9**, 1066-1073, doi:10.1038/ncb1627 (2007).
117 Shioi, G. *et al.* Mutations affecting nerve attachment of Caenorhabditis elegans. *Genetics* **157**, 1611-1622 (2001).
118 Naslavsky, N. & Caplan, S. C-terminal EH-domain-containing proteins: consensus for a role in endocytic trafficking, EH? *J Cell Sci* **118**, 4093-4101, doi:10.1242/jcs.02595 (2005).
119 Chen, C. C. *et al.* RAB-10 is required for endocytic recycling in the Caenorhabditis elegans intestine. *Mol Biol Cell* **17**, 1286-1297, doi:10.1091/mbc.E05-08-0787 (2006).
120 Sharma, M., Naslavsky, N. & Caplan, S. A role for EHD4 in the regulation of early endosomal transport. *Traffic* **9**, 995-1018, doi:10.1111/j.1600-0854.2008.00732.x (2008).
121 Rondanino, C. *et al.* RhoB-dependent modulation of postendocytic traffic in polarized Madin-Darby canine kidney cells. *Traffic* **8**, 932-949, doi:10.1111/j.1600-0854.2007.00575.x (2007).
122 Pant, S. *et al.* AMPH-1/Amphiphysin/Bin1 functions with RME-1/Ehd1 in endocytic recycling. *Nat Cell Biol* **11**, 1399-1410, doi:10.1038/ncb1986 (2009).
123 Shi, A. *et al.* A novel requirement for C. elegans Alix/ALX-1 in RME-1-mediated membrane transport. *Curr Biol* **17**, 1913-1924, doi:10.1016/j.cub.2007.10.045 (2007).

124 Ren, M. *et al.* Hydrolysis of GTP on rab11 is required for the direct delivery of transferrin from the pericentriolar recycling compartment to the cell surface but not from sorting endosomes. *Proc Natl Acad Sci U S A* **95**, 6187-6192 (1998).
125 Moore, R. H., Millman, E. E., Alpizar-Foster, E., Dai, W. & Knoll, B. J. Rab11 regulates the recycling and lysosome targeting of beta2-adrenergic receptors. *J Cell Sci* **117**, 3107-3117, doi:10.1242/jcs.01168 (2004).
126 Bucci, C. *et al.* The small GTPase rab5 functions as a regulatory factor in the early endocytic pathway. *Cell* **70**, 715-728 (1992).
127 Stenmark, H. *et al.* Inhibition of rab5 GTPase activity stimulates membrane fusion in endocytosis. *Embo J* **13**, 1287-1296 (1994).
128 Hirata, R. *et al.* Molecular structure of a gene, VMA1, encoding the catalytic subunit of H(+)-translocating adenosine triphosphatase from vacuolar membranes of Saccharomyces cerevisiae. *J Biol Chem* **265**, 6726-6733 (1990).
129 Zeidler, M. P. *et al.* Temperature-sensitive control of protein activity by conditionally splicing inteins. *Nat Biotechnol* **22**, 871-876, doi:10.1038/nbt979 (2004).
130 Tan, G., Chen, M., Foote, C. & Tan, C. Temperature-sensitive mutations made easy: generating conditional mutations by using temperature-sensitive inteins that function within different temperature ranges. *Genetics* **183**, 13-22, doi:10.1534/genetics.109.104794 (2009).
131 Szewczyk, E. *et al.* Fusion PCR and gene targeting in Aspergillus nidulans. *Nat Protoc* **1**, 3111-3120, doi:10.1038/nprot.2006.405 (2006).
132 Amitai, G., Callahan, B. P., Stanger, M. J., Belfort, G. & Belfort, M. Modulation of intein activity by its neighboring extein substrates. *Proc Natl Acad Sci U S A* **106**, 11005-11010, doi:10.1073/pnas.0904366106 (2009).
133 Sheffield, M., Loveless, T., Hardin, J. & Pettitt, J. C. elegans Enabled exhibits novel interactions with N-WASP, Abl, and cell-cell junctions. *Curr Biol* **17**, 1791-1796, doi:10.1016/j.cub.2007.09.033 (2007).
134 Tomasevic, N. *et al.* Differential regulation of WASP and N-WASP by Cdc42, Rac1, Nck, and PI(4,5)P2. *Biochemistry* **46**, 3494-3502, doi:10.1021/bi062152y (2007).
135 Shakir, M. A. *et al.* The Arp2/3 activators WAVE and WASP have distinct genetic interactions with Rac GTPases in Caenorhabditis elegans axon guidance. *Genetics* **179**, 1957-1971, doi:10.1534/genetics.108.088963 (2008).
136 Puthenveedu, M. A. *et al.* Sequence-dependent sorting of recycling proteins by actin-stabilized endosomal microdomains. *Cell* **143**, 761-773, doi:10.1016/j.cell.2010.10.003 (2010).
137 Riedl, J. *et al.* Lifeact: a versatile marker to visualize F-actin. *Nat Methods* **5**, 605-607, doi:10.1038/nmeth.1220 (2008).
138 Schermelleh, L. *et al.* Subdiffraction multicolor imaging of the nuclear periphery with 3D structured illumination microscopy. *Science* **320**, 1332-1336, doi:10.1126/science.1156947 (2008).